CERTIFICATO DI FIRMA DIGITALE

Si certifica che questo documento informatico

PhD-thesis-Angela-Subbiani.pdf

composto da n°141 pagine

È stato firmato digitalmente in data odierna con Firma Elettronica Qualificata (FEQ), avente l'efficacia e gli effetti giuridici equivalenti a quelli di una firma autografa, ai sensi dell'art. 2702 del Codice Civile e dell'art. 25 del Regolamento UE n. 910/2014 eIDAS (electronic IDentification Authentication and Signature).

PROCESSI INFORMATICI COMPLETATI

- **Apposizione di Firma Elettronica Qualificata Remota** emessa da Intesi Group S.p.A. in qualità di prestatore di servizi fiduciari qualificati autorizzato da AgID, per garantire con certezza l'autenticità, l'integrità, il non ripudio e l'immodificabilità del documento informatico e la sua riconducibilità in maniera manifesta e inequivoca all'autore, ai sensi dell'art. 20 comma 2 del CAD - D.lgs 82/2005.
- **Apposizione di Marca Temporale Qualificata** emessa da Intesi Group S.p.A. in qualità di prestatore di servizi fiduciari qualificati autorizzato da AgID, per attribuire una data e un orario opponibile a terzi, ai sensi dell'art. 20 comma 3 del CAD - D.lgs 82/2005 e per far sì che la Firma Elettronica Qualificata apposta su questo documento informatico, risulti comunque valida per i prossimi 20 anni a partire dalla data odierna, anche nel caso in cui il relativo certificato risultasse scaduto, sospeso o revocato.
- **Apposizione di Contrassegno Elettronico**, l'unica soluzione tecnologica che permette di prorogare la validità giuridica di un documento informatico sottoscritto con firma digitale e/o marcato temporalmente, rendendolo inalterabile, certo e non falsificabile, una volta stampato su supporto cartaceo, ai sensi dell'art. 23 del CAD - D.lgs 82/2005.

  Per risalire all'originale informatico è necessario scansionare il Contrassegno Elettronico, utilizzando l'applicazione HONOS, disponibile per dispositivi Android e iOS.

UNIVERSITÀ
DI SIENA
1240

Università degli Studi di Siena

Department of Biotechnology, Chemistry and Pharmacy

Research Doctorate in Biochemistry and Molecular Biology

BIBIM2.0

Cycle XXXIV°

Coordinator: Prof. Lorenza Trabalzini

Multiple roles of β3-adrenergic receptor in pediatric cancers.

Scientific-disciplinary sector: BIO/10

PhD student: Angela Subbiani

Co-tutor: Dr. Maura Calvani

Supervisor: Prof.ssa Paola Chiarugi

Academic year 2020/2021

Index

Abstract

The *β*3-Adrenergic Receptor (*β*3-AR) is one of the *β*-ARs subtypes regulating various physiological responses, including thermogenesis, vasodilatation and cardiac functions, following activation mediated by catecholamines. Recently, increasing evidence demonstrated the role of *β*3-ARs in the tumorigenesis, growth and progression of various cancer types. Despite the efficacy of current therapies and the identification of several genes involved in the onset and growth of pediatric cancers, they remain the second leading cause of death in children.

This thesis had two major aims. First, to investigate the link between *β*3-ARs and cancer-evoked pain and tumor metabolism in pediatric cancers. We found that the development of cancer-evoked pain is mediated by oxidative stress in a murine osteosarcoma model, associated with the recruitment of neuronal macrophages, and that the *β*3-ARs, but also *β*2-ARs, antagonism contributes to the reduction of tumor growth and cancer-associated pain. Second, to characterize the metabolic adaptation of malignant rhabdoid tumor of the kidney (MRTK) G-401 cells to nutrient deprivation to sustain cell survival. In particular, we identify that tyrosine/phenylalanine and glutamine deprivation leads to enhanced glucose metabolism, regulated by *β*3-ARs.

These results indicating the *β*3-ARs as possible pharmacological targets for preventing cancer-evoked pain and metabolic compensatory mechanism that allow MRTK cell survival even during nutrient deprivation.

.

Abbreviations used in thesis

2-DG	2-Deoxy-Glucose
5-HT	5-hydroxytryptamine
AC	Adenylate cyclase
ACLY	ATP citrate lyase
ADRB2	Adrenergic beta2 receptor
ADRB3	Adrenergic beta3 receptor
AKAP250	A-kinase-anchoring protein 250
AMPA	α-amino-3-hydroxy-5-methyl-4-isoxazolepropionic acid receptor
AP-2	Adaptor complex 2
APC	Antigen-presenting cells
AQP5	Aquaporin 5
Arg	Arginine
ASICs	Acid-sensing ion channels
ASS	Argininosuccinato synthase
ATP	Adenosine triphosphate
BAT	Rodent brown adipose tissue
BDNT	Brain-derived neurotrophic factor
C358	Cysteine-358
CAFs	Cancer-associated fibroblasts
cAMP	Cyclic adenosine monophosphate
CCO	Conventional central osteosarcoma
CDK4	Cyclin-dependent kinase
CL316243	5-(2-[[2-(3-chlorophenyl)-2-hydroxyethyl]-amino]propyl)1,3-benzodioxole-2,2-dicarboxylate (),
COMT	Catechol-O-methyltransferase
DCs	Dendritic cells
DIO2	Type 2 deiodinase Mitochondrially Encoded NADH:Ubiquinone
DMP1	Dentin matrix acidic phosphoprotein 1

DNM3	Dynamin-3 gene
dPOS	differentiate POS
E2F3	E2F transcription factor 3
ECM	Mineralized extracellular matrix
EGFR	Epidermal growth factor receptor
EMA	Epithelial membrane antigen
eNOS	Endothelial NO synthase
ERK1/2	Extracellular regulated kinase ½
ET-1	Endothelin 1
ETAR	Endothelin Type A receptor
$FADH_2$.	Flavin adenine dinucleotide
FBP	Fructose-1-6-biphosphate
FFAs	Free fatty acid
GCLc	Glutamate-cysteine ligase catalytic subunit protein
GCPR	Calcitonin gene-related peptide
GDH	Glutamate dehydrogenase
GDP	Guanosine diphosphate
GIPC	PDZ Domain Containing Family Member 1
Gln	Glutamine
GLS	Glutaminases
Glu	Glutamate
GLUTs	Glucose transporters
GOT1	Aspartate transaminase
GPCRs	G-protein-coupled receptors
GRKs	G-protein coupled receptor kinases
GS	Glutamine synthetase
GSA	Glutamic-γ-semi-aldehyde
GTP	Guanosine triphosphate
GW427353	Solabegron
$G\alpha_i$	Inhibitory G protein
$G\alpha_s$	Stimulatory G protein
HGSOS	High-grade osteosarcoma
HIF-1	Hypoxia-inducible factors 1

HK	Hexokinases
HPD	4-hydroxyphenylpyruvate dioxygenase
HREs	Hypoxia Response Elements
HSCs	Hematopoietic myeloid progenitors
HSL	Hormone-sensitive lipase
IGF-1	Insulin-like growth factor 1
IGFR1b	Insulin-like growth factor receptor 1b
IL-10	Interleukin 10
IL-12	Interleukin 12
IL-13	Interleukin 13
IL-17	Interleukin 17
IL-1β	Interleukin 1 beta
IL-6	Interleukin 6
iNOS	Inducible Nitric Oxide Synthase
K305	Lysine305
KRAS	Kirsten rat sarcoma viral oncogene homolog
KUC-7483	Ritobegron
L-cells	Ltk-cells
LDH	Lactate dehydrogenase
L-DOPA	L-dihydroxyphenylalanine
Leu	Leucine
LOH	Loss of heterozygosity
LOS	Low-grade osteosarcoma
LPL	Lipoprotein lipase
MAGI-2	WW And PDZ Domain Containing 2
MAGI-3	WW And PDZ Domain Containing 3
MCP-1	Chemokine monocyte chemoattractant protein-1
M-CSF	Macrophage colony-stimulating factor
MCTs	Monocarboxylate transporters
Met	Methionine
MOR	Morphine receptors
MPC	Mitochondrial pyruvate carrier
MRGPRB2	Mas-related G-protein coupled receptor member B2

MRTK	Malignant rhabdoid tumor of the kidney
MSCs	Mesenchymal stem cells
MT-ND2	Mitochondrially Encoded NADH:Ubiquinone Oxidoreductase Core Subunit 2
mtROS	mithocondrial ROS
NADH	Nicotinamide adenine dinucleotide NAD^+ reduced
NADPH	Nicotinamide adenine dinucleotide phosphate
NAFLD	Nonalcoholic fatty liver disease
NDO	Neurogenic detrusor overactivity
NeSCCs	Neuron-evoked single-channel currents
NF-kB	Nuclear factor kappa B
NGF	Neurotrophic nerve growth factor
NMDA	*N*-methyl-D-aspartate receptor
nNOS	Neuronal NO synthase
NO	Nitric Oxide
NPD1	Neuroprotectin D
NTBC	Nitisinone
OAA	Oxaloacetate
OS	Osteosarcoma
OXPHOS	Oxidative phosphorylation
P5C	α-pyrroline-5-carboxylate
PAH	Phenylalanine hydroxylase
Panx1	Pannexin 1
PBN	Phenyl-alpha-tert-butyl nitrone
PBS	Phosphate buffered saline
PDGH	Phosphoglycerate dehydrogenase
PDH	Pyruvate dehydrogenase complex
PDK	Phosphoinositide-dependent kinases
PDK1	Pyruvate dehydrogenase kinase 1
PEP	Phosphoenolpyruvate
PET	Positron emission tomography
PGE_2	Prostaglandin E_2
Phe	Phenylalanine

PI3K	Phosphoinositide 3-kinase
PIOS	Periosteal osteosarcoma
PKA	Protein kinase A
PKB	Protein kinase B
PKC	Protein kinase C
PKG	Protein kinase G
PKM1	Pyruvate kinase M1
PLC	Phospholipase C
PMA	Phorbol-myristate-acetate
pOB	Preosteoblasts
POS	Parosteal osteosarcoma
PP2A	Protein phosphatase 2A
PP2B	Phosphatase 2B
PPARγ	Peroxisome proliferator-activated receptor gamma
PPAT	Phosphoribosyl pyrophosphate amidotransferase
PPP	Pentose phosphate pathway
PRIM1	DNA primase subunit 1
Pro	Proline
PRODH/POX	Proline dehydrogenase (oxidase)
PSD-95	Postsynaptic density protein 95
Rb	Retinoblastoma
RMS	Rhabdomyosarcoma
ROS	Reactive oxygen species
RUNX2	Run-related transcription factor 2
$S1P_2$	Sphingosine 1 phosphate receptor 2
SDF1	Stromal-derived factor
Ser	Serine
SK2	Sphingosine kinase 2
SNPs	Single-nucleotide polymorphism
SNS	Sympathetic nervous system
SOS	Small-cell osteosarcoma
SPM	Specialized pro-resolving mediator
SR58611A	Amibegron

TCA	Tricarboxylic acid
TGF-β	Transforming growth factor
TH	Tyrosine hydroxylase
Thr	Threonine
TM	Seven-transmembrane-spanning
TMJ	Temporomandibular joint
TNF-α	Tumor necrosis factor alpha
TOS	Telangiectatic osteosarcoma
TRP	Transient receptor potential
Trp	Tryptophan
Tyr	Tyrosine
UCP1	Uncoupling-Protein 1
VEGF	Vascular endothelial growth factor
WAT	Rodent white adipose tissue
WES	Whole-exome sequencing
WGS	Whole-genome sequencing
Y105	Tyrosine-105
YM178	Mirabegron
α-KG	α-ketoglutarate
β-ARs	Beta-adrenergic receptors

List of figures

Chapter 1. Introduction

1.1 General introduction

Beta-Adrenergic Receptors (*β*-ARs) are members of the large family of the G-protein-coupled receptors (GPCRs), responsible for mediating a wide range of physiological responses following their activation elicited by catecholamines, such as adrenaline or noradrenaline. Presently, three subtypes of *β*-ARs have been characterized, *β*1-, *β*2-, *β*3-AR, with a fourth *β*4-AR remaining controversial [1]. Different *β*-ARs are expressed in numerous cell types and tissues, where they are able to activate downstream pathways that can be distinct for each subtype of *β*-ARs or even overlapped. *β*-ARs signaling regulates multiple cellular processes that contribute to thermogenesis, cardiac functions, vasodilatation, increasing metabolism, and other various responses in healthy tissues. While the *β*1-AR and *β*2-AR are expressed almost ubiquitous in humans, the *β*3-AR exhibits a restricted expression pattern in humans.

Since its discovery in 1989, *β*3-AR has been detected in various human tissues such as adipose tissue, myocardium, urinary bladder, blood vessels, brain and retina [2]. Several studies have shown that *β*3-AR plays an important role in metabolic homeostasis by stimulating lipolysis and releasing fatty acids in the white adipose tissue and activating thermogenesis in brown adipose tissue [3]. Growing evidence suggests a role of *β*-ARs signaling in the initiation and progression of cancer, including inflammation, angiogenesis, cell motility, cellular immune response and epithelial-mesenchymal transition. The role of *β*-ARs in cancer initiation and progression is supported by several studies which reported that *β*-blocker treatment significantly reduced cancer metastasis, recurrence and mortality [4]. In view of the emerging role of *β*-ARs in new pathologies, it becomes all the more pertinent better to understand the regulation of *β*-ARs function and signaling.

1.2 *β*3-Adrenergic Receptors

*β*3-AR belong to the GPCRs family, the largest family of membrane-localized proteins in mammals, whose function consists of transmitting extracellular stimuli such as peptides, chemokines, hormones into intracellular functional changes. *β*3-AR consists of a seven-transmembrane-spanning (TM) domains, with three intracellular and three extracellular loops. The C-terminus of *β*3-AR is intracellular, whereas the N-terminal tail is extracellular and glycosylated. The classical signal transduction via GPCRs depends on receptor-mediated activation of heterodimeric G proteins, which are composed of three subunits, Gα, Gβ and Gγ that provide specificity and functionality of GPCRs. G proteins are classified into four families according to the α subunit, G_i, G_s, $G_{12/13}$, and G_q whit different activities. The G_i and G_s families regulate adenylyl cyclase (AC) activity, whereas G_q activates phospholipase C (PLC) and $G_{12/13}$ activates small GTPase families [5]. The G_q family is composed of four members, $G_{q,}$ G_{11}, G_{14} and $G_{15/16}$ and their respective subunits are $G\alpha_q$, $G\alpha_{11}$, $G\alpha_{14}$ and $G\alpha_{15/16}$. When bound to GDP, Gα associates with Gβγ to form the inactive heterotrimer. After ligand binding, the receptor undergoes a conformational change that induces an exchange of guanosine diphosphate (GDP) for guanosine triphosphate (GTP), leading to dissociation of the G protein into Gα and Gβγ protein subunits causing their activation (Figure 1).

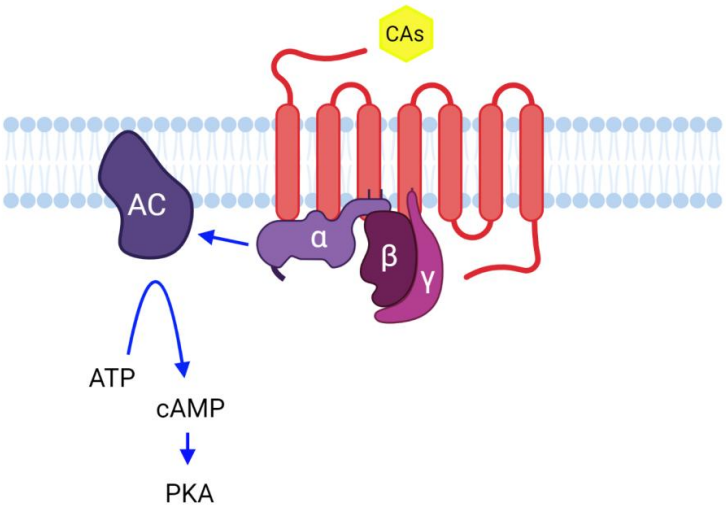

Figure 1. *β*3-AR signaling.

Both subunits modulate the activity of different downstream effector proteins. Activation of $G\alpha_s$ subunits leads to activation of AC that catalyzes the conversion of adenosine triphosphate (ATP) into cyclic adenosine monophosphate (cAMP). The second messengers, cAMP, activates protein kinase A (PKA), which phosphorylated effector molecules and subsequently mediates a functional response. The type of the downstream effectors is determined by the subtype of *β*-AR that is activated; all *β*-ARs are coupled with the stimulatory G protein ($G\alpha_s$) activation, but only *β*2-AR and *β*3-AR can be coupled to the inhibitory G protein ($G\alpha_i$) [6]. One of the functional responses of cAMP-mediated PKA activation is the mobilization of Ca^{2+} mediating the cardiac contraction [7]. Furthermore, PKA activation can also mediate relaxation by phosphorylation of protein involved in Ca^{2+} sensitivity and cross-bridge cycling of smooth muscle cells [8] (Figure 1).

1.2.1 *β*-ARs signaling regulation

Once the cell manifests a functional response, the *β*-ARs initiated signal need to be dampened despite continuing agonist stimulation through an adaptive mechanism called desensitization, which occurs through three different processes; the uncoupling of GPCR/G-protein signal mediated by phosphorylation of *β*-ARs, recruitment of β-arrestin that suppress further *β*-AR-G-protein coupling, and endocytosis of GPRCs into endosomes.

The functional uncoupling of *β*-ARs from G-protein occurs through receptor phosphorylation by PKA or G-protein coupled receptor kinases (GRKs) family. The second messenger cAMP activates PKA, which in turn phosphorylates *β*-ARs, reducing G-protein coupling, a process known as heterologous desensitization or non-agonist-specific desensitization. In contrast, agonist-occupied GRKs' phosphorylation through a mechanism called homologous desensitization or agonist-specific desensitization. There are seven-member of the GRKs family (GRK 1-7) and four arrestins. GRK2, 3, 5, and 6 are ubiquitously expressed and mediated agonist dependent *β*-AR phosphorylation recruiting the cytosolic adaptor protein β-arrestin to the receptor. In particular, GRK2 and GRK3 are recruited to the activated *β*-ARs by Gβγ subunits, whereas GRK5 and GRK6 are associated with the plasma membrane [9, 10]. Arrestin1 and arrestin4 have restricted tissue expression,

localizing primarily to visual sensory tissue, while arrestin2 and arrestin3, also called β-arrestin1 and β-arrestin2, respectively are ubiquitously expressed and interact with the majority of G-protein coupled receptors [2]. The phosphorylation of agonist-occupied GPCRs by GRKs enhances the receptor's affinity for interaction with β-arrestin, which binds to the *β*-ARs, forming a complex that interdicts further G-protein coupling. This process prevents further activation of the stimulatory protein $G\alpha_s$ and the subsequent stimulation of AC. The increase of GRKs activity induces *β*-AR towards the inactive state and subsequently reduced responsiveness to catecholamines [11, 12]. Receptor binding produces significant conformational changes in arrestin with the exposition of the C-terminus tail, whereas arrestin binding stabilizes the receptor [13].

β-arrestin1 and β-arrestin3 also play a crucial role in desensitization followed by the internalization of GPRCs through the clathrin-dependent mechanism. The arrestin C-terminus directly binds the clathrin heavy chain and the adaptor complex 2 (AP-2) subunit, a complex involved in protein transport via vesicles in different membrane traffic pathways. The binding between clathrin and AP-2 induces arrestin-bound receptors to cluster in clathrin-coated pits, which are pinched off membrane by the motor protein dynamin [14-16]. This arrestin-dependent endocytosis removes receptors from the cell surface, leading to minor responsiveness to stimuli. The *β*-ARs exhibit a higher affinity to β-arrestin1 and β-arrestin3 and forms transient receptor-arrestin complexes that dissociated rapidly after the receptor internalized, with subsequent resensitization and recycling back to the plasma membrane (Figure 2).

In addition to the above classical mechanism of desensitization, *β*-ARs are predisposed to become dysfunctional during inflammation. Evidence suggests that in the human airway smooth muscles and in cardiomyocytes have shown that the pro-inflammatory cytokines such as tumor necrosis factor-alpha (TNF-α), interleukin 1 -beta (IL-1β), and interleukin 13 (IL-13) predispose *β*-ARs to desensitization [17, 18]. Resensitization of *β*-ARs is an important process that restores the responsiveness of the desensitized receptor either in the continued presence or absence of desensitizing stimulus, to maintain tissue homeostasis as receptor becomes refractory to responding to their environment upon desensitization [19, 20]. Following dynamin mediated pinching of the clathrin

vesicle, receptor-containing vesicle could be transported as a recycling endosome or targeted to lysosomal mediated degradation. Multiple processes, including nitrosylation, regulate dynamin function. Inhibition of nitrosylation of dynamin results in a reduction in *β*-ARs internalization that affects resensitization [21].

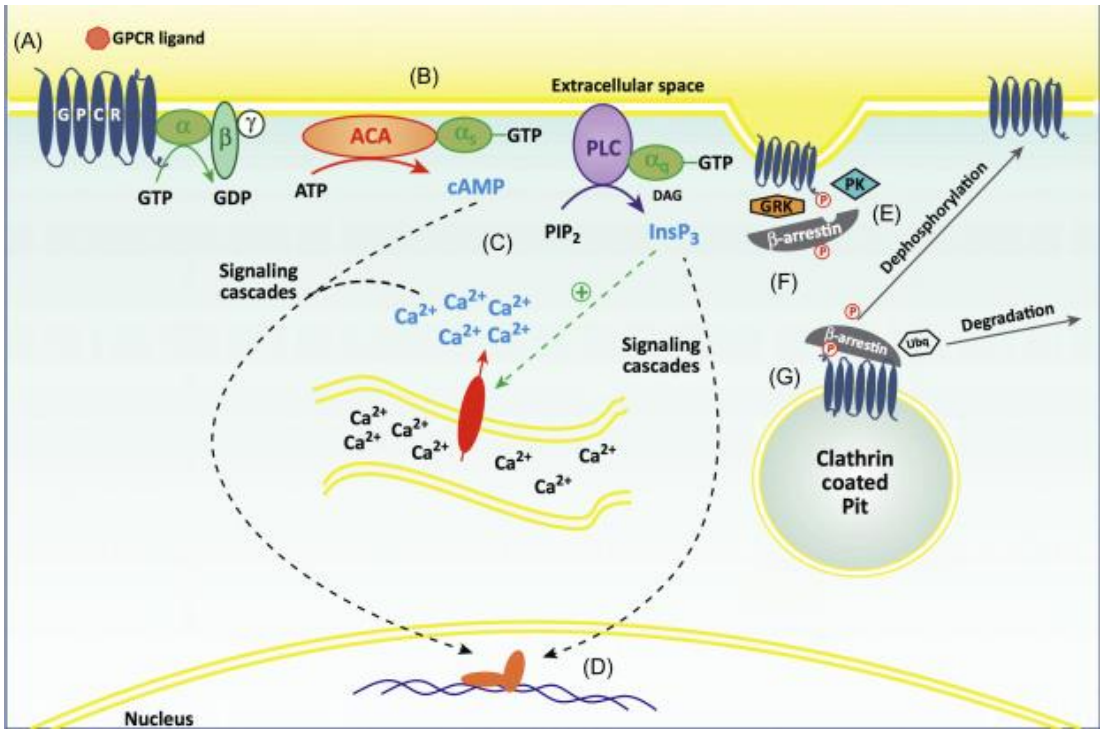

Figure 2. GPCRs activation and regulation. (A) Binding of a GPCR ligand to the extracellular side of the receptors enables the exchange of GDP to GTP by the α subunit of the G protein. (B) The GTP-bound α subunit then acts as a second messenger leading to the activation of adenylate cyclase (AC) or phospholipase C (PLC). (C) Second-messenger molecules such as cAMP and inositol-1,4,5-triphosphate ($InsP_3$) are products of enzymatic conversion of ATP and phosphatidylinositol-4,5-bisphosphate (PIP_2) respectively, whereas cytosolic Ca^{2+} is released upon activation of reticular calcium channels. (D) Second messenger molecules can induce a cascade reaction that lead to gene expression regulation. (E) Protein kinase or G protein-coupled receptor kinases (GRKs) phosphorylates the intracellular side of the receptor and decouple the G protein. (F) β-arrestin recognize the phosphorylated GPCR and induced the internalization process. (G) Modification on β-arrestin define the fate of internalized molecules; the dephosphorylation lead to the recycling of the molecule, whereas ubiquitination lead to its degradation (adapted from [22]).

Resensitization is also due to the transport of the endocytosed β-ARs to an appropriated location in cells, dependent on local actin synthesis and reorganization, and mediated by small Rab GTPases, which are critical to the formation of recycling endosomes in which resensitization occurs. The alteration of these processes leads to improper localization of the endocytosed receptor and reduced resensitization efficiency [23-26]. Many GPCRs, including β-ARs, contain carboxyl-terminal motifs that interact with PDZ scaffold proteins like postsynaptic density protein 95 (PSD-95), PDZ Domain Containing Family Member 1 (GIPC) and Membrane Associated Guanylate Kinase, WW And PDZ Domain Containing 2 (MAGI-2) that regulate multiple biological processes such as receptor trafficking, ion channel signaling and other signal transduction system. PSD-95 binding to β1-AR results in inhibition of receptor internalization, which in turn affects the process that regulates resensitization, whereas binding of PDZ domain on β1-AR by WW And PDZ Domain Containing 3 (MAGI-3) initiated a signaling pattern but did not affect internalization, suggesting that the binding of PDZ domain on the receptor by different PDZ containing scaffolding proteins will elicit a specific transport for the receptor [27].

Once internalized, β-ARs undergo dephosphorylation in the endosomes by protein phosphatase 2A (PP2A) and are recycled to the plasma membrane [28]. Several studies have observed that sequestered receptors in the endosomal compartments are less phosphorylated than desensitized receptors on the plasma membrane. Moreover, isolated vesicles containing sequestered receptors showed higher phosphatase activity than plasma membrane, suggesting that internalization was required for dephosphorylation and functional resensitization [29-33]. However, it has been shown that blocking the internalization with inhibitors does not lead to a block of receptor resensitization [34]. To better understand if resensitization could occur at the plasma membrane, it has been demonstrated that inhibition of phosphorylated β-ARs internalization results in β-ARs dephosphorylation at GRK and PKA sites. Moreover, although the use of β-ARs agonists leads to a block of receptor internalization, β-ARs can still undergo dephosphorylation following selective PKA site phosphorylation which occurs at the plasma membrane under conditions precluding agonist-induced GRK phosphorylation, β-arrestin binding,

or internalization [35, 36]. Although inhibiting *β*-ARs internalization, agonist treatment had an effect also in GRK site dephosphorylation, albeit to a lesser extent. In these conditions, resensitization measured by AC activity occurred faster than the rates of PKA and GRK site dephosphorylation, suggesting that the rapid phase of resensitization occurs by the dissociation of arrestin after blockade of agonist stimulation and that the GRK site phosphorylation causes little desensitization, confirming a rapid dissociation of β-arrestin from the *β*-ARs after agonist removal. *In vivo* studies show that short-term desensitization of *β*-ARs is incomplete due to a continued balancing of resensitization that constantly restores the responsiveness of desensitizing *β*-ARs, indicating that internalization and resensitization due to dephosphorylation may be two independent events linked due to the absence of a blocking process [19] (Figure 3).

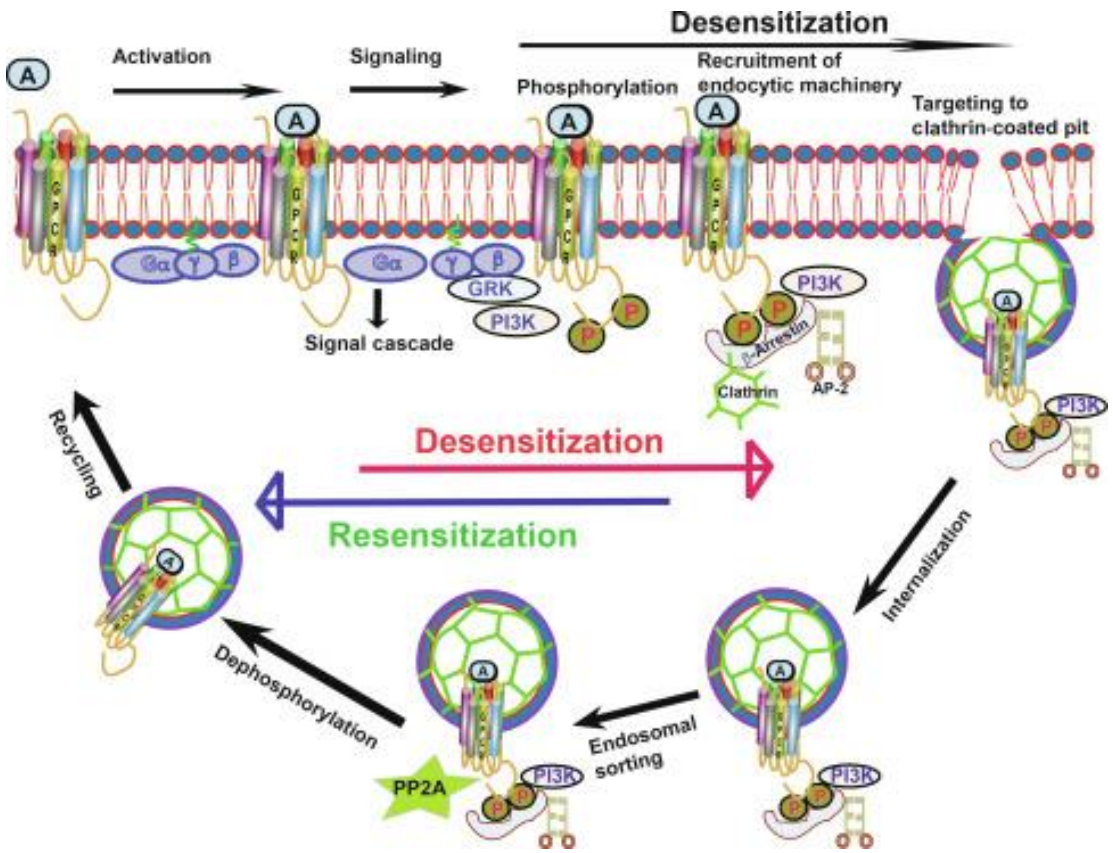

Figure 3. Classical view of *β*-ARs resensitization. Receptors on the cell membrane are phosphorylated (desensitized) in response to agonist stimulation, internalized by arrestin and

the internalization machinery, dephosphorylated (resensitized) in the endosomes, and subsequently recycled to the membrane as naïve receptors (taken from [37]).

Although the analysis of β-ARs dephosphorylation has been used to understand the receptor function, the mechanism underlying resensitization of β-ARs is poorly known. Recently, various studies have identified the A-kinase-anchoring protein 250 (AKAP250), also known as gravin or AKAP12, which acts as a scaffold protein that binds PKA, protein kinase C (PKC), and protein phosphatases, associating reversibly with the β-ARs and required for recovery from agonist-induced desensitization to occur. AKAP250 interaction with β-ARs increases with agonist stimulation recruiting PP2A to the receptor complex. Suppression of AKAP250 expression interrupts recovery from agonist-induced desensitization, indicating the role of these scaffold proteins in the organization of β-ARs signaling complex [38, 39]. Another AKAP associated with β-ARs is AKAP79 which influences β-ARs phosphorylation by complexing to PKC and the protein phosphatase 2B (PP2B or calcineurin). It has been shown that overexpression of AKAP79 with the β-ARs enhances receptor phosphorylation, whereas mutants of AKAP79, which fail to bind to PKA or to β-ARs, are ineffective in reducing phosphorylation. Moreover, AKAP79 regulates the ability of GRK2 to phosphorylate agonist-occupied β-ARs, enhancing receptor phosphorylation [40]. In addition, AKAP79/150, also known as AKAP5 has a central role in mediating the localization of second messenger kinases, such as PKA, PKC and PP2B, to the β-ARs at the plasma membrane, increasing receptor phosphorylation. Furthermore, it has been reported that PKA phosphorylation of the β-ARs promotes a receptor-regulated MAP kinase pathway [41]. In this context, suppression of AKAP79/150 results in loss of extracellular regulated kinase 1/2 (ERK1/2) activation and the ability of the cells to resensitize internalized desensitized β-ARs [42]. These studies suggest that dephosphorylation of β-ARs occurs due to factors present constitutively at the plasma membrane or recruited following agonist stimulation and represent a critical step in the regulation of receptor function.

Although the increasing studies in β-ARs resensitization, the mechanism that underlying this process is poorly understood. *In vivo* studies showed that downregulation of cardiac β-ARs can be prevented by inhibition of

phosphoinositide 3-kinase (PI3K) activity within the receptor complex since PI3K is necessary for *β*-ARs internalization. Cardiac-overexpression of a catalytically inactive PI3Kγ isoform and PI3Kγ knockout in mice prevents *β*-ARs downregulation despite the presence of cardiac stress. In contrast, *β*-ARs were desensitized in the wild-type controls indicating that the presence of active PI3K leads to significant *β*-ARs desensitization [43-45]. Based on these observations, it has been hypothesized that PI3Kγ negatively regulates *β*-ARs resensitization. However, a recent study reveals that pharmacological and genetic inhibition of PI3Kγ results in PP2A activation which, in turn, dephosphorylates *β*-ARs resulting in resensitization and maintenance of *β*-ARs function. Furthermore, since PI3Kγ is necessary for *β*-ARs internalization, inhibition of PI3Kγ attenuates *β*-ARs internalization, suggesting that receptors undergo resensitization at the plasma membrane [46].

1.2.2 *β*3-AR gene and protein

The adrenergic beta3 receptor (*ADRB3*) gene has been identified in various species, including mouse, rat, bovine, goat and dog [47-50]. In humans, *ADRB3* is localized on chromosome 8 and is identical for 81% to the mouse gene, with the highest homology in the transmembrane domain and the lowest in the third intracellular loop and C-terminal tail. However, the latter differs in sequence and length, ranging from 6 and 12 additional residues in human and mouse/rat, respectively. Moreover, the human and mouse *ADRB3* differs in the number of exons/introns. In particular, the human *ADRB3* comprises two exons and a single intron, whereas in mice, there are three exons and two introns. Sequence analysis of the human *ADRB3* identified regions in the intron that were homologous to the rat gene's second intron and second exon. In both species, exon 1 spans the 5' untranslated region and the major part of the coding block and utilizes homologous 3' acceptor sites of the final exon. However, in humans, exon 2 contains 19 bp of the coding region and the 3' untranslated region, while in mice it contains 37 coding nucleotides and 31 bp of 3' untranslated region. The rest is carried by exon 3. Although intron presence, no spliced variants have been described for the human *ADRB3*, while two have been identified in the mouse, which differs within the coding region [51-53].

ADRB3 encodes a single 408-amino acid residue-long peptide chain that shares approximatively 40-50% of amino acid sequence homology with *β*2-AR and *β*1-AR, respectively whit main differences located in the third intracellular loop and C-terminal tail, which contains an S-palmitoylation site on $Cys^{361/363}$ involved in G-protein coupling and AC activation. S-palmitoylation on $Cys^{361/363}$ of *β*3-AR is involved in both G-protein coupling, in receptor abundance and stability, and in mediating AC stimulation by the agonist bound receptor, leads to the promotion of various adjacent residues into the plasma membrane and forming an additional intracellular loop resulting in an active conformation for G-protein coupling. Recently, two new specific *β*3-AR S-palmitoylation sites on Cys^{153} and Cys^{292} within the second and third intracellular loops, respectively, have been described, which regulate membrane receptor abundance and stability [54]. Notably, based on the absence of threonine and serine residues sequences targeted by GRKs, and the lack of PKA phosphorylation on the third cellular loop and C-terminal tail in *β*3-AR that are present in *β1*- and *β*2-AR, *β*3-ARs have been assumed to be resistant to agonist-induced desensitization. Unlike *β*1-AR desensitization that occurs by internalization/degradation of the receptor, *β*3-AR desensitization occurs through downregulation of downstream components of the signaling pathway or mRNA regulation. It has been reported that a chimeric receptor constituted of a *β*3-AR with substitution of its third cytoplasmic loop and C-terminal tail for the corresponding region of the *β*2-AR in Chinese hamster fibroblast (CHW) and murine Ltk-cells (L cells), resulting in a less reduction in AC stimulation and a higher reduction in agonist potency, leading to the resistance to desensitization [55, 56]. Moreover, has been demonstrated a down-regulation of *β*3-AR mRNA expression due to changes in expression of functional receptor protein, indicating that the reduction in mRNA expression is caused by changes in transcription and not for mRNA stability. Several studies reconsidered the potential of *β*3-AR to be desensitized during prolonged agonist exposure. In hamsters treated for 6 days with *β1*-, *β2*- and *β*3-AR agonists, the responses to *β1*- and *β2*-AR were reduced, those to *β*3-AR were unchanged, indicating that in contrast to *β1*- and *β2*-AR, the *β*3-AR was refractory to desensitization [57]. In mouse ileum, treatment with *β*3-AR selective agonist reduced maximum relaxation in a time-dependent manner, indicating that the

occurrence of desensitization upon long-term stimulation but not shorter-time stimulation [58]. This feature contributed to making *β*3-AR an attractive therapeutic target suitable for chronic treatments in various diseases in which the *β*3-AR appears to be up-regulated, including heart failure.

1.2.3 *β*3-AR polymorphism

Each subtype of *β*-AR is known to have some recognized single-nucleotide polymorphism (SNPs) in humans. To date, only one major polymorphism has been described for the *ADRB3* at codon 64 at the beginning of the first intracellular loop, a tryptophan (Trp) is substituted by an arginine (Arg) (Trp64Arg), reducing the activation of *ADRB3*. This mutation occurs in approximately 8-10% of the Caucasian population, 20% in the Japanese population and 40% in the Alaskan population. Several groups reported homozygotes for Trp64Arg exhibited abdominal obesity and resistance to insulin, increased capacity to gain weight, earlier onset of type 2 diabetes and a lower resting metabolic rate, confirming the association of Trp64Arg polymorphism with disorders in different populations. Kurabayashi et al. investigated the relationship of Trp64Arg with obesity-related traits in 686 subjects in Australia and showed that female heterozygotes exhibit significantly increased total body weight and Body Mass Index, with an allelic frequency of 7.5% [59]. Two studies conducted with Chinese subjects confirm the direct involvement of Trp64Arg polymorphism in the development of obesity but not in diabetes, with a higher frequency in obese hypertensive male patients than in the non-obese hypertensive population and healthy controls [60, 61]. In Japanese, most of the subjects with the Trp64Arg polymorphism exhibit abnormal obesity and/or higher Body Mass Index, earlier onset of type 2 diabetes and hyperinsulinemia [62-64]. Moreover, it has been demonstrated that the Trp64Arg polymorphism had a positive correlation with insulin resistance. Considering that insulin resistance is associated with obesity, further analysis indicated that the association between Trp64Arg and insulin resistance was significant in obesity. Garcia-Rubi et al. have found that obese women with Trp64Arg polymorphism had greater insulin resistance than those without based on age, physical activity and body composition [65]. In addition to insulin

resistance, the Trp64Arg polymorphism is associated with insulin secretion. In a study of male twins who carried the Trp64Arg polymorphism, insulin resistance and secretion were significantly lower, without any effects in plasma glucose response [66, 67].

In addition to the association with obesity and type 2 diabetes, the Trp64Arg polymorphism has a prominent role in other disorders, such as hypertension, cardiovascular disease and overactive bladder. For example, a study based on meta-analysis revealed that Trp64Arg polymorphism was associated with the significantly increased risk of hypertension, and particularly, the heterozygotes carry were 1.23-times more likely to develop hypertension than the homozygote carries [68]. Recently, a study based on meta-analysis reveals the role of Trp64Arg polymorphism in the development of hypertension in Chinese and Caucasian populations. The meta-analysis study including 9555 patients showed a significant relationship between *ADRB3* Trp64Arg polymorphism and hypertension in the whole population had been described, especially in the Chinese and Caucasian population [69].

Another study conducted with 218 women showed that both heterozygous and homozygous carries of Trp64Arg polymorphism were associated with overactive bladder [70]. However, some studies report no correlation between Trp64Arg polymorphism and overactive bladder. Indeed, although the Trp64Arg allele was reported to be significantly more frequent in subjects with overactive bladder than in those without, no significant association was detected between Trp64Arg and lower urinary tract function in a cohort of more than 1000 men [71]. This may be because, clinically, Trp64Arg is considered to encode a hypofunctional variant of the receptor-associated with reduced bladder compliance, suggesting that the polymorphism may have functional relevance in a situation when it is activated such as overactive bladder syndrome.

Although several studies have reported a correlation between Trp64Arg polymorphism of *ADRB3* and various disorders, many studies showed no association due to significant differences between subjects with Trp64Arg polymorphism and controls. These different results may be due to the number

and ethnic origin of the subject's studies, and interaction between Trp64Arg polymorphism and variants in other genes [72].

Furthermore, a strong linkage between the Trp64Arg polymorphism and other polymorphic variants of the same gene or other genes has been shown. It has been identified a linkage between the occurrence of Tpr64Arg polymorphism and the Gln27Glu *ADRB2* variant. The Gln27Glu polymorphism consists of the substitution of glutamine (Gln) for glutamate (Glu) at protein position 27 of the *ADRB2*. A study carried out on 1054 diabetic and non-diabetic subjects revealed that homozygote subjects for the low-risk alleles Glu27 in the *ADRB2* and Trp64 in the *ADRB3* had a lower prevalence of diabetes than subjects with other genotype combinations [73]. In addition, it has been shown that the Gln27Glu *ADRB2* and the Trp64Arg *ADRB3* polymorphisms affect gain in body weight or blood pressure elevation in male subjects who were previously non-obese. Notably, the subjects carrying the polymorphism of Glu27 and Trp64 alleles show higher frequency in those who had significantly gained weight or blood pressure elevation over 5 years [74]. Other than this association, Trp64Arg polymorphism has been reported to be associated whit several noncoding variants in the *ADRB3* intronic region or 3'-UTR and 3'-downstream region that possibly affect transcription of the gene and the stability of the mRNA transcript, influencing receptor expression [71, 75]. Moreover, various studies reported the association of Trp64Arg polymorphism with SNPs in other genes, such as lipoprotein lipase (*LPL*), type 2 deiodinase (DIO2) and Mitochondrially Encoded NADH:Ubiquinone Oxidoreductase Core Subunit 2 (MT-ND2) genes that are critical in lipid and energy metabolism [76-78].

Various in vitro studies have been performed to understand the effect of Trp64Arg polymorphism on the metabolic function of *β*3-AR. In CHO-K1 and HEK293 cells, polymorphism of ADRB3 results in reduced maximal cAMP accumulation independent of G_i coupling under stimulation of *β*3-AR agonists [79]**.** Similarly, in 3T3-l1 and rat insulinoma cells, the mutant receptor is less responsive to *β*3-AR agonists with lower maximal cAMP accumulation [80, 81]. In contrast, Vrydag et al. reported no difference in cAMP accumulation and receptor desensitization between Trp64Arg polymorphism of *ADRB3* and the wild-type receptor upon agonists stimulation in CHO-K1 and HEK293 cells [82].

Besides Trp64Arg polymorphism, other SNPs and mutations have been identified in the coding region of *ADRB3*, which results in being associated with human diseases. It has been reported a very rare SNP in the intracellular loop 3 of the receptor, which consists of the substitution of threonine (Thr) with methionine (Met) at protein position 265 (Thr265Met) of *ADRB3*. Teitsma et al. described a leucine (Leu) substituted with phenylalanine (Phe) at protein position 306 (Leu306Phe), which is involved in catecholamine binding [71]**.** Recently, a study carried out in 1337 healthy Chinese healthy subjects and related patients identified two other SNPs in the coding region that are significantly higher in the patient's group compared to control: a substitution of serine (Ser) with proline (Pro) at protein position 165 (Ser165Pro) and 257 (Ser257Pro). These two polymorphisms reduce receptor function lead to lower fasting, insulin resistance, and the development of type 2 diabetes [83]. Furthermore, two studies have reported SNPs in the noncoding region of *ADRB3*. Voruganti et al. showed that SNP rs35361594 in the 5'-UTR could be involved in the development of obesity since this SNP shows an association with Body Mass Index and percentage of fat [84]. In addition, SNP rs4998 in the 3'-UTR of *ADRB3* has been found to be associated with Alzheimer's disease [85]. The Trp64Arg polymorphism, in combination with Thr265Met and Leu306Phe variants, affects ligand binding, function and regulation of receptor responsiveness [82]. A functional study regarding the association of Ser165Pro and Ser257Pro polymorphism with type 2 diabetes in the Chinese population has been proposed. Huang et al. showed that these two variants do not affect receptor expression and trafficking but impair cAMP accumulation in response to different concentrations of *β*3-AR agonist in HEK293 and CHO-K1 cells. It is hypothesized that Ser165Pro and Ser257Pro, preferentially affect receptor interaction with G_s protein rather than G_i protein, leading to impaired cAMP signaling [83].

1.2.4 Pharmacology of the *β*3-AR

Several studies have helped identify and define the *β*3-AR pharmacological response to develop agonists and antagonists of *β*3-AR. However, in general, the affinity, selectivity and potency of the *β*3-AR agonist and antagonist widely

vary between species due to differences in the β3-AR amino acid sequences and levels of expression. In humans, β3-AR has emerged as a novel potential target for treating several pathologies, such as obesity, type 2 diabetes, heart failure, overactive bladder and preterm labor.

β3-AR agonists

Besides endogenous ligands, β3-AR is activated with high affinity and potency by two main classes of preferential antagonists, which differs according to the time of their discovery: the first-generation compounds such as BRL37344 and 5-(2-[[2-(3-chlorophenyl)-2-hydroxyethyl]-amino]propyl)1,3-benzodioxole-2,2-dicarboxylate (CL316243) were developed in the 1990s. In contrast, the second-generation such as mirabegron (YM178), solabegron (GW427353), ritobegron (KUC-7483) and amibegron (SR58611A) were improved later [86].

BRL37344 is the most used β3-AR agonist in human and mouse models. The affinity for β3-AR and the potency, as measured as the ability to stimulate AC, is higher in rodents than humans. Various studies have reported the high potency of BRL37344, which is similar to the selective agonist mirabegron on human bladder strips, and the higher selectivity for β3-AR whit respect to β1- and β2-AR [87, 88]. In addition, BRL37344 was recently used to corroborate the hypothesis that β3-ARs are involved in the protection against myocardial infarction injury, in the relaxation of corpus cavernosum and detrusor smooth muscle, liver steatosis and inflammation associated with nonalcoholic fatty liver disease (NAFLD) [89-91].

CL316243 exhibits the lowest potency but good selectivity for the human β3-AR than β1- and β2-AR, and it has been used in the relaxation of urinary bladder strips, in skeletal muscles where improve muscle force production and skeletal muscle strength and in the relaxation of endothelium during vascular complication of diabetes [92-94].

Second-generation agonists have been tested for their abilities to induce human detrusor relaxation in adults with overactive bladder and is currently the most promising agent in over 30 years. Recently, mirabegron has also been investigated in pediatric patients with neurogenic detrusor overactivity (NDO)

and received the first approval in patients aged 3 years or older [95]. This drug has been extensively studied with Phase II and Phase III trials worldwide, showing a good balance between efficacy and tolerability [96]. Mirabegron was approved in Japan, the United States and Canada for the treatment of overactive bladder, and in Europe in 2013. Solabegron has been found to relax isolated human bladder strips at low concentrations and reduce detrusor spontaneous contractile activity by almost 80% [97]. Amibegrom was first described for its inhibitory effects on colon motility in rats and later for its potential use as an antidepressant and in the reduction of portal pressure in a mouse model [98-100].

*β*3-ARs antagonists

Two of the most used *β*3-AR antagonists are SR59230A and L748337. SR59230A has been reported to improve ventricular function in pulmonary arterial hypertension in a mouse model [101] and reduce the induction of lipolysis, the stimulation of AC, and the increase of cAMP in isolated murine adipocytes [102]. Moreover, it has been reported that SR59230A can promote the differentiation of progenitor cells in hematopoietic tumors. Calvani et al., reported that SR59230A treatment promotes hematopoietic differentiation by increasing the ratios of lymphoid/hematopoietic stem cells and myeloid progenitor cells/ hematopoietic stem cells, the number of granulocytes precursors, and inducing the mesenchymal stem cells differentiation into adipocytes of melanoma cells [103].

L748337 is a selective *β*3-AR antagonist with higher selectivity for *β*3-AR whit respect to *β*1- and *β*2-AR [104], and it has been reported to increase cAMP in CHO cells expressing *β*3-AR, leading to induction of thermogenesis and lipolysis [105].

1.2.5 *β*3-ARs function and expression

Since its discovery, *β*3-AR has been detected in several human tissues such as adipose tissue, myocardium, urinary bladder, retina and brain, suggesting that *β*3-AR is an important regulator of various physiological functions (Figure 4). *β*3-ARs are expressed predominantly in rodent white (WAT) and brown (BAT)

adipose tissue, where it mediates lipolysis and thermogenesis triggered by the sympathetic nervous system [47, 106]. In humans, β3-AR expression appears to be lower when compared with rodent adipose tissue [51].

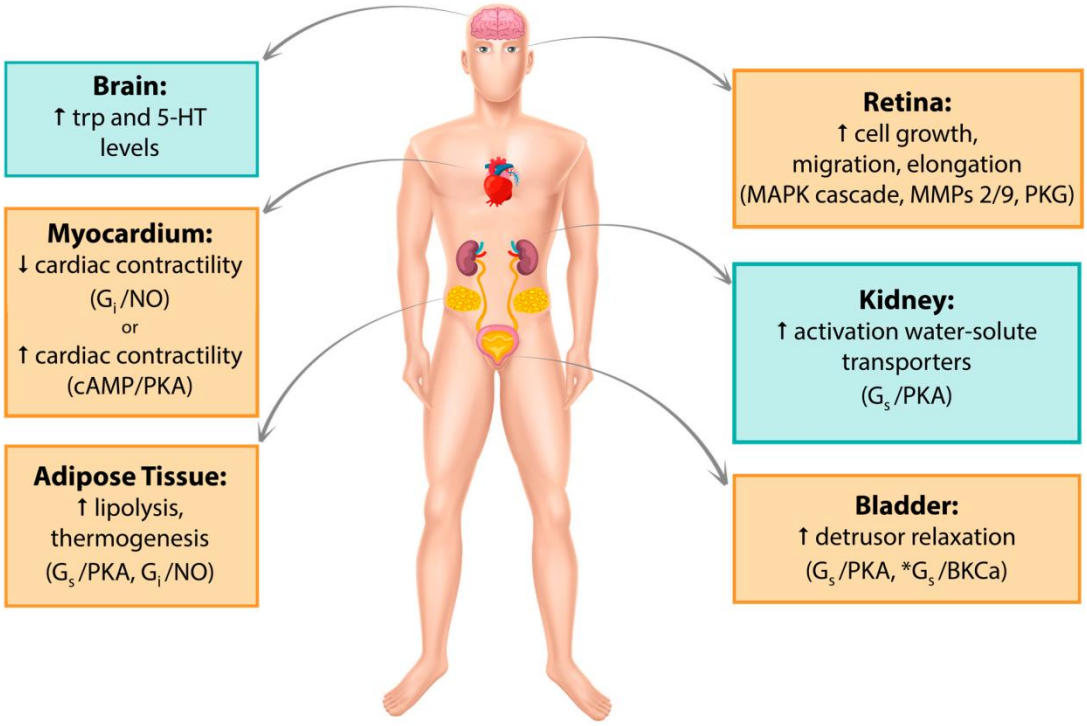

Figure 4. Graphic summary of β3-ARs localization. Pathway studied in human tissues and cell lines are in the yellow boxes. Pathway studied in mouse are in the blue boxes (taken from [107]).

Norepinephrine-mediated β3-AR activation results in the coupling of β3-AR to the G_α subunits and induces the activation of the cAMP-PKA axis, which stimulates lipolysis of lipid droplets protein as hormone-sensitive lipase (HSL) and perilipin in the adipocytes. However, HSL activation can also be triggered by β3-AR coupling to G_i and consequent activation of the ERK1/MAPK signaling, resulting in the hydrolysis of triglycerides stored in the lipid droplets and the release of free fatty acid (FFAs). In brown adipocytes, FFAs activate Uncoupling-Protein 1 (UCP1) in mitochondria, inducing thermogenesis. Moreover, β3-AR activation can induce lipolysis by increasing the expression of the inducible nitric oxide synthase (iNOS) and, in turn, nitric oxide (NO) levels in a PKA-dependent manner [108]. Recently, β3-AR activation seems to be involved in the generation of hyperthermia arising from WAT lead to tissue remodeling and impairment in

triglyceride storage capabilities [109]. β3-AR knock-out mice showed impaired cold-induced thermogenesis with a reduction in white adipocytes, according to the observation that β3-AR activation induces transdifferentiation of mature white adipocytes. β3-AR KO mice also show a compensatory overexpression of β1-AR in WAT and BAT and can survive cold exposure through β1-AR-mediated thermogenesis and UCP1 increase [110].

In humans, the β3-AR expression level is reduced in obese patients, raising the interest in developing compounds for the treatment of type 2 diabetes. Unfortunately, clinical studies have shown poor selectivity of the drugs for the human β3-AR, and no agonist has overcome beyond phase II clinical trials [111-113]. Recently, a clinical study investigated the use of mirabegron in patients with detectable cold-activated BAT. Mirabegron induced BAT activation and increased resting energy expenditure via cardiovascular stimulation and BAT activation [114].

The human β3-AR was first identified in human cardiac biopsies in 1996 [115]. Under physiological conditions, β3-AR is expressed at low levels in myocardial tissue compared to β1- and β2-AR. During diseases, including failing heart, the expression of β3-AR results to be upregulated, while β1-AR is downregulated, and β2-AR remains stable but is functionally desensitized [116, 117]. After catecholamines stimulation of β3-AR, PKA phosphorylates Ca^{2+} handling proteins in the myocardium leading to positive ionotropic and chronotropic effects. Moreover, in the heart, the stimulation of β3-AR leads to increased endothelial NO synthase (eNOS) or neuronal (nNOS) activation, inducing NO generation and activation of cGMP and cGMP-dependent protein kinase G (PKG) activation. PKG is a serine/threonine kinase that mediates the biological effects of NO/cGMP. PKG downstream of β3-AR enhances myocytes' relaxation, resulting in a cardioprotective mechanism that can be beneficial in failing myocardium [118].

Evidence has reported that the β3-AR has specific beneficial effects in the cardiovascular system, including cardioprotection [119]. However, chronic exposure of the heart to high levels of catecholamines can lead to progressive deterioration of cardiac function and structure. β3-AR desensitization represents a protective mechanism at lower catecholamines stimulation, but chronic

stimulation can cause β1- and β2-AR dysregulation and promote the progression of the disease [120]. However, β3-ARs are not subject to desensitization and downregulation, and their levels within the failing human heart remain unchanged or become upregulated. Therefore, this mechanism could represent either a protective process against the effects of chronic β3-AR stimulation or a mechanism that may lead to deterioration of the heart. Some reports have suggested that sustained activation of β3-AR in failing hearts could contribute to impaired cardiac function [121]. A potential strategy proposed against failing heart development has resulted in being the use of β3-AR antagonists. In contrast, it has been demonstrated that in the failing myocardium, β3-ARs are able to inhibit the accumulation of Na^+ in cardiac myocytes leading to a block of cAMP generation and reducing the activation of cAMP-downstream oxidative pathways [122]. Accumulating evidence supports the idea that overexpression or persistent activation of β3-AR has a cardioprotective effect and can attenuate pathological left ventricular hypertrophy induced by activation of NOS and subsequent NO generation responsible for β3-AR-induced cardioprotection in mice [123].

Since 2007, various studies have investigated the relationship between β3-AR and β-blockers and proposed that β1-AR blockers and their protective effects in heart failure could induce enhancement of β3-AR expression and protection signaling [124], [117]. Moreover, it has been recently showing the potential of the selective β1-AR blocker nebivolol as a β3-AR blocker. In particular, nebivolol administration activated β3-AR leading to a significant reduction of infarct and cardiac fibrosis and improved cardiac function [125, 126].

The evidence of the expression of the β3-AR transcript was first reported in the detrusor smooth muscle, and protein was first described in the detrusor and urethelium, where it predominantly mediates the relaxation of the detrusor muscle [127, 128]. The first studies conducted in human detrusor muscle strips showed bladder relaxation following the use of β3-AR agonists, indicating that the β3-AR activation in the bladder represents the most relevant mechanism to increase bladder capacity without affecting bladder contraction [129-131]. Few information regarding β3-AR presence in the kidney has been reported.

Recently, it has been demonstrated the presence of β3-AR in the mouse nephrons. The use of BRL37344 in isolated kidney tubules and slices from wild type and β3-AR knock-out mice showed that β3-AR coupling to G_s/AC had a positive effect on water and solute transporters, indicating a role of β3-AR in renal homeostasis [132]. Various evidence showed the presence of β3-AR also in the lower urinary tract where undergoes expression changes due to ureteral stenosis, chronic kidney disease, or carcinoma [133, 134].

β3-ARs are also expressed in different human brain regions, such as the hippocampus and frontal cortex [135]. Given the involvement of β3-AR in the regulation of depressive states, the administration of amibegron has been demonstrated to have anxiolytic-like effects in rats [136]. In addition, the treatment with amibegron increased 5-hydroxytryptamine (5-HT) levels and noradrenaline release via activation of β3-AR [137]. Improving evidence has shown the involvement of β3-AR in memory consolidation, a process that required both modulations of hippocampal neuron excitability and activation of brain glucose metabolism. Notably, the administration of β3-AR antagonist in chicks enhanced memory and learning by increasing glucose uptake via GLUT3, suggesting that β3-AR also modulates glucose uptake [138].

β3-ARs also exert antiangiogenic and vasorelaxant effects in the retina blood vessels and retinopathies. β3-AR stimulation with BRL37344 increased vascular endothelial growth factor (VEGF) release in hypoxic conditions, while treatment with β3-AR antagonist prevented VEGF increase in the same conditions, indicating a potential role for β-blockers in the treatment of retinal diseases [139]. In contrast, non-selective inhibition of NOS abolished BRL37344-induced VEGF increase while supplementation of NO bypassed the beneficial effect of the β3-AR blockade, suggesting NO as a key effect in this pathway [140].

1.2.6 β-ARs and cancer

Recently, it has been widely demonstrated the role of β3-AR in sustaining the pathogenesis of various cancer types, from benign tumors, such as the infantile hemangioma [141, 142], to several malignant cancer types, including melanoma [143], breast cancer [144], ovarian cancer [145], lung carcinoma [146] and some

pediatric cancers, like neuroblastoma [147] and Ewing sarcoma [148]. Several studies have investigated the relationship between *β*3-AR and tumorigenic processes such as cellular proliferation and apoptosis, angiogenesis and vasculature normalization, which are important in cancer cell invasion and metastasis during cancer development, and the influences of *β*3-AR on energy metabolism and immune system (Figure 5).

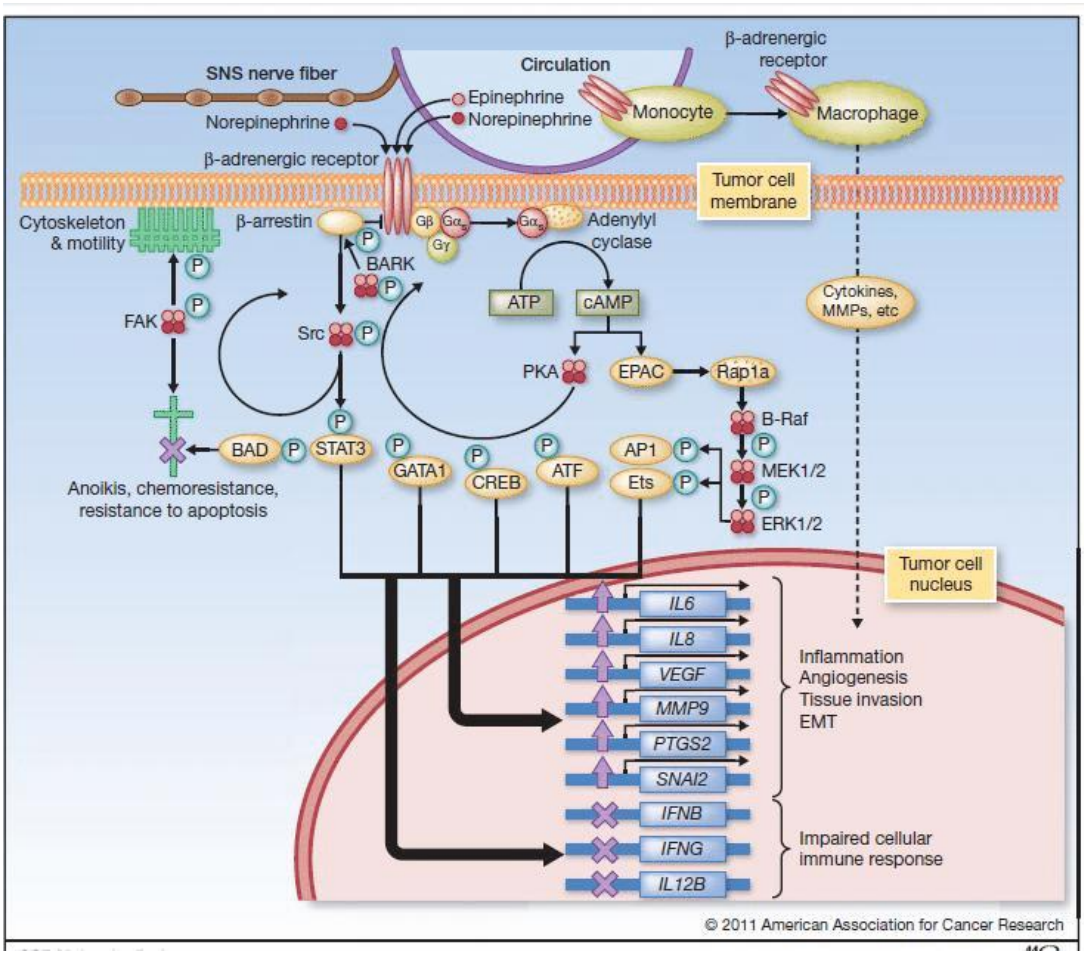

Figure 5. The *β*-ARs signaling pathway in cancer. Abbreviations: ATP: adenosina triphosphate, cAMP: cyclic adenosine monophosphate, IL6: interleukin 6, IL8: interleukin 8, IL12B: interleukin 12B, PKA: protein kinase A, EPAC: Exchange Protein activated by Adenylil Cyclase, FAK: Focal Adesion Kinase (taken from 147).

The relationship between stress, chronic depression, and other psychological factors, and tumor onset has been demonstrated in the last years through various experimental and clinical investigations [149, 150]. The *β*-adrenergic system mediates sympathetic nervous system (SNS)-induced fight-or-flight responses lead to the release of catecholamine norepinephrine, whose concentration increase in response to physiologic, psychologic, and environmental threats to homeostasis [151]. The catecholamines epinephrine and norepinephrine are stress hormones released in a stress reaction that induce an increase in heart muscle contraction, dilatation of airways, and glycogen broke down. Notably, SNS and catecholamine exert pro-tumorigenic actions through the modulation of *β*-ARs, which in turn affect numerous biological processes related to cancer progression and metastasis, such as tumor cell proliferation, invasiveness, vascularization, and migration [152]. *In vivo* models have shown the ability of *β*-ARs agonists to enhance tumor metastasis, corroborating the involvement of *β*-ARs in cancer biology [153-155]. In contrast, *β*-ARs antagonists have been found to block stress-induced enhancement of tumor progression in various cancer types, including leukemia [156], melanoma [157], breast [153], and prostate cancers [154]. Besides the direct effects on tumor cells, *β*-ARs are involved in regulating pathways of non-tumoral cells of tumor microenvironment [158].

The first report showing that *β*3-AR influences the risk of cancer, suggested that the Trp64Arg polymorphism decreased the risk of breast cancer in Japanese woman. In particular, a woman who simultaneously carried the association of Trp64Arg polymorphism of *ADRB3* and the Gln27Glu polymorphism showed a markedly reduced risk for breast cancer, with an odds ratio of 0.37 even if not statistically significant [159]. Another study conducted on 169 subjects has reported an association between the Trp64Arg polymorphism and endometrial cancer in overweight/obese patients, suggesting involvement of *β*3-AR cancer biology [160]. Perrone M.G. et al., for the first time, have described a significant up-regulation of *β*3-AR mRNA, compared to *β*1- and *β*2-AR mRNA in patients operated for colorectal carcinoma [161]. Interestingly, Magnon et al., have investigated the role of SNS in prostate cancer

development. To assess the contribution of β-ARs in tumor development, the human prostate PC-3 cell line was injected into the prostate of mice genetically deficient for β2-, β3-, or both β2- and β3-ARs. Whereas tumor development was slightly delayed in mice lacking a single adrenergic receptor, it was severely compromised in both ADRB2-/- and ADRB3-/- mice. Moreover, tumor dissemination into the lymph nodes and distant organs was significantly reduced in the double knockouts. These results were confirmed by using human prostate LNCaP cell line in the same animal model, indicating that both β2- and β3-ARs expressed in stromal cells of the tumor microenvironment appear to be critical for the tumor development in this mouse model [162]. In the last few years, β3-AR mRNA and protein have found expressed in various cancer types, including infantile hemangioma, breast cancer, acute lymphoblastic leukemia, lung carcinoma, and thyroid carcinoma, confirming the hypothesis that β3-AR could play a role in the onset and progression of multiple cancers [163-165]. Recently, several studies have reported the expression of β3-AR in melanoma. Dal Monte et al., have demonstrated for the first time the involvement of β3-AR in melanoma growth and vascularization, using murine melanoma B16-F10 cell line injected in C57BL mice and treated with β3-AR antagonists. Tumor cell proliferation and growth were reduced, while apoptosis was increased after administration with SR59230A and L-748,377 [166]. In addition, the use of β3-AR blockers was able to reduce tumor vasculature through apoptosis of endothelial cells, suggesting that β3-AR is necessary for the proliferation and survival of melanoma cells [167]. The effect of β3-AR modulation on melanoma cell proliferation and survival was found mediated by iNOS. The treatment with β3-AR blockers reduced iNOS expression and NO levels, suggesting that NO mainly produced by iNOS represents a major downstream effector of β3-AR in melanoma [168].

Interestingly, the treatment with β3-AR antagonists leads to inhibition of melanoma cell proliferation either in the presence or not of noradrenaline stimulation, indicating a partial constitutive β3-AR activity in melanoma cells, which was previously reported [166, 169]. β3-AR was found expressed in different stromal cells of the tumor microenvironment, including cancer-associated fibroblasts (CAFs), endothelial cells, and macrophages. Calvani et

al., showed the ability of primary melanoma cells to recruit stromal cells in response to ligand activation of β3-AR and in eliciting stromal reactivity, to sustain secretion of proinflammatory cytokines, and to drive de novo angio/vasculogenesis. In addition, β3-AR appears to be responsible for instructing melanoma cells to respond to environmental cell signals and induce CAFs and macrophages to enhance their motility and stem-like straits [170]. The β-adrenergic system has been identified as a regulator of the immune system. The use of the β3-AR antagonist SR59230A, and siRNA targeting of β3-AR, injected in B16-F10 melanoma-bearing mice, indicated an involvement of β3-AR in the regulation of the immune-tolerance in the melanoma microenvironment. In particular, the β3-AR antagonist increased the number of natural killer (NK) and $CD8^+$ cells as well as their cytotoxicity, M1/M2 macrophages ratio and N1 granulocytes, while abrogated Treg and MDSC subpopulations in the tumor microenvironment. The reduction of the immune-suppressive and the increase of the immune-competent subpopulation cells in the tumor microenvironment suggests a role of β3-AR in promoting of immune tolerance in melanoma [171]. Recently, it has been demonstrated that in murine B16-F10 melanoma-bearing mice, the pharmacological β3-AR blockade was able to attenuate the expression of stemness markers, such as CD44, NANOG, OCT3/4 and CD24, and to induce MSCs differentiation in adipocytes and a differentiated phenotype of numerous hematopoietic progenitors recruited in the tumor microenvironment. Thus, targeting the metastatic potential of melanoma using β3-AR blockers could represent an efficacious strategy to counteract the progression to advanced states of this malignancy [103]. Induction of β3-AR protein expression during hypoxia has been reported in murine B16-F10 and human A375 melanoma cells [166], [170]. Hypoxia is a condition of solid tumors, including melanoma, that reduces in the normal level of tissue oxygen tension, contributing to the malignant phenotype and to aggressive tumor behavior. The induction of β3-AR expression in a hypoxic microenvironment suggests that melanoma cells exploit the activation of β3-AR to acquire aggressiveness features required in the tumorigenic process [172].

Clinical investigations of β3-AR expression in melanoma patients are not still available. However, the expression of β3-AR has been confirmed in melanoma

biopsies from different patients. Immunohistochemical analysis for β3-AR expression in melanoma biopsies, including *in situ* primary melanoma, common and atypical melanocytic nervi, nodular melanoma, superficial spreading melanoma and cutaneous and lymph-nodal metastatic melanoma, showed that all examined melanocytic lesions expressed β3-AR higher than benign lesions [170]. β3-AR was also found to be also expressed in stromal, inflammatory and endothelial cells of the tumor microenvironment, suggesting that β3-AR expression correlates with melanoma malignancy features in human melanocytes lesions. Recently, a preliminary clinical investigation of β3-AR expression has been conducted in Ewing Sarcoma patients. Clinical data have shown β3-AR expression on peripheral blood of all patients with no statistical differences between the metastatic and non-metastatic patients. In addition, a higher β3-AR expression was shown in the surface of bone marrow and microenvironmental cells of metastatic patients compared to a lower expression in non-metastatic patients, suggesting a possible role of β3-AR as a new marker for the prediction of recurrence or disease severity in Ewing Sarcoma patients [173]. Bruno et al., demonstrated that β3-AR is constitutively expressed in both murine and human neuroblastoma cell lines and in tumor biopsies from neuroblastoma patients. In this study, the pharmacological antagonism of β3-AR was able to reduce tumor growth by affecting the neuronal differentiation of neuroblastoma cancer cells through its functional cross-talk with sphingosine kinase 2 (SK2)/sphingosine 1 phosphate receptor 2 ($S1P_2$) axis. Since the available therapies are still not compelling enough for metastatic neuroblastoma, the crucial role of β3-AR in regulating neuroblastoma tumorigenesis may have implications for therapeutic purposes [147].

1.2.7 β3-ARs and oxidative stress

The relationship between β3-AR and reactive oxygen species (ROS) production has recently been evidenced in various physiological and pathological diseases. Studies have reported an essential role of ROS in modulating adrenergic function. Increased ROS production following β-AR activation contributes to altering downstream signals and a feedback loop that mediates receptor phosphorylation and internalization [174, 175]. As previously reported, β3-ARs

are upregulated in failing hearts, representing a potential target for the treatment of cardiovascular diseases. It has been demonstrated that β3-AR stimulation leads to an Akt/PKB-dependent phosphorylation of $eNOS^{Ser117}$ associated with dephosphorylation of $eNOS^{Ser114}$. The complementary alteration of these two sites leads to NO release in the cardiac myocytes of human nonfailing ventricular myocardium [176]. The antioxidant effects of β3-ARs were also observed in the myometrium. β3-AR stimulation exhibits dual antioxidant proprieties by directly inhibiting NADPHoxidase activity and inducing the expression of catalase, an enzyme that plays an endogenous antioxidant role. In addition, β3-AR exerts an anti-inflammatory effect since its functional expression in the human macrophages, confirming the protective role of β3-AR in the human myometrium [177]. In the last few years, various studies have reported the involvement of β3-AR in the modulation of NO release, contributing to tumor growth and metastatic process in various cancer types [178]. Different works have associated reduced NO levels with decreased growth of melanoma cells, whereas increased NO levels promote melanoma growth. Sikora et al., showed that targeting iNOS in NOD/SCID mice bearing mel624 xenografts model inhibited iNOS-dependent NO production and suppressed melanoma growth, associated with a decrease in tumor vessels and increased number of intratumoral apoptotic cells. In addition, a combination of iNOS inhibitor with cisplatin, enhanced cytotoxic therapy of melanoma, suggesting a promising approach to melanoma and other solid tumor therapy [179]. The first report showing the antioxidant effect of β3-AR suggested the involvement of iNOS in the antitumoral effects exerted by pharmacological β3-AR blockade in melanoma cells. In particular, the use of β3-AR antagonist induced a reduction of iNOS expression, resulting in a decreased activity in the NO pathway, leading to a reduction of melanoma tumor growth [166]. Pharmacological inhibition of β3-AR inhibited iNOS expression by reducing the basal nitrite production, while β3-AR stimulation increased this production by activation iNOS expression. Moreover, β3-AR blockade effects were prevented by NOS activation, and β3-AR activation effects were prevented by NOS inhibition, indicating that iNOS-induced NO production is a crucial event in melanoma growth and that β3-AR could regulate melanoma cell proliferation and survival through the NO pathway

[168]. Yoshioka et al., showed that treating human U-251 MG astrocytoma cells with norepinephrine leads to an increase in intracellular glutathione concentration by inducing glutamate-cysteine ligase catalytic subunit (GCLc) protein. This increase was inhibited by SR59230A, while the treatment with β3-AR agonist increased the intracellular GSH in U-251 MG cells, indicating that norepinephrine increased the GSH concentration in astrocytes by inducing GCLc protein via β3-AR stimulation [180].

Recently, has been identified a relationship between nutraceutical compounds, mitochondrial ROS production, and β3-AR expression in human A673 Ewing Sarcoma cells. Bioactive nutraceutical compounds with antioxidant activity have recently attracted the attention as a supplement used during cancer treatments; *in vitro* and *in vivo* experiments have demonstrated the efficacy of nutraceutical compounds in the inhibition of different pathways involved in tumorigenesis, angiogenesis, and metastasis in pediatric and adult cancers [181, 182]. In particular, the intracellular expression of mitochondrial ROS (mtROS) was low in Ewing sarcoma cells treated with prosurvival antioxidants, such as ascorbic acid, flavon, capsaicin and formononetin, and was increased when Ewing sarcoma cells were treated with curcumin, retinoic acid, gingerol and genistein. Interestingly, A375 cells treated with curcumin, retinoic acid, gingerol and genistein showed reduced cell survival and β3-AR expression, while no change in cell viability but upregulation of β3-AR was observed in A375 cells treated with prosurvival antioxidants compounds, indicating that since β3-AR is expressed in mitochondria, it may drive mitochondrial bioenergetics and redox state of the cells inducing or not cell survival under nutraceutical treatment [183]. These results suggest that β3-AR may be considered one of the regulators of cellular response to oxidative stress. Thus, inhibiting β3-AR could dramatically increase ROS levels lead to cell death due to the inhibition of antioxidant response.

1.3 Osteosarcoma

Childhood cancers comprise less than 1% of all new cancer diagnoses each year and represent the second leading cause of death in children. The 5-year

survival of children and adolescents diagnosed with cancer is approximately 80% in many high-income countries because of the access to modern treatments and supportive care. Unfortunately, only 40% of children who live in low- and middle-income countries tend to survive 5 years after diagnosis [184]. Among pediatric cancers, leukemia is by far the most common, representing about 28% of childhood cancers, brain tumors represent about 27%, lymphomas about 12% and certain bone cancers, such as osteosarcoma and Ewing sarcoma, represent approximately 4% [185].

Osteosarcoma (OS) is the most common primary malignant tumor of bone in children and young adults and the eighth-most frequent childhood cancer. Osteosarcoma accounts for 20% of all primary malignant bone tumors, with a worldwide incidence of 3.4 per million people per year [186, 187]. Osteosarcoma has an annual incidence of 4.1 cases per million children under the age of 15 years [188, 189] and 5.0 cases per million for the range 0-19 years, with approximately 400 new cases diagnosed each year in the United States [190]. Osteosarcoma has characterized by a bimodal age distribution; the first peak occurs during adolescence, and the second occurs in older adults. Osteosarcoma is rare in children younger than 5 years of age, representing 2% of osteosarcoma patients. The first peak incidence of osteosarcoma ranges between 10 and 14 years of age, coinciding with the puberal growth spurt, followed by an incidence decline. The second peak of incidence occurs in adults older than 65 years, representing a second malignancy, frequently related to Paget's disease that is a disorder of the bone remodeling process. The incidence rate is higher in males (5.4 cases per million) than in females (4.0 cases per million) [191], and are different across the world regions and ethnicities, whit rates ranging from 5.2 per million in African Americans to 4.6 per million in white children. The highest incidence of osteosarcoma is reported in Hispanic patients (6.5 per million) between 15 and 29 years of age and the lowest is in white [187]. According to the stage of the disease, the general overall 5-year survival rate for children aged 0-19 with osteosarcoma is 68%. If osteosarcoma is diagnosed and treated before its spreading outside the bone, the 5-year survival rate is 74%, while it is 66% if osteosarcoma has invaded other tissues and/or regional lymph nodes, and it is reduced to 27% if the tumor

has metastasized distant tissues or organs of the body. The 5-year survival rates for patients younger than 45 years of age with osteosarcoma was greater than 65% but continued to be less than 45% for the 45 years and older age group. The lower 5-survival rate (19-39%) has been observed in Estonia, Slovakia and Denmark [192], while the highest (58%) has been reported in Finland [193]. In Italy, the 5-year survival rate was 57% for patients of all ages, 68% for those younger than 41 years, and 22% for patients older than 65 years [194, 195].

Numerous studies have established a correlation between rapid bone growth during puberty and osteosarcoma development. Bone is a mineralized connective tissue that exerts important functions, including locomotion, support and protection of soft tissues, harboring bone marrow, and calcium and phosphate storage [196, 197]. Bones are present in the body in different sizes and shapes. A long bone consists of two main regions: the diaphysis and the epiphysis. The diaphysis is the tubular part between the proximal and distal ends of the bone, containing the medullary cavity filled with yellow bone marrow in an adult. The outer of the diaphysis is composed of dense, compact bone called cortex or cortical bone. The epiphysis consists of the wider section at each end of the bone filled internally with spongy bone, another type of osseous tissue. Each epiphysis is connected to the diaphysis through the metaphysis. The latter contains the site of long bone elongation, which is present during growth and is called epiphyseal plate. In adulthood, when the bones stop growing, the epiphyseal plate becomes the epiphyseal line. Inside the bone is present a layer of bone cells, called endosteum, which contains the bone cells responsible for bone growth, repair and remodel. These cells are part of the outer double layered structure called the periosteum that contains blood vessels, nerve and lymphatic vessels. Except for the region where the epiphysis meets other bones, which is covered by the articular cartilage, the periosteum covers the entire surface of the bone. In addition, the periosteum is the attachment site for tendons and ligaments (Figure 6). Osseous tissue is a connective tissue that contains few cells and a large amount of extracellular matrix. The latter consists of calcium phosphate salt for the most part and collagen for the rest part. The collagen provides a surface for the adhesion of inorganic salt crystals developing after calcium phosphate and calcium carbonate combine to form hydroxyapatite.

These crystals provide hardness and strength to bones or flexibility if they calcify on the collagen fibers.

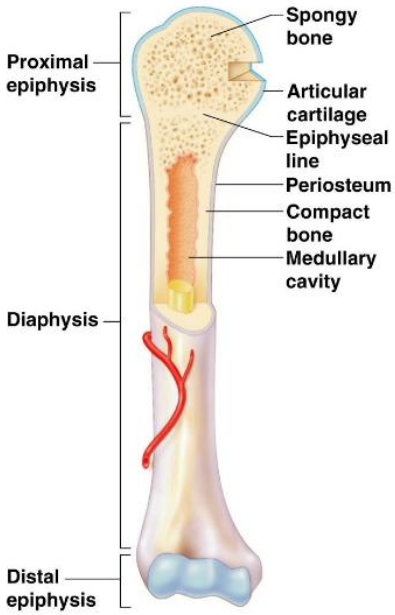

Figure 6. Anatomy of long bones.

Bone is continuously remodeled through the concerted action of four types of cells: osteoblast, osteocytes, osteoclast and bone lining cells. Osteoblasts are cells derived from mesenchymal stem cells (MSCs) located along the bone surface responsible for bone forming function. When the collagen matrix is synthesized and secreted from osteoblast calcified, the osteoblast become trapped within it, changing their structure and becoming osteocytes, the primary cell of mature bone [198]. Osteocytes are the most abundant cells that have a different morphology depending on the bone types. For example, osteocytes from cortical bone have an elongated morphology, while osteocytes from trabecular bone display a rounded morphology. Osteocytes are derived from osteoblasts differentiation and are involved in bone remodeling through the regulation of osteoblast and osteoclast activity [199]. Osteoclasts are differentiated multinucleated cells responsible for bone resorption, which derives

from mononuclear cells of the hematopoietic stem cell lineage. This differentiation is regulated by various stimulatory factors, including the macrophage colony-stimulating factor (M-CSF), secreted by osteoprogenitor mesenchymal cells and osteoblasts, and the receptor activator for nuclear factor κ-B ligand (RANKL) secreted by osteoblast, osteocytes and stromal cells [200, 201]. Osteoclasts are continually breaking down old bone, while osteoblasts are continually forming new bone. In addition to resorption, osteoclasts have also involved a source of cytokine that influences the activity of other cells, including osteoblast and hematopoietic stem cells niche [202]. Bone limiting cells are quiescent flat-shaped osteoblasts that cover the bone surface. The function of these cells is not fully understood. However, it has been described as a preventive action of bone limiting cells in osteoclast differentiation and preventing the direct interaction between osteoclasts and bone matrix [203].

Osteosarcoma commonly occurs in the long bones of the extremities near the metaphyseal growth plates and arises as an enlarging and palpable mass, with progressive pain. The most common bone affected the knee area. In particular, the femur for the 42% of cases with 75% of tumors in the distal femur, the tibia for the 19% of cases with 80% of tumors in the proximal tibia and the humerus for 10% of cases with 90% of tumor in the proximal humerus. Other locations are the skull or jaw and the pelvis [190].

1.3.1 Osteosarcoma pathogenesis

A better understanding of the cellular origin of osteosarcoma is essential to improve the outcomes of patients. In the last few years, various hypotheses concerning the origin of osteosarcoma have been made. Some reports propose that osteosarcoma originates from MSCs; others suggest osteoblast precursor cells as the origin of osteosarcoma [204]. MSCs are non-hematopoietic precursors cells that have been found in various human tissues, such as bone marrow, peripheral blood, and adipose tissue, that contribute to the maintenance and regeneration of a variety of tissues, including bone [205]. MSCs also exhibit an ability to differentiate into a variety of mesenchymal cell lineage, like osteocytes, chondrocytes, and adipocytes based on the predominant cancer cell type, suggesting that MSCs may be the cells of origin of osteosarcoma [206,

207]. Several *in vivo* studies support the hypothesis of the origin of osteosarcoma from MSCs. The overexpression of c-Myc with loss of Ink4a/Arf, the locus that encodes two tumor suppressor proteins that regulate the Rb and p53 pathways, may induce the malignant transformation from MSCs to osteosarcoma [208]. Moreover, the simultaneous knockdown of Rb and overexpression of c-Myc, a combination observed in patients with poor survival, have been described to induce MSCs differentiation and osteosarcoma in murine models [209]. In contrast, increasing evidence suggests that osteosarcoma arises from defective differentiation of osteoblast-committed cells. Yang et al., have demonstrated that the implantation of MSCs and preosteoblasts (pOB) differentiated from the same MSCs, induced tumor growth simultaneously. However, compared to MSCs, only the pOB tumors showed a histological appearance characteristic of osteosarcoma [210]. The most compelling evidence that supports the hypothesis of osteosarcoma deriving from osteogenic progenitors comes from *in vivo* experiments deleting p53 or both p53 and Rb after MSCs differentiation. Mouse with these deletions induced the formation of osteosarcoma-like tumors, suggesting that osteoblast rather than MSCs are the cells of origin of osteosarcoma [211].

Another factor that affects the differentiation of MSCs is the bone microenvironment, a specialized and highly dynamic system composed of bone cells, stromal cells, vascular and immune cells, and a mineralized extracellular matrix (ECM). Osteosarcoma communicates with the bone microenvironment via growth factors, such as transforming growth factor β (TGF-β) and stromal-derived factor (SDF1), and plasminogen that induces homing of MSCs to the tumor site, where it changes to acquire a phenotype that promotes tumor progression and metastasis [212]. Rubio et al., have shown that p53, Rb, or both p53 and Rb MSCs depletion into immunodeficient mice developed into osteosarcoma-like tumors in the recipients' bone. In addition, tumor position far away from the host bone exhibited a different pathology from osteosarcoma, indicating that the host bone environment might be another factor in programming the sarcoma phenotype of transformed MSCs [211]. Recently, it was reported that osteosarcoma might also arise from osteocytes. In fact, injection of osteocyte cell lines in immortalized mice induces tumor development,

and the osteocyte marker dentin matrix acidic phosphoprotein 1 (DMP1) was increased in human osteosarcoma samples, suggesting that osteocytes might also constitute an osteosarcoma progenitor cell type [213].

A vicious cycle between bone and osteosarcoma cells occurring during the development of osteosarcoma, promoting tumor growth and dissemination (Figure 7). Osteosarcoma cells produce interleukin 6 (IL-6), interleukin 11 (IL-11), tumor necrosis factor alpha (TNF-α) and RANKL that activates osteoclastogenesis and bone degradation, leading to the release of TGF-β in the bone microenvironment, which stimulates tumor growth and metastatic progression [214, 215].

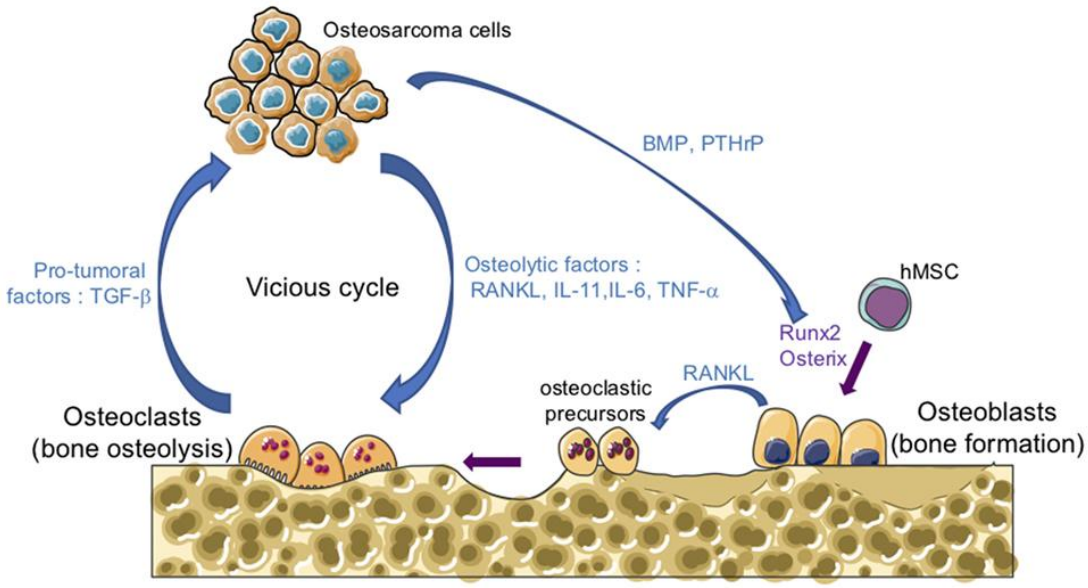

Figure 7. The vicious cycle between tumor and bone cells during osteosarcoma development. Osteosarcoma cells produce receptor activator of nuclear factor kappa-B ligand (RANKL), interleukin 11 (IL-11), interleukin 6 (IL-6), and tumor necrosis factor alpha (TNF-α) that activate osteoclastogenesis, lading to bone degradation. Osteosarcoma cells produce bone morphogenetic protein (BMP) or parathyroid hormone-related protein (PTHrP), that stimulate the production of RANKL by osteoblasts and increase osteoclasts activity. Following bone degradation, the transforming growth factor β (TGF-β) are released into the bone microenvironment and stimulate tumor growth and dissemination (taken from [216]).

1.3.2 Osteosarcoma subtypes

Osteosarcoma is a highly heterogeneous disease. Over the last decades, morphological analysis, but also genomic, transcriptomic, and proteomic analysis, were applied to identify new molecular markers with prognostic and predictive value to better determine the appropriate therapy.

Microscopic heterogeneity is the first marker for osteosarcoma. Depending on the morphological features of the cancer cells, osteosarcoma can be classified into central or surface tumors.

Central osteosarcoma, also called medullary tumor, can be divided into four subtypes depending on the histology: conventional, telangiectatic, small-cell, and low-grade osteosarcoma. Conventional central osteosarcoma (CCO) is a high-grade intraosseous sarcoma containing neoplastic bone-producing cells, usually arising from the intramedullary cavity. CCO is the most common type of osteosarcoma and represents 80% of all osteosarcoma cases affecting children between 0-14 years of age and adults older than 40 years [217]. CCO can be divided into osteoblastic, chondroblastic, and fibroblastic, depending on the histological features of the cells. In most cases, CCO is located in the metaphysis of long bones, but it can also arise in the axial skeleton and the metaphysis of long bones [218]. Telangiectatic osteosarcoma (TOS) is a rare, high-grade osteosarcoma which represent the 4% of all osteosarcomas. TOS occurs between 5 and 25 years of age with a higher incidence in males than females (median male-to-female 2:1). The exact etiology of TOS is still unknown but is presumed to derive from either transformed osteoblast or stem cells of mesenchymal origin. In most cases (42%), TOS arises in the distal femoral metaphysis, but also in the proximal tibia (17%), proximal humerus (9%), and the proximal femur (8%). Histologically, TOS is composed of blood-filled or empty cystic spaces resembling an aneurysmal bone cyst [219]. Although the TOS prognosis is worse than CCO, recent studies suggest that there are no differences between the two types [220, 221]. Small-cell osteosarcoma (SOS) is a very rare type of osteosarcoma, representing 1-2% of all osteosarcomas, mainly in young adolescents with a mild female incidence compared to males. Histologically, SOS cells are small cells with scant cytoplasm and round hypochromatic nuclei, making it difficult to distinguish from Ewing's sarcoma,

another type of pediatric cancer of the bone [222]. However, SOS cells are characterized by focal osteoid production, a morphologic feature that represents the diagnostic hallmarks of all types of osteosarcoma, allowing to distinguish SOS from other small cell malignancies [223]. Low-grade osteosarcoma (LOS) accounts for 1-2% of all osteosarcomas ad usually arise in the third or fourth decade of life, with equal gender distribution. LOS is a well differentiated osteosarcoma that consists of the fibroblastic stroma of variable cellularity and amounts of osteoid production, resembling parosteal osteosarcoma, making LOS diagnosis difficult [224].

Surface sarcoma, also called peripheral tumor, arises from the cortical and periosteal surface of the bone, in contrast to conventional osteosarcoma, which has an intramedullary site of origin. Surface sarcoma is divided into three different subtypes: parosteal, periosteal, and high-grade osteosarcoma. Parosteal osteosarcoma (POS) is low-grade osteosarcoma and accounts for 5% of all osteosarcomas. POS usually arises in early adult and middle age with a peak incidence in the third decade, with a slightly higher incidence in females than males [225]. POS usually arises from the outer layer of the distal femur, but it may also occur in other sites, including the proximal tibia and humerus. Histologically, it is a well-differentiated tumor with the woven bone formation that rarely metastasizes unless it undergoes malignant transformation into a differentiate POS (dPOS) [226]. Periosteal osteosarcoma (PIOS) is an intermediate-grade tumor that represents 1.5% of all osteosarcomas. PIOS usually occurs in patients between 15 and 25 years of age with a higher incidence in females than males and commonly involves the diaphysis of long bones, such as the tibia and femur. PIOS is characterized by zonated lobules that are primarily composed of malignant cartilage [227]. High-grade osteosarcoma (HGSOS) accounts for only 0.5% of all osteosarcomas, whit a peak incidence in the second and third decade of life. It usually arises in the lower limb diaphysis, with a local growth higher than POS [228].

1.3.3 Genetics of osteosarcoma

In the last few years, numerous molecular genetic studies have allowed identifying somatic mutation and mutational processes involved in osteosarcoma

to understand better the pathogenesis of the disease and ongoing therapeutic approach for osteosarcoma patients. Several genomic studies using whole-genome sequencing (WGS) and whole-exome sequencing (WES) have allowed us to identify chromosomal abnormalities, mutations, and candidate driver genes involved in osteosarcoma pathophysiology [229]. *RB1* encodes the tumor suppressor protein Rb that is essential in preventing cell cycle progression through G1/S phase after DNA damage [230]. Inactivation of *RB1* or Rb pathway deregulation is frequent in sporadic osteosarcoma. For example, amplification of the cyclin-dependent kinase (*CDK4*) and DNA primase subunit 1 (*PRIM1)*, which are involved in the transition from G1 to S, has been detected respectively for about 10% and 40%of osteosarcoma tumors [231, 232]. *TP53* is another driver of osteosarcoma development. Mutation of *TP53* has been detected in 30-42% of sporadic osteosarcoma [233, 234], whereas deletions and loss of heterozygosity (LOH) for 10-40% of cases [235]. Functional inactivation of p53 can also occur through the regulation of other proteins, including MDM2 that is a p53 inhibitor. Amplification of *MDM2* accounts only for 3.-25% of cases of osteosarcoma, but this amplification was highly frequented in metastasis and recurrence [232, 236]. *E2F3* (E2F transcription factor 3), which encodes the E2F2 transcription factor, was detected gained or amplified in approximately 60% of osteosarcoma. Increasing levels of this gene were associated with DNA damage and increased proliferation rate in cancer [237-239]. Also, *RUNX2* (Run-related transcription factor 2), which encodes for a transcription factor involved in osteogenesis, was found gained for about 60% of osteosarcoma, correlating with poor response to chemotherapy [240].

1.4 Malignant rhabdoid tumor of the kidney

Pediatric renal tumors account for around 7% of all cancers occurring before 15 years [241]**.** In Europe, each year, about 1000 children are diagnosed with renal tumors. This is a highly heterogeneous group of tumors, each with its therapeutic management, outcome, and association with germline predispositions.

Malignant rhabdoid tumor of the kidney (MRTK) is a rare, highly aggressive tumor occurring in infancy and early childhood. It was recognized as a distinct

tumor type in 1978, although initially, it was classified as a possible rhabdomyosarcomatoid variant of Wilms' tumor [242]. Subsequent studies identified tumors with similar histology at other sites, particularly soft tissues and the central nervous system [243]. MRTK is a rare tumor, accounting for 0.9-2% of renal cancers, with a peak of incidence between 10 and 18 months of age and 85% of cases occurring within the first 2 years of age. The incidence rate in men is slightly higher than in women (1:5) [244]. In the United States, the annual incidence among children less than 15 years is 0.19 per million. MRTK is considered one of the deadliest malignant solid tumors of childhood, with overall survival rates of not more than 20% to 25% [245]. The overall 3-years survival rate in patients with MRTK ranges from 12% to 38%; it is the highest in children aged 24 months or older and the lowest in those between 0 and 5 months of age. In China, a recent study reported that within a 5-year follow-up, out of 35 cases, one survived [246]. In addition, in children younger than 6 months, this condition is often accompanied by distant metastases, including brain metastasis [247]. Over 70% of children with MRTK are already in stages III and IV at the time of diagnosis, with overall survival of 15% compared to 40% of stages I and II. Progression on therapy and relapse are common in patients with MRTK, with about half of patients having a relapse after initial remission. The median time from diagnosis to relapse is less than 8 months, but the majority of patients with MRTK have disease progression far earlier (3–4 months after diagnosis) without ever obtaining a complete remission [242, 247].

The kidneys are the central organs in maintaining body homeostasis through the filtration of blood from metabolic waste products, blood pressure regulation, calcium and phosphate levels, the resorption of nutrients, and the maintenance of a homeostatic balance of tissue fluids. The kidneys are bilateral bean-shaped organs located retroperitoneally in the abdomen, one for each side of the vertebral column. Each kidney typically extends for three vertebrae in length, although the right kidney is generally slightly and smaller compared to the left due to the presence of the liver. The kidneys are encased in complex layers of fascia and fat that entirely surround and protect the kidneys. Internally, the parenchyma of the kidney consists of the outer renal cortex and the inner renal medulla. The cortex extends into the medulla, dividing it into triangular

structures, known as renal pyramids (8-18 per kidney). The apex of the renal pyramid is the renal papilla which opens to the minor calyx that collects urine from the pyramids. Several minor calyces unite to form a major calyx that merges to form the renal pelvis, from which urine drains the ureter that emerges and leaves the kidney through the renal hilum (Figure 8).

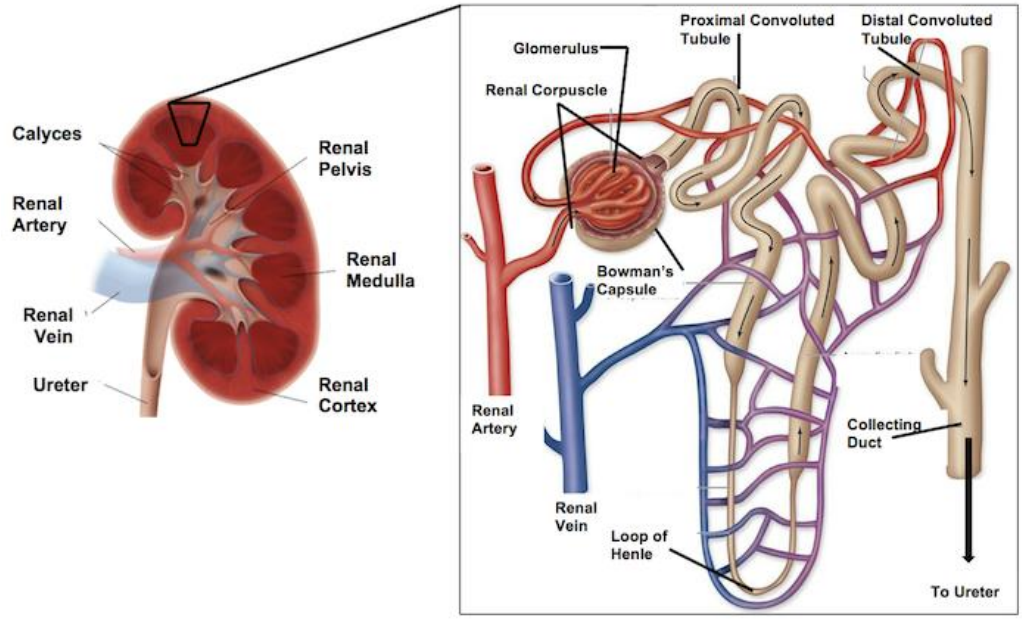

Figure 8. Anatomy of nephrons.

The kidney's functional units are the nephrons (1.000.000 per kidney), contained inside the renal pyramids, that filter the blood to produce urine. Each nephron contains a renal corpuscle and a renal tubule which filters the blood and carries the filtered fluid to the system of calyces, respectively. The renal corpuscle comprises the glomerular capsule, also called Bowman's capsule, which lies the glomerulus consisting in arterioles and capillaries able to filter the blood through the glomerular membrane. After living the renal corpuscle, the filtrate passes through the renal tubule that consists in the proximal convulted tubule, the Loop of Henle, and the distal convoluted tubule, responsible for reabsorption and

recovery of water and small molecules, such as glucose, amino acid, and ions, and then flow into the collecting duct for the final reabsorption of water and urine storage. The kidneys are richly supplied with blood and lymph vessels that contribute to the draining excess fluid and protein under physiological and pathological conditions. Each kidney has a single renal artery which is a direct lateral branch of the abdominal aorta, and a single renal vein that conducts the blood out of the kidney.

The lymph vessels collect and move lymph fluid away from the kidney into the small bean-shaped masses of lymphatic tissue, called lumbar lymph nodes that are placed around the origin of the renal artery. The lymph vessels and the lymph nodes are part of the lymphatic system, which has a crucial role during the extravasation of cancer cells, together with blood vessels. Once cancer cells detached from the primary site, they can arrive at the lymph nodes outside the abdomen through the lymph vessels and invade other tissues and metastasize.

1.4.1 MRTK histology

MRTK often presents as masses centered in the renal hilum with a grossly indistinct tumor border between the tumor and normal renal tissues. There are many variant patterns histologically, but characteristically, these tumors stain diffusely positive for vimentin. Epithelial membrane antigen (EMA) and cytokeratin appear to be the next most frequently expressed markers. Expression of a variety of other markers has been less commonly (neuron specific enolase [NSE], S-100, and Leu 7) or only sporadically (CD99 and desmin) identified [248].

Histologically, MRTK is characterized by rhabdoid cells, large polygonal cells with juxtanuclear, globular, eosinophilic cytoplasmatic inclusions, and vesicular nuclei that often contain single prominent nucleolus. A solid pattern is the most common without architectural organization, but trabecular, pseudo-alveolar and myxoid patterns may also be seen. Although for most cases of renal MRTK, the diagnosis is relatively straightforward, the combination of histologic heterogeneity and potential to occur in a diverse array of sites can create a diagnostic challenge for any given case. Among the more challenging

differential, diagnostic considerations are epithelioid sarcoma and a subset of rhabdomyosarcomas exhibiting rhabdoid-type inclusions [249], [250].

1.4.2 Genetics of MRTK

The cause of MRTK is largely unknown, and the histogenetic origin of this tumor has not yet been determined [251]. Most MRTKs demonstrate a normal karyotype, but few studies report numerical or structural chromosomal abnormalities, involving mainly chromosome 22. Molecular genetic investigation of MRTK cells has revealed heterozygous or homozygous deletions at of the region 11.2 of the long arm of chromosome 22 (22q11.2) as a recurrent genetic characteristic of MRTK, indicating that this locus may encode a tumor suppressor gene [252, 253]. Versteege et al., have mapped the most frequently deleted region of chromosome 22q11.2 from a panel of MRTK cell lines and delineated a common region of deletion that includes marker A006E25, which is an expressed sequence tag for *hSNF5/INI1*, a human homolog of the yeast *SNF5* gene [254]. *hSNF5/INI1* encodes a member of the SWI/SNF complexes, which are thought to facilitate the transcriptional activation of inducible genes through the remodeling of chromatin [255, 256]. hSNF5/INI1 works as an indirect cell cycle suppressor or increases mutually retroviral DNA intake with some viral proteins. Thus, it could be involved in other malignancies, including cervical and anogenital cancer, due to stimulation of human papillomavirus DNA replication [257]. Recently, *hSNF5/INI1* gene mutations were found in medulloblastoma [258], rhabdomyosarcoma (RMS) [259], plexus choroid carcinoma, plexus choroid atypical papilloma, and glioblastoma [260]. Several studies have reported an abnormal expression of the tumor suppression gene SMARCB1/INI-1 in MRTK patients. The *SMARCB1*/*INI1* gene is located in chromosome band 22q11.2 and is inactivated by deletions and/or mutations. SMARCB1 is an invariant member of the SWI/SNF chromatin-remodeling complex of proteins and thus controls gene transcription. *SMARCB1/INI1* is inactivated homozygously in most of the malignant rhabdoid tumors; up to 20% of tumors show no alterations at either the DNA or RNA levels. Different immunochemistry staining for SMARCB1/INI1, have reported that expression of SMARCB1/INI1, was not detected in neoplastic cells in the rhabdoid tumors of the kidney [261,

262]. The expression of SMARCB1/INI1 was also evaluated in other models of rhabdoid tumors and kidney tumors. Interestingly, immunochemistry staining for SMARCB1/INI1 has shown nuclear expression by neoplastic cells in all renal carcinomas, clear cell sarcomas and, Wilms' tumor, while no nuclear staining in atypical teratoid/rhabdoid tumors and soft tissue malignant rhabdoid tumors, indicating SMARCB1/INI1 as a candidate tumor suppressor gene involved in renal and extra-renal rhabdoid tumor pathogenesis. In addition, it has been demonstrated that SMARCB1 is required for the integrity and stabilization of SWI/SNF complexes, enabling them to bind and facilitate enhancer formation and function. SMARCB1 loss results in a marked reduction in the amount of SWI/SNF complexes, decreasing their levels since they are not able to maintain normal enhancer function. The small amount of residual SWI/SNF complex that remains is preferentially bound to super-enhancers. Loss of SMARCB1 impairs the function of enhancers required for differentiation, while super-enhancers were largely unaffected and could drive oncogenic transformation by locking cells into a lower differentiated and highly proliferative state [263].

Recently, RNA-seq technology has allowed the identification of new possible targets related to the occurrence and development of MRTK. RNA-seq analysis of MRTK tissues showed 2203 differential genes expressed compared to healthy kidney tissues; 1123 were downregulated, and 1080 genes were upregulated, and most of them involved in protein binding, suggesting that many proteins involved in protein binding are implicated in MRTK development. In addition, the INI1 protein corresponding gene *SMARCB1* showed a significant downward trend, corroborating the involvement of this gene in the pathogenesis of MRTK. Subsequently, KEGG signaling pathways analysis has reported 62 genes involved in the phosphoinositide 3-kinase (PI3K)-AKT signaling pathway, indicating the crucial role in the occurrence and development of MTRK. PI3K-AKT pathway is the most commonly activated pathway in human cancers. Oncogenic activation of the PI3K-AKT pathway in cancer cells reprograms cellular metabolism by augmenting the activity of nutrient transporters and metabolic enzymes, supporting the anabolic demands of growing cells. Besides PI3K-AKT, other signaling pathways such as the cell cycle and calcium signal pathway were found in MRTK tissues. PI3K-AKT pathway signaling in MRTK

was confirmed *in vitro*. Primary rhabdoid tumors and G-401, TTC549, and TTC709 cell lines have shown p-AKT expression, associated with higher levels of epidermal growth factor receptor (EGFR) expression, an upstream growth factor that positively regulates AKT signaling. In addition, insulin-like growth factor receptor 1b (IGFR1b) is expressed in MRTK G401, TM87-16, and TTC549 cell lines [264]. Furthermore, up to 33 miRNA-related genes were found changed in MRTK compared to health tissues [246]. Among miRNA, RNA-seq analysis has shown and high upregulation of miR-214-3p in human G-401 and WT-CLS1 MRTK cell lines compared to Kelly and SH-SY5Y neuroblastoma cell lines. miR-214 is a conserved mammalian miRNA located in the intron 14 of the Dynamin-3 gene (*DNM3*), which plays an important role in development, myogenesis, and neurogenesis. In addition, miR-214-3p was found significantly elevated in the serum of BALB/c-nu mice injected with WT-CLS1 and G-401 cell lines, indicating miR-214-3p as a possible marker for MRTK [265].

1.5 Pain

Chronic pain is a major health concern that affecting for 25-35% of European adults [266]. It is estimated that 20% of adults in the United States had chronic pain, and 8% had high-impact chronic pain, with a higher prevalence among women and older adults [267]. A prevalence between 3% and 17% of neuropathic pain is reported worldwide, with an incidence higher in women than men and in manual workers and among people from rural areas [268]. There is also a different ethnic prevalence of pain-related conditions. Caucasians have less painful experience than black and lower chronic pain than Asians, black, or mixed ethnicity [269, 270]. The most common reported pains in children and adolescence are low back, abdominal and headache pain. The 1-year incidence of low back pain ranges from 12% to 33% in children and adolescents, while the incidence of neck pain is 49% and 30% for upper back pain. The 1-month prevalence of low back pain ranges from 10% to 36%, whereas chronic back pain ranges from 18% to 24%. The prevalence of multiple pains in children and adolescents ranges from 12% to 36% [271, 272].

1.5.1 Nociceptors: transducers of pain

Nociceptors are sensory neurons that function as the primary unit of pain, associated with receptors and ion channels that facilitate the detection of stimuli that may potentially cause damage. Some nociceptors are myelinated Aδ-fibers, and others are unmyelinated C-fibers that are sensitive to different stimuli and terminate in the skin, muscle, and visceral organs [273]. Nociceptors have three functions: transduction, conduction and transmission of the noxious stimuli. These receptors are activated by inflammatory mediators such as prostaglandin E_2 (PGE_2), bradykinin and cytokines such as TNF-α, IL-1β and pro-inflammatory chemokines that bind and stimulate GPCRs, tyrosine kinase receptors and ionotropic receptors [274-276]. Activation of these latter receptors induces modulation of various ion channels, such as transient receptor potential (TRP) channels (TRPA1, TRPV1 and TRPV4) and sodium channels ($Na_v1.7$, $Na_v1.8$, and $Na_v1.9$) that results in hypersensitivity and hyperexcitability of nociceptors [274, 277].

TRPA1 responds to electrophilic reactive chemicals and inflammatory products, including oxidized lipids and lipid peroxidation products. TRPA1 activation by bradykinin induced the bradykinin receptor B2R signaling that leads to PLC activation and the release of IP3, which in turn gates TRPA1 opening [278]. TRPA1 activation may also drive by tyrosine kinases, such as p38 MAPK, PKA and PKC signaling [279, 280].

TRPV1 is also known as the capsaicin receptor and mediates thermal hyperalgesia during inflammation. The expression and activity of this large-pore cation channel are mediated by cytokines, prostaglandins, neurotrophic nerve growth factor (NGF) and bradykinin signals released during tissue inflammation or damage [281, 282]. In particular, NGF and bradykinin potentiated TRPV1 via PLC-dependent hydrolysis of diacylglycerol and IP3 [283]. The latter mediates the intracellular calcium release, leading to TRPV1 sensitization as well as TRPA1 [278, 284]. In addition, immune mediators activate MAPK, PKA and PKC that phosphorylate residues of TRPV1 and facilitate its opening. In particular, p38 MAPK activation induces peripheral sensitization by increasing TRPV1 and sodium channel activity in response to TNF-α and IL-1β, respectively [285, 286].

TRPV4 is a Ca^{2+}-permeable ion channel that is activated by warm temperatures, hypotonicity and acidic pH. Moreover, TRPV4 mediates pain-related behaviors in response to inflammatory mediators and contributes to mechanical hyperalgesia induced by PGE2, serotonin and bradykinin involved in cAMP-PKA and PKC signaling [287, 288]. In addition, TRPV4 has been reported to be involved in the activation and differentiation of innate immune cells, adhesion and chemotaxis, and production of reactive oxygen species in response to inflammatory stimuli [289].

$Na_v1.7$, $Na_v1.8$, and $Na_v1.9$ are essential for the generation of electrical impulses. Pro-inflammatory mediators, such as TNF-α and IL-1β, signal through tyrosine kinases facilitating the opening of sodium channels [285, 290].

1.5.2 Nociceptors and immune response

Nociceptors directly interact with immune cells in a bidirectional way, forming an integrated protective mechanism. Indeed, nociceptors release pro-inflammatory mediators, including cytokines and chemokines, that act on innate and adaptive immune cells, such as macrophages, neutrophils, mast cell and dendritic cells, to modulate their functions, and immune cells, in turn, release mediators that modulate nociceptors activity and pain sensitivity [291]. Thus, pain is not only a sign of inflammation but also participates in regulating immunity. Innate and adaptive immune cells express receptors for calcitonin gene-related peptide (CGPR) and substance P, two neurotransmitters released from nociceptors following noxious stimulation or activation of TRPA1 and TRPV1 [291], [292] (Figure 9). Macrophages are mononuclear phagocytes that originate from hematopoietic myeloid progenitors (HSCs) in the bone marrow responsible for phagocytosis, antigen presentation and cytokine production. Once macrophages are activated after infection and tissue lesion, they release inflammatory cytokines, lipids and growth factors that directly stimulate nociceptors to generate pain.

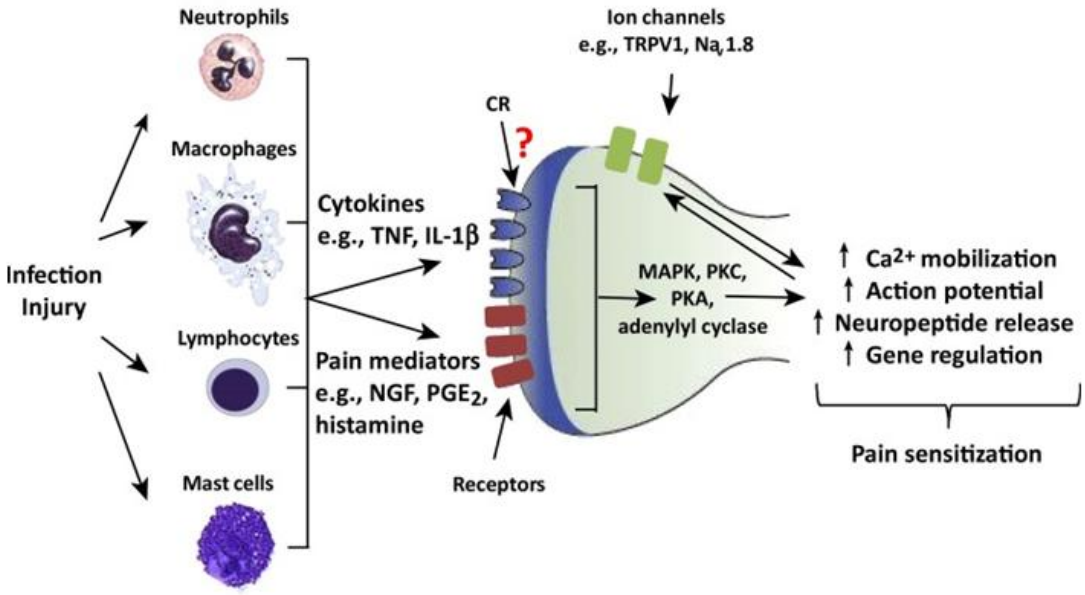

Figure 9. Immune cytokines as important mediators in the activation of nociceptors during inflammatory pain. Abbreviations: TNF: Tumor necrosis factor, IL-1β: interleukin 1 beta, PGE_2: Prostaglandin E_2, NGF: Neurotrophic nerve growth factor, PKA: protein kinase A, PKC: protein kinase C, MAPK: Mitogen-activated protein kinase (taken from [293]).

Substance P induces the release from murine macrophages of pro-inflammatory cytokines, including TNF-a, IL-1β and IL-6 via activation of ERK-p38 MAPK-mediated nuclear factor kappa B (NF-kB) activation [294], whereas CGPR has an anti-inflammatory effect through down-regulation of interleukin 10 (IL-10) in macrophages and dendritic cells [295]. Nociceptors also interact with macrophages via neuropeptides, including the pro-inflammatory chemokine CCL2, also known as chemokine monocyte chemoattractant protein-1 (MCP-1), produced by immune cells and neurons [296]. Nociceptor-produced CCL2 induces peripheral sensitization through activation of TRPV1 and macrophages infiltration and activation after nerve injury [286, 297]. Several evidences suggest the role of macrophages in the resolution of pain through the release of IL-10 and specialized pro-resolving mediator (SPM). It has been demonstrated that GRK2 regulates the resolution of inflammatory pain through IL-10 secretion in myeloid cells [298]. In fact, loss of GRK2 was associated with reduced production of IL-10 in macrophages [299]. Among SPM, neuroprotectin D (NPD1) promoted macrophage phagocytosis, limited neutrophil infiltration and

analgesic action during inflammatory and neuropathic pain in a mouse model [300]. Importantly, GPR37 has been identified as a receptor for NPD1, which turned out to be necessary for NPD1 activity. In addition, GPR37 is responsible for upregulation of the anti-inflammatory cytokines IL-10 and TGF-β and down-regulation of the pro-inflammatory cytokines IL-1β and TNF-α in macrophages [299, 301].

Neutrophils are short-lived leukocytes generated by myeloid precursors in the bone marrow and represent the first immune cells recruited to the damaged tissue to fight against infection [302]. During neurogenic inflammation, the release of neuropeptides, such as chemokines, TNF-α and interleukin 17 (IL-17), by nociceptors activation, facilitates chemotaxis that promotes the infiltration and accumulation of neutrophils in nerves [303, 304]. In contrast, some studies showed a suppressive role of nociceptors in recruiting and activating neutrophils during inflammation [305, 306]. Moreover, neutrophils at the site of inflammation can secrete analgesic mediators, such as opioid peptides, that can inhibit nociceptive transmission [307].

Mast cells are granulated immune cells that reside close to nerve fibers and participate in innate defense through their degranulation and release of histamine, pro-inflammatory cytokines, chemokines, NGF and serotonin, which acts on the nervous system and/or immune cells contributing to pain sensitization [308]. The interaction between mast cells and nociceptors in pain conduction has been described in inflammatory disease, indicating a correlation of mast cells with pain symptoms [309, 310]. Indeed, *in vivo* studies conducted in mast cell-deficient mice have shown a reduction in pain, demonstrating the involvement of mast cells in the regulation of peripheral sensitizations [311, 312]. Furthermore, mast cells have been found to contribute to hyperalgesia in transgenic mice by releasing neuropeptides [313]. Degranulation of mast cells can be due to the activation of numerous cell surface receptors, including GPCR and Fcε receptors. The latter induces the secretion of S1P, which recruits mast cells to the injury site and stimulates their degranulation by binding to GPCR [314]. In addition, substance P was able to activate mast cells by Mas-related G-protein coupled receptor member B2 (MRGPRB2) lead to the release of pro-inflammatory cytokines and chemokines that facilitates immune cells infiltration

[315]. Moreover, pannexin 1 (Panx1) is a pore membrane channel expressed in neurons and immune cells that promotes sensitization following activation and induces degranulation of mast cells during hypersensitivity [316, 317].

Dendritic cells (DCs) are a type of antigen-presenting cells (APC) that are in contact with nociceptors in peripheral tissues and modulate cutaneous immunity. Intact skin of mice model revealed that depletion of nociceptors suppresses IL-23 production from DCs and IL-17 by γδ T cells and recruitment of other inflammatory cells [318]. Mikami et al., have shown that CGPR acts through the cAMP/PKA pathway lead to inhibition of interleukin 12 (IL-12) from DCs, a decrease of DCs activation and migration, and suppression of Th1 cell responses [319].

1.5.3 Neuropathic pain

The definition of neuropathic pain was released by the International Association for Study of Pain (IASP), which indicate that neuropathic pain is caused by a lesion or disease of the somatosensory nervous system, including peripheral fibers and central neurons, representing the most common chronic pain condition that affects for the 7-10% of the general population. The somatosensory system enables the perception of touch, pain, temperature, position, movement and pressure which arise from the muscles, skin and fascia. Conditions associated with neuropathic pain include metabolic disorders, neuropathies associated with viral infects, chemotherapy-induced peripheral neuropathies and autoimmune disorders affecting the central nervous system [320]. Usually, the perceived neuropathic pain is spontaneous without stimulus and affects the quality of life of patients. Notably, neuropathic pain differs from inflammatory pain in terms of diagnosis and treatment [321]. In general, neuropathic pain is unrecognized and challenging to diagnose due to how the pain message is modulated in the CNS. The pain signal can be augmented, relayed, or altered from other interfering pathways. In addition, most of the pharmacological and nonpharmacological approaches that are used target the clinical symptoms instead of the causative factors, making difficult the treatment of neuropathic pain [322].

Chronic neuropathic pain includes central and peripheral neuropathic pain conditions. Central neuropathic pain results from any type of injury to the central nervous system, including vascular, infectious, traumatic or neoplastic disorders. However, central neuropathic pain is commonly following stroke, spinal cord injury, or multiple sclerosis [323]. Peripheral neuropathic pain results from damage of the nerves located in the peripheral nervous system due to traumatic injuries, metabolic problems, infections, inherited causes and diabetes. Peripheral neuropathic pain is more common than central neuropathic pain because of the aging of the global population, the increased incidence of diabetes and cancers. Peripheral neuropathic pain disorders can be subdivided into generalized distribution and focal distribution. Generalized peripheral neuropathies include diabetes and metabolic disorders, infectious diseases, immune and inflammatory disorders, chemotherapy and inherited neuropathies. These types of disorders involve the distal extremities, such as feet and hands, and are characterized by progressive sensory loss, weakness and pain. Focal distribution disorders involve one or more peripheral nerves and include post-traumatic and post-surgical neuropathy, post-herpetic neuralgia, HIV infection and diabetes [324]. Peripheral neuropathy alters the electrical proprieties of sensory nerves leading an imbalance between the inhibitory and central excitatory signaling and alteration of the transmission of sensory signals. These changes produce a gain of hyperexcitability that contributes to the neuropathic state becoming chronic.

Neuropathic pain also causes alterations in both ion channels called channelopathies and second-order nociceptive neurons. Yang et al., have reported that increased expression and function of sodium channels lead to an increase of excitability, signal transduction, and release of neurotransmitters [325]. The enhanced excitability due to the release of excitatory amino acids and neuropeptides induces changes in the second-order nociceptive neurons, including an excess of signaling due to phosphorylation of *N*-methyl-D-aspartate (NMDA) and α-amino-3-hydroxy-5-methyl-4-isoxazolepropionic acid (AMPA) receptors [326]. Furthermore, neuropathic pain contributes to interneuron dysfunction lead to an alteration between excitation and inhibitory signaling in

favor of excitation. For this, the brain receives altered and abnormal sensory messages which cause high pain, anxiety and depression [327].

1.5.4 β-ARs and pain

In the last few years, an increased number of studies have demonstrated the involvement of noradrenergic transmission in neuropathic pain. Among β-ARs, the β2- and β3-ARs subtypes can directly produce pain by increasing the excitability of primary nociceptors and activating immunoregulatory cells. Indeed, it has been reported that the increase in catecholamine levels after stress or pharmacologic targeting leads to β2-ARs-mediated activation of macrophages, mast cells, T-cells, and β3-ARs-mediated activation of adipocytes and pro-inflammatory cytokines that sensitize nociceptors. Recently, it has been demonstrated that the inhibition of catechol-O-methyltransferase (COMT), an enzyme that metabolized catecholamines, induced the β2- and β3-ARs-mediated the increase in plasma levels of TNF-α, IL-6 and IL-1β, and the phosphorylation and activation of MAPKs in nociceptors resulting in neuroinflammation and allodynia [328]. Notably, the combination of persistent COMT-inhibition with TNF-α or p38 MAPK inhibition reversed COMT-dependent allodynia, suggesting that pain is maintained by TNF-α or p38 MAPK following β2- and β3-ARs stimulation [329]. The involvement of the adrenergic system and pain is further demonstrated by using the β2- and β3-ARs antagonists in mouse model of nerve injury. Kanno et al., have shown that the treatment with propanolol following noradrenaline administration inhibited the increased frequency of neuron-evoked single-channel currents (NeSCCs), whereas the treatment with the β3-AR antagonists, but not with β1- and β1-AR antagonists, abolished the noradrenaline effect, indicating that noradrenaline increases the frequency of NeSCCs via β3-AR stimulation. In addition, the treatment with β2- and β3-AR antagonists, reduced the NADPH signal in DRG neurons mediated by noradrenaline, indicating that noradrenaline stimulates ATP release from DRG neurons via β3-AR after peripheral nerve injury, triggering allodynia. In fact, treatment with SR59230A relieved mechanical allodynia in a rat model [330]. Furthermore, it has been reported a correlation between β3-ARs and temporomandibular joint (TMJ) pain. In fact, the treatment with atenolol, ICI

118.551 and SR59230A in the rat's TMJ significantly reduces inflammatory pain resulting from injection of formalin in a dose dependent response, indicating that blockade of *β*-ARs might be beneficial in the treatment of TMJ pain [331].

1.5.5 Neuropathic pain and cancer

Neuropathic pain in cancer is debilitating and affects up to 39% of patients with advanced cancer. The presence of neuropathic pain in cancer patients could delay treatment, limit treatment options or lead a patient to refuse treatment. Neuropathic cancer pain is divided into tumor-related and treatment-related pains. In particular, about 60% of neuropathic pain in cancer is tumor-related, while around 20% is related to cancer treatment, and the last 10-15% is associated with comorbid diseases. The association of neuropathic cancer pain with anti-cancer treatment lead to worse physical, social and cognitive functioning and poor outcome [332].

Neuropathic cancer pain is the result of a multi-step process that contributes to neuronal sensitization. However, the final event that induces neuropathy differs between individuals. Indeed, neuropathic cancer pain may be due to direct infiltration by the primary tumor or metastasis into a component of the central or peripheral nervous system, or to compression of the nerve, or changes in the neuronal milieu resulting from cancer growth, or from inflammatory response such as acidosis and the release of chemokines and cytokines [333]. These mechanisms have been reported to be more critical in neuropathic cancer pain compared to other neuropathies. In addition, also paraneoplastic neurological syndromes and infection may lead to neuropathic damage or hypersensitivity in cancer patients [334]. Neuropathic pain is also related to cancer therapy, such as radiotherapy, chemotherapy and surgery. Radiation can result in chronic painful-induced neuropathy. Indeed, local damage to the nervous system due to radiation-induced fibrosis or nerve and blood vessels injury could appear months or years after radiation treatment, as in lung and breast cancer [335]. Chemotherapy-induced neuropathy is a common and painful side effect of chemotherapy [336]. Common drugs such as paclitaxel, cisplatin, vincristine and bortezomib have been reported to induce

sensory neuropathies, paraesthesias in the distal extremities and nerve fiber loss and demyelination in the first two months of treatment [337]. Seretny et al., have reported that chemotherapy-induced neuropathy affects the 60% of patients in the first three months of treatment and the 30% at six months or more [338]. Surgery could cause direct damage to peripheral nerves, for example, during thoracotomy or mastectomy. In addition, up to 40% of 5-year cancer survivors report pain [339].

Increasing studies have been performed to understand the mechanism of neuropathic cancer pain. Inoculation of HCa-1 murine hepatocarcinoma cells in the thigh or dorsum of the foot of mouse model induced mechanical and cold allodynia and hyperalgesia 4 weeks after inoculation. In particular, mechanical and cold allodynia were developed in mice inoculated into the foot, while only cold allodynia was observed in mice that received an inoculation into the thigh [340]. Moreover, subcutaneous inoculation of SCC-7 squamous cell carcinoma in a mouse model induced spontaneous heat hyperalgesia and mechanical allodynia after 12 days from inoculation and a decrease after 15 days post-inoculation [341]. The involvement of the TRPA1 and TRPV1 channels in cancer pain was also demonstrated in melanoma and bone cancer, respectively. Inoculation of B16-F10 murine melanoma cells into the plantar region of the paw induced mechanical allodynia and thigmotaxis behavior, which are absent in TRPA1-deficient mice [342]. De Logu et al., have reported that inoculation of B16-F10 cells into the paw C57BL/6J mice induced cold and mechanical hypersensitivity and increased the number of monocytes and macrophages within the tumor and adjacent tissue. In addition, they showed that the increased levels of the growth factor M-CSF induced macrophages expansion and cancer-evoked allodynia via TRPA1. In fact, in TRPA1-depleted mice, M-CSF failed to induce mechanical allodynia [343]. Finally, in an *in vivo* model of bone cancer pain, TRPV1 depletion or administration of TRPV1 antagonist attenuated movement-evoked pain-related behaviors, suggesting TRPV1 as a novel target for pharmacological treatment of bone cancer pain [344].

1.5.6 Cancer-induced bone pain

Cancer-induced bone pain is the most common type of pain in cancer. Approximately 60-84% of patients with advanced cancer are estimated to experience varying degrees of bone pain, with a reduction of patients' quality of life [345]. Cancer-induced pain is a complex phenomenon that is distinct from other forms of chronic pain, such as inflammatory or neuropathic pain, due to the interaction between tumor cells, bone cells, activated inflammatory cells and bone-innervating neurons [346]. In addition, it has been demonstrated that the crosstalk between bone microenvironment cells, including those that regulate bone remodeling, immune cells, stromal cells, and endothelial cells, and bone metastatic cancer cells is crucial for bone metastatic progression [347-349].

During bone metastatic progression, osteolytic cancer cells originated from the primary tumor, stimulate osteoblasts to release RANKL, a protein member of the cytokine family of TNF-α produced by tumor cells, the osteoblastic cell line and activated T cells. The osteoblast-derived RANKL binds to its receptor RANK expressed on osteoclasts inducing osteoclasts maturation and increasing osteolytic activity. This process results in enhanced bone resorption which causes the release of growth factors such as TGF-β, insulin-like growth factor 1 (IGF-1) leading to metastatic progression. During the bone resorption process, osteoclasts acidify the extracellular space stimulating the sensory nerves to thermal, mechanical and chemical stimuli through the activation of acid sensing receptors, including TRPV1 and acid-sensing ion channels (ASICs) expressed on sensory nerves and triggers cancer-induced bone pain [350-352]. In addition, osteoclasts release accumulated intracellular ATP into the extracellular space, inducing the activation of purinergic receptors such as P2X, also known as the ATP-gated ion channels, expressed in the afferent neurons innervating bone and involved in cancer-evoked bone pain development [353-355]. Thus, pharmacologically targeting the ATP/P2X axis could be a potential therapeutic strategy for cancer-evoked bone pain (Figure 10).

Unlike osteoclasts, the mechanism driving osteoblastic bone metastatic progression is not yet well known. However, it has been demonstrated that overexpression of endothelin-1 (ET-1), a vasoconstrictor and an osteoblast

inducing factor, induced osteoblastic metastases along with new bone formation after inoculation of breast cancer cells into murine bone [356, 357]. Therefore, treatment with the endothelin A receptor (ETAR) antagonist reduced osteoblastic lesion and cancer-induced bone pain [358].

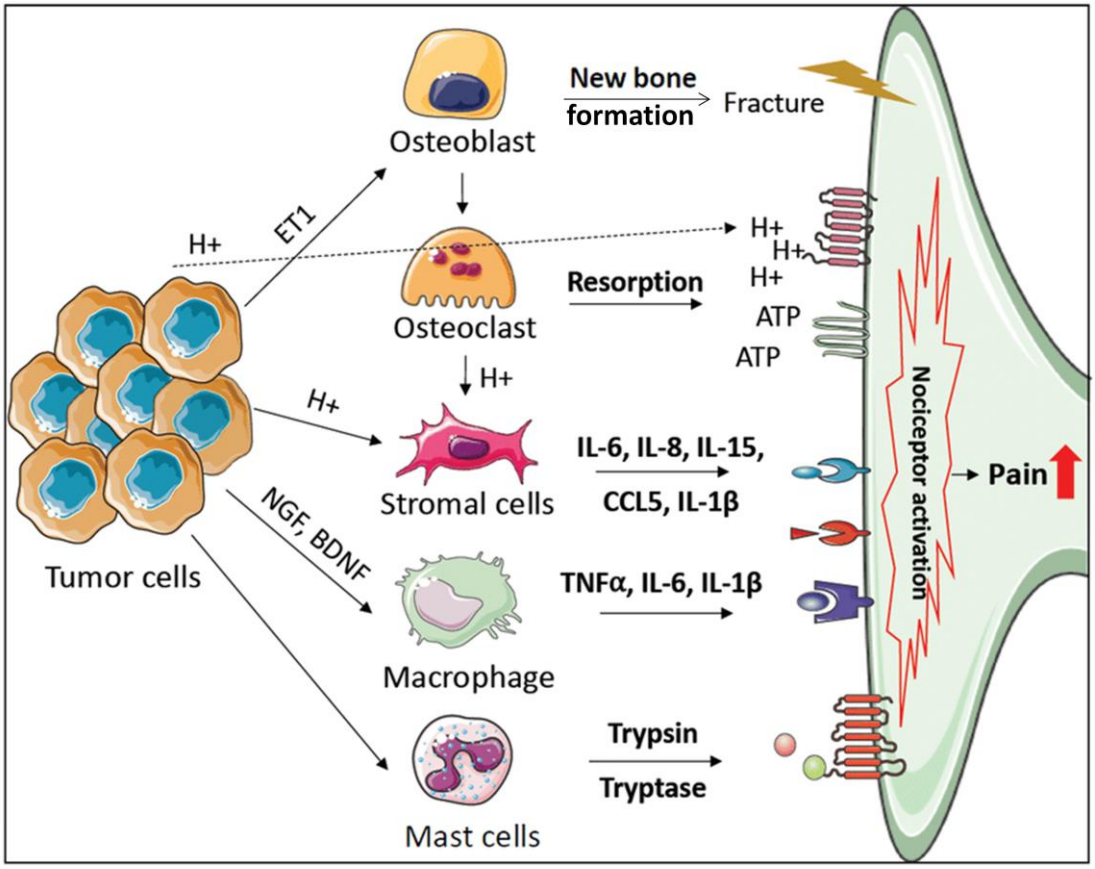

Figure 10. Mechanism of bone microenvironment involvement in cancer-induced bone pain. Abbreviation: IL-6: interleukin 6, IL-8: interleukin 8, IL-15: interleukin 15, IL-1β: interleukin 1 beta, TNFα: tumor necrosis factor alpha, NGF: neurotrophic nerve growth factor, BDNF: brain neurotrophic growth factor, CCL5: Chemokine Ligand 5 (taken from [359]).

Macrophages contribute to the tumor microenvironment through the release of inflammatory factors, following interaction with tumor cells, which induced both disease progression and cancer-induced pain [360, 361]. Different types of cancer cells that metastasize to the bone, secreted NGF and the brain-derived neurotrophic factor (BDNF) that activated macrophages, which express the NGF

and BDNF receptors, inducing the release of pro-inflammatory cytokines, such as TNF-α, IL-6 and IL-1β, and inflammatory regulator, such as PGE_2, that sensitize nociceptors [290, 362].

Mesenchymal stem cells (MSCs) and fibroblasts express high levels of acid sensing receptors, including ASIC3, ASIC4, G-protein coupled receptor 4 (GPR4) and GPR65, which results activated by the acid environment generated by metastatic tumor cells. This interaction induced the expression and secretion of inflammatory cytokines, such as IL-6, IL-8, IL-15 and CCL5, NGF and BDNF, leading to cancer-induced bone pain [363].

1.6 Tumor metabolism

The hallmarks of cancer are the different biological capabilities that cancer cells acquire during tumor development and progression [364]. Genomic instability and thus mutability is the most important enabling characteristic of the cancer cell alteration that drives tumor progression through increased sensitivity to mutagenic agents and breakdown in one or several components of the genomic maintenance machinery [364]. Reprogramming of energy metabolism is an established hallmark of cancer. Most cancer cells exhibit metabolic adaptations that promote their survival and progression under nonphysiological conditions to support enhanced proliferation and cell division. Although cellular transformation occurring in different cell types arises from many different pathways, the metabolic reprogramming of different cancer cells is generally similar [365]. To sustain the metabolic demands of this increased growth and proliferation, cancer cells must generate energy in the form of ATP, promote macromolecules synthesis and manage the high oxidative stress levels. Cancer cells are surrounded by different cell components of the tumor microenvironment that contribute to the acquisition of hallmarks traits. The metabolic adaptations also affect the tumor microenvironment by exerting additional selective pressure on the cancer cells to adapt to the harsh condition, such as acidity, hypoxia and/or nutrient starvation (Figure 11).

Figure 11. Hallmarks of cancer: the next generation. There are now 10 established hallmarks of cancer, including inflammation, metabolism and genomic instability (taken from 220).

1.6.1 Glucose metabolism

Under aerobic conditions, normal cells metabolize glucose, first to pyruvate via glycolysis in the cytosol and after that to the mitochondria tricarboxylic acid (TCA) cycle for its complete oxidation. This reaction produces nicotinamide adenine dinucleotide NAD^+ reduced (NADH) that fuels oxidative phosphorylation (OXPHOS) for maximum ATP production. Under anabolic conditions, glycolysis is favored, and relatively little pyruvate undergoes OXPHOS, while a high pyruvate quantity is converted in lactate in a process called fermentation. Otto Warburg first observed that even in the presence of oxygen, cancer cells could reprogram their glucose metabolism, and thus their energy production, consuming glucose at a high rate compared to normal cells by an increase of glycolysis and lactate release, leading to a state that has been termed “aerobic glycolysis” or “Warburg effect” (Figure 12) [366]. Warburg initially hypothesized that cancer cells developed a defect in mitochondria which led to an impairment in aerobic respiration and subsequent reliance on glycolytic metabolism [366].

Nevertheless, subsequent studies showed that mitochondrial function was not affected in most cancer cells [367, 368].

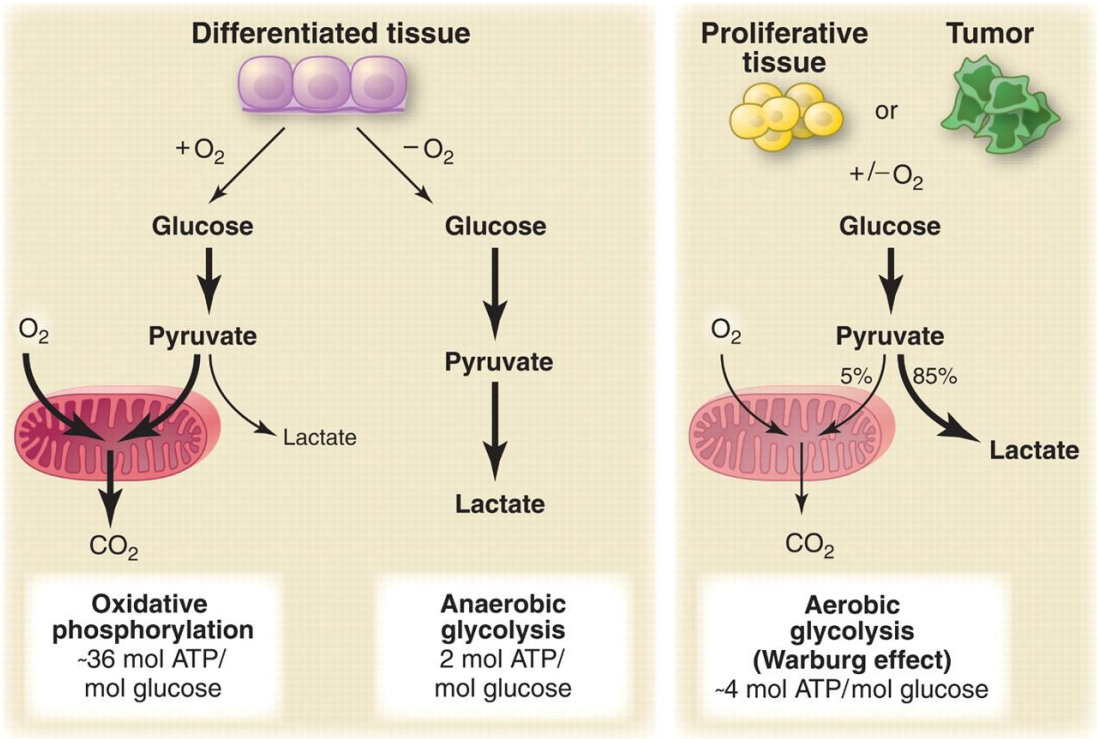

Figure 12. Comparison of glycolysis between a normal tissue and tumor/proliferated tissue (taken from 339).

Although ATP production by glycolysis can be more rapid than OXPHOS, it is far less efficient in terms of ATP generated per unit of glucose consumed. This shift, therefore, demands that tumor cells implement an abnormally high rate of glucose uptake to meet their increased energy, biosynthesis, and redox needs [366, 369]. To promote glucose uptake, many cancer cells upregulate the glucose transporters (GLUTs), a family of 14 transporters that can contribute to a substantial increase in glucose import into the cytoplasm. Among these transporters, GLUT1, GLUT3, and GLUT4 are the most overexpressed and studied in cancer [370]. Indeed, markedly increased uptake and utilization of glucose have been documented in many human tumors using positron emission tomography (PET) with the radiolabeled analog of glucose (^{18}F-fluorodeoxyglucose, FDG) [371]. In addition to producing ATP, glucose could be

used to generate biomass needed to support cell proliferation. Degradation of this metabolite provides cells with intermediates of the glycolytic flux that represent precursors for biosynthetic pathways, including non-essential amino acids for protein synthesis and/or citrate for lipogenesis. In addition, glucose-6-phosphate derived from the first step of glycolysis can be oxidized into the pentose phosphate pathway (PPP) to produce nicotinamide adenine dinucleotide phosphate (NADPH), essential for biosynthetic reactions and protection against ROS, and ribose-5-phosphate for nucleotides synthesis [372]. The availability of biosynthetic precursors is enhanced by regulating the last rate-limiting step of the glycolytic pathway, which is catalyzed in normal cells by pyruvate kinase M1 (PKM1). PK catalyzes the conversion of phosphoenolpyruvate (PEP) to pyruvate, with concomitant phosphorylation of ADP to ATP. In addition to PKM1, it also exits another PK isoform, which has reduced catalytic activity. PKM1 and PKM2 are produced by alternative splicing of the primary RNA transcript of the PKM gene. The non-allosteric PKM1 isoform is constitutively active and expressed in a differentiated tissue with a great demand for ATP, such as the brain and muscles. PKM2 is allosterically activated by fructose-1-6-biphosphate (FBP) and expressed in tissue with anabolic functions, including proliferating cancer cells [373, 374]. PKM2 can exist as both dimer and tetramer forms. The PKM2 dimer is less active compared to its tetrameric form in converting PEP to ATP and pyruvate. While tetrameric PKM2 favors ATP production through the TCA cycle, dimeric PKM2 plays a critical role in aerobic glycolysis [375, 376]. This reduced catalytic activity allows the reduction of the glycolytic flux rate and causes the accumulation of intermediates that fuel several biosynthetic pathways [374]. The dynamic equilibrium between the dimeric and the tetrameric form of PKM2 allows proliferating cells to regulate their need for anabolic and catabolic metabolism [377]. PKM2 activity can be regulated by post-translational modifications, which favor the dimeric state of PKM2, such as phosphorylation at tyrosine-105 (Y105), acetylation of the lysine305 (K305) and the oxidation at cysteine-358 (C358) [378-381]. The genetic transcription of PKM2 can be mediated by various factors, including Hypoxia-inducible factors 1 (HIF-1) that binds Hypoxia Response Elements (HREs) regions, promoting PKM2 transcription and c-Myc either directly by

binding with the gene promoter or indirectly by activating genes that facilitate alternative splicing [382, 383]. Moreover, a missense mutation in the PKM2 gene, including H391Y and K422R, may promote cancer metabolic reprogramming, conferring advantages in tumor growth [384].

In addition, the PI3K/AKT/mTOR pathway has a crucial role in controlling glucose metabolism and in the regulation of biological processes, such as cell proliferation, apoptosis, and angiogenesis. The AKT serine/threonine kinase, also known as protein kinase B (PKB), is an oncogenic protein that regulates cell survival, proliferation, growth, apoptosis, and glycogen metabolism. AKT is activated by phosphorylation on Thr308 or Ser473 by PI3K or phosphoinositide-dependent kinases (PDK) as well as growth factors, inflammation, and DNA damage, and it phosphorylates a variety of downstream protein substrates and induces signals that interfere with normal regulatory mechanisms activating mTOR [385]. AKT directly and/or indirectly regulates the transcription and translation of GLUT1 leads to the switch to glycolytic metabolism in cancer [386, 387]. mTOR is the conserved serine/threonine kinase that regulates nutrient uptake, cell growth, metabolic state, proliferation, and cell survival [388, 389]. Notably, multiple points along the glycolytic pathway are influenced by mTOR via regulation of critical transcription factors such as HIF-1α and Myc. During normoxia, HIF-1α undergoes a degradation following posttranscriptional modifications, while during hypoxia, HIF-1α expression is normally elevated. However, in several cancer cells, HIF-1α is stable in the presence of oxygen, and this is due to mutations that can involve HIF-1α itself or its regulators [390]. Increased HIF-1α expression is sufficient to induce the expression of genes whose products increase glycolytic flux [391]. Another effector of mTOR that promotes glycolytic gene expression is the transcription factor Myc. HIF-1α and Myc have overlapping metabolic gene targets. For example, both regulate the expression of lactate dehydrogenase (LDH), which converts pyruvate to lactate [392, 393]. Lactate is transported out of the cancer cells across the plasma membrane by the monocarboxylate transporters (MCTs) family. MCT1 is an importer used in oxidative tumors to transport exogenous lactate, produced by glycolytic cells in the tumor microenvironment, as an energy source, which can be metabolized through OXPHOS. Conversely, MCT4 acts as an exporter that

releases lactate produced from glycolytic cancer cells [394]. The lactate produced and released in the tumor microenvironment by glycolytic cancer cells results in increased acidity in the tumor microenvironment, which promotes tumor cells adaptation and contributes to the evolution of the tumor niche [395].
In addition to HIF-1α and Myc, p53 is another transcription factor involved in regulating the glycolytic pathway. Hexokinases (HK) are important enzymes that regulate the first step of glycolysis, converting glucose into glucose 6-phosphate. HK2 is the isoform expressed specifically in skeletal muscle, adipocytes, and cancer cells. In cancer cells, the HK2 gene is amplified, activated and induced by multiple signal cascades [396]. HK2 can be regulated from both p53 and HIF-1α. The upstream regulatory elements of the HK2 gene contain response elements for protein kinase A, protein kinase C, HIF1-α, and p53 [397, 398]. In cancer cells, the HK2 gene is amplified, activated and induced by multiple signal cascades [399]. Moreover, HIF-1-α induces the expression of [400, 401]. The inhibition of PDH impairs the entry of pyruvate into the TCA cycle and promotes the conversion of pyruvate into lactate.

1.6.2 Amino acids metabolism

Cancer cells have a continued and increased requirement for amino acids to sustain their rapid growth and proliferation. Amino acids can be divided into two classes: essential amino acids (isoleucine, leucine, methionine, valine, phenylalanine, tryptophan, histidine, threonine and lysine) and non-essential amino acids (alanine, glutamate, glutamine, aspartate, asparagine and serine). Amino acids can be used as substrates for protein synthesis but also as a source of energy (Figure 13).

Serine and glycine are linked to biosynthetic pathways and represent essential precursors for synthesizing building blocks including protein, nucleic acids and lipids. Serine can be an external source or internal when driven from glucose metabolism. Upregulation of *de novo* serine and glycine synthesis has increased as a result of general metabolic reprogramming of glycolysis by the Warburg effect in various cancer types. Several studies suggested that cancer cells increase de novo serine synthesis via the phosphoglycerate dehydrogenase (PDGH) pathway. PHGDH oxidases around 10% of 3-

phosphoglycerate produced during glycolysis by converting it to 3-phospho-hydroxypyruvate [402-404]. This compound is then transaminated and dephosphorylated to serine. Both *de novo* synthesized and imported serine can be further converted into glycine by the serine hydroxymethyl transferase (SHMT) enzyme, a direct transcriptional target of c-Myc [405].

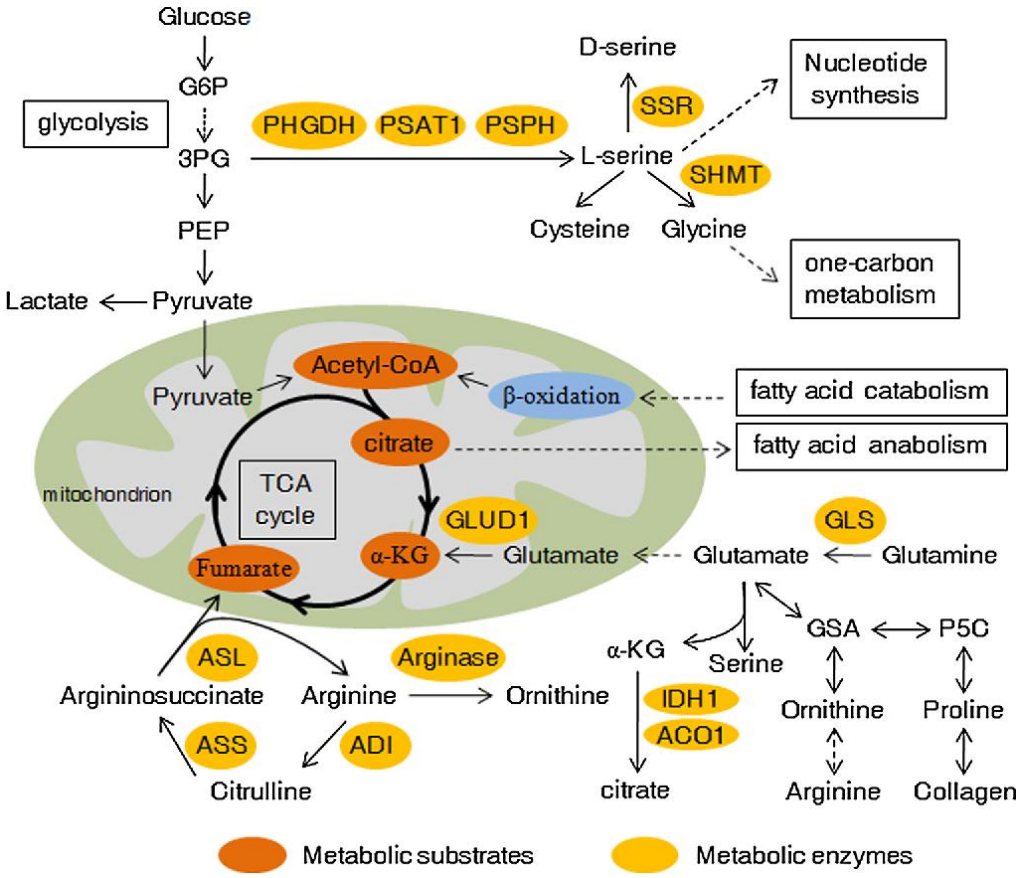

Figure 13. Amino acids metabolism in cancer cells and its crosstalk with other metabolism pathways. Amino acids synthesis, utilization, and involvement in other metabolism pathways are usually changed in cancer cells. Abbreviations: α-KG, α-ketoglutarate; GSA, glutamic semialdehyde; P5C, pyrroline-5-carboxylate; GLS, glutaminase; GLUD1, glutamate dehydrogenase 1; ASS, argininosuccinate synthetase; ASL, argininosuccinate lyase; ADI, arginine deaminize; IDH1, isocitrate dehydrogenase-1; ACO1, aconitase 1; SSR serine racemase. Dashed arrows represent indirect effects or serial reactions (taken from [406]).

The glycine cleavage system represents a major metabolic pathway of the one-carbon metabolism that provides cofactors for purine and pyrimidine nucleotides biosynthesis essential for proliferating lymphocytes, cancer cells and fetal tissue [407, 408]. In addition to PHGDH, SHMT is also implicated in tumorigenesis. Numerous studies have reported that exogenous glycine cannot be replaced by serine to support cell proliferation. In fact, cancer cells use exogenous serine, which is then converted into glycine and one carbon units for nucleotide synthesis [409]. In contrast, uptake of exogenous glycine without the presence of serine impaired the synthesis of nucleotides indicated that cancer cell proliferation is supported by serine rather than glycine consumption.

Another important essential amino acid involved in numerous metabolic pathways, including biosynthesis nucleotides, nitric oxide, glutamate and proline, in several cancer types is arginine. Arginosuccinate, derived from the reaction catalyzed by argininosuccinato synthase (ASS), is converted into L-arginine and fumarate, an intermediate of TCA. Therefore, arginine is linked to glucose-generate energy metabolism via the TCA cycle. Recent clinical investigations have shown that some human cancers do not express ASS, leading to the inability of these cancer cells to generate *de novo* arginine. Thus, they were susceptible to arginine deprivation therapy [410].

Proline is a proteinogenic amino acid that contributes to collagen formation, the most abundant protein in the body [411]. Proline can be converted by a reversible reaction to glutamate, in which α-pyrroline-5-carboxylate (P5C) and glutamic-γ-semi-aldehyde (GSA) are used as intermediates. During this reaction, FAD is reduced to $FADH_2$, which may be used to generate ATP through OXPHOS. Proline dehydrogenase (oxidase) (PRODH/POX), which catalyzes the reaction from proline to P5C has a mitochondrial suppressor function and is induced by p53 and peroxisome proliferator-activated receptor gamma (PPARγ) and suppressed by c-Myc and microRNA-23, a small non-coding RNA molecule with RNA silencing function that thus inhibits gene expression of mRNA target [412]. The role of PRODH-mediated proline oxidation in cancer proliferation and survival has been well described [413].

Phenylalanine and tyrosine are aromatic amino acids involved in synthesizing protein and secondary metabolites implicated in various anabolic pathways. Phenylalanine is an essential amino acid required for the synthesis of the nonessential amino acid tyrosine. This conversion is catalyzed by the enzyme phenylalanine hydroxylase (PAH), which expression could be altered during inflammation and malignancy [414, 415]. Deficiency of the PAH gene correlates with phenylketonuria, an autosomal recessive disorder characterized by phenylalanine accumulation, which causes brain dysfunction [416]. Tyrosine is further catabolized into several catabolites, including pyruvate [417] fumarate, phenol [418], and catecholamines [419]. Tyrosine-derived catecholamine synthesis is efficiently regulated by the rate-limiting enzyme tyrosine hydroxylase (TH), which catalyzes the convection of tyrosine to L-dihydroxyphenylalanine (L-DOPA). TH protein synthesis primarily controls long-term regulation of TH activity, while short-term regulation is modulated by phosphorylation of three key Ser residues on TH, Ser19, Ser31, and Ser40 [420]. In particular, phosphorylation on Ser40 directly increases TH activity by relieving end-product feedback inhibition by the inhibition by the catecholamine [421]. Various studies have reported the dependency of different cancer types on tyrosine and phenylalanine. Restriction of tyrosine and phenylalanine induces apoptosis and inhibits invasion via inhibition of the GTP binding to Ras and Rho, two G proteins involved in cell movement and actin cytoskeletal arrangement, melanoma and prostate cancer cells [422]. The induction of apoptosis also depends on the alteration of mitochondrial integrity and function. Thus, loss of this integrity leads to the release of cytochrome c and apoptosis [423]. In addition, tyrosine and phenylalanine deprivation affects other mitochondrial functions. Restriction of these specific amino acids decreased ATP synthesis and mitochondrial ROS in melanoma cancer cells [424]. A recent study has reported that the impairment in tyrosine metabolism due to inactivation of the second tyrosine catabolic enzyme 4-hydroxyphenylpyruvate dioxygenase (HPD) regulated metabolic alteration through the activation of the AKT/mTOR signaling pathway in liver cancer, suggesting that tyrosine catabolism is closely associated with poor clinical outcome in liver cancer patients [425]. Several clinical investigations have reported decreased serum concentration of tyrosine and phenylalanine, while an

increase of these aromatic amino acids in tissue and urine of gastroesophageal cancer patients [426]. Moreover, a low expression of tyrosine catabolic enzyme correlates with poor survival in patients with liver cancer [427]. Despite tyrosine metabolism has not been well investigated in cancer development, there have been efforts to take advantage of tyrosine metabolism in the clinic. In fact, tyrosine PET tracers are a readout of the activity of the amino acid transporter LAT1 which expression and activity are elevated in various cancer types [428, 429]. Thus, tyrosine-based PET imaging techniques could be effective for therapeutic responses [430, 431].

Glutamine is the most important amino acid for the survival and proliferation of human cancers, which cancer cells use for both energy generation and, as a source of carbon and nitrogen, for biomass accumulation [432]. Glutamine is transported into cells through several membrane transporters and used for biosynthesis or exported back out of the cell by antiporters in exchange for other amino acids [433]. In addition, glutamine-derived glutamate can also be exchanged through the xCT (a heterodimer of two solute carrier transporters, SLC7A11 and SLC3A2) antiporter for cystine, which is quickly reduced to cystine inside the cell [434]. Glutamine is converted by mitochondrial glutaminases (GLS) to an ammonium ion and glutamate upon entry into the cells. In mitochondria, glutamate can then be converted to α-ketoglutarate (α-KG), which enters the TCA cycle to generate ATP through the production of NADH and flavin adenine dinucleotide ($FADH_2$). This reaction can be catalyzed by either glutamate dehydrogenase (GDH), an ammonia-releasing process, or by numerous non-ammonia-producing aminotransferase that transfer nitrogen from glutamate to produce another amino acid and α-KG [435]. In addition to energy and amino acids production, glutamine is involved in the lipogenesis process. Glutamine metabolism can serve as an alternative source of carbons for fatty acids synthesis. Indeed, glutamine-derived α-KG can be exported to the cytosol and reduced through reductive carboxylation to citrate, which is then cleaved to generate oxaloacetate (OAA) and acetyl-CoA, the substrate for fatty acid synthesis. It has been demonstrated that this reaction is important for cancer growth and involved in tumor progression [436-438]. Alternatively, glutamine-derived α-KG can generate pyruvate in the TCA cycle from malate via

glutaminolysis [439]. Many cancer cells utilized acetyl-CoA produced from glucose-derived pyruvate, but under glucose deprived-conditions, citrate produced by glutamine-derived α-KG can be converted to acetyl-CoA by ATP citrate lyase (ACLY) enzyme [440], inducing glutamine dependent lipid synthesis. A recent study showed that the import of glucose-derived pyruvate into mitochondria by mitochondrial pyruvate carrier (MPC) suppressed GDH activity and glutamine-dependent acetyl-CoA formation. The MPC inhibition activated GDH and diverted glutamine metabolism to generate both oxaloacetate and acetyl-CoA, indicating a compensatory mechanism that allows cancer cells to generate lipid in glucose deprived-conditions [441]. In addition, glutamine-derived fumarate, malate and citrate were increased during glucose deprivation, indicating that glutamine drives the glucose-independent TCA cycle during nutrient deprivation [440]. Moreover, glutamine provides carbon and nitrogen for the biosynthesis of non-essential amino acids and nucleotides. Indeed, glutamine provides an amide (γ-nitrogen) group contributing directly to *de novo* biosynthesis of purines and pyrimidines, which functions as a rate-limiting factor in cancer cell proliferation [442, 443]. It has been demonstrated that growth-promoting signals regulate the glutamine-derived nitrogen production, including c-Myc, which induces the expression of various enzymes of the nucleotide biosynthetic pathways, such as phosphoribosyl pyrophosphate amidotransferase (PPAT), a rate-limiting enzyme in the purine biosynthesis [444, 445]. In fact, PPAT expression has been observed to increase in human lung cancer and related to disease in patients [446]. Moreover, glutamine can contribute to nucleotides synthesis through other pathways. Aspartate derivate from glutamine via the TCA cycle is required for *de novo* purine synthesis and provides carbons for *de novo* pyrimidine synthesis [447]. Indeed, aspartate supplementation can rescue cell cycle arrest caused by glutamine deprivation in cancer cells [448]. Glutamine metabolism reprogramming is activated by oncogenic alteration, such as c-Myc and Kirsten rat sarcoma viral oncogene homolog (KRAS) gene, and anti-oncogenic alterations, such as p53 and retinoblastoma (Rb). c-Myc overexpression upregulates GLS [449] and increases both the expression of high-affinity glutamine transporters and glutamine synthetase (GS) [450-452], making cells dependent on exogenous

glutamine for cell survival. KRAS has been shown to reprogram glutamine metabolism by aspartate transaminase (GOT1) and repressing GDH in pancreatic cancer [453]. Glutamine metabolism is regulated by p53, a tumor suppressor that induces GLS, reducing cellular sensitivity to ROS-associated apoptosis via glutathione-dependent antioxidant defense [454]. Another tumor suppressor, Rb, can regulate glutamine metabolism through the modulation of various glutamine transporter leading to a reduction of glutamine uptake [455].

Chapter 2. Materials and Methods

2.1 Materials

- Unless specified, all reagents used for cells culture were purchased from Euroclone group, Invitrogen and Sigma-Aldrich.
- Reagents for real-time PCR were from Qiagen.
- Solutions and equipment for protein analysis were purchased from Biorad.
- Ripa buffer, proteases and phosphatases inhibitors were from Sigma-Aldrich.
- Bradford reagent for protein dosage and all materials for SDS-PAGE were from Biorad.
- Chemiluminescence revelation kit was from Biorad.

2.1.2 Drugs and Compounds

- Tyrosine: dissolved in 1 M HCl at 25 mg/ml stored at RT purchased from Merck Life Science (T4321 - 100G).
- Phenylalanine: dissolved in 1 M HCl at 50 mg/ml stored at RT purchased from Merck Life Science (P5482 – 10 MG).
- 2-DG: dissolved in Phoshate buffered saline (PBS) at 100 mg/ml stored at +4°C purchased from Merck Life Science.
- SR59230A: dissolved in H_2O at 10 mM stored at – 20°C purchased from Tocris Bioscence (1511).
- Propanolol: dissolved in H_2O at 50mg/mL stored at 4°C purchased from Merck Life Science.
- Atenolol: dissolved in H_2O at 0.3 mg/mL stored at RT purchased from Merck Life Science.
- PMA: dissolved in DMSO at 10 mg/mL stored at – 20°C purchased from Merck Life Science.
- PBN: dissolved in DMSO at 50 mg/mL stored at – 20°C purchased from Merck Life Science.

- NTBC: dissolved in DMSO at 5 mg/mL stored at – 20°C purchased from Merck Life Science

2.1.3 Common use solution

- PBS (Phosphate buffered saline): 0.27 g/L KH2PO4, 0.2 g/L KCL, 8.0 g/L NaCl, 2.16 g/L Na2HPO4-7H2O.
- SDS−PAGE 4X Sample Buffer: 40% Glycerol, 240 mM Tris/HCl pH 6.8, 8% SDS, 0.04% bromophenol blue, 5% β-mercaptoethanol.
- SDS-PAGE 1X running buffer: 25 mM Tris, 192 mM glycin, 0.1% (W/V) SDS, pH 8.3.
- SDS-PAGE 1X blotting buffer: 25 mM Tris, 192 mM glycin, 10% methanol, pH 8.3.
- Blocking solution: non-fat dry milk 5 %, tween 0.05 % in PBS.
- Washing solution: tween 0.1 % in PBS (T-PBS).

2.1.4 Antibodies

Antibody	Application	Diluition	Use	Source	Manifacturer
HK2	WB	1:1000	O/n 4°C	Mouse	Abcam
β-actin	WB	1:1000	O/n 4°C	Mouse	Santa Cruz

2.1.5 Cell lines

The rhabdoid tumor G-401 (CRL-1441) cells, osteosarcoma K7M2 (CRL-2836) murine cells and macrophages RAW 264.7 (TIB-71) murine cells were from American Type Culture Collection (ATCC). G-401 cells were cultured in McCoy's 5A Modified Medium (Sigma-Aldrich) supplemented with 10% Fetal Bovine Serum (FBS, Euroclone), 2 mM L-glutamine and penicillin/streptomycin solution (1x) (both Euroclone). K7M2 cells were cultured in Dulbecco's Modified eagle's medium high glucose (4.5 g/L) (DMEM) (Gibco, Euroclone) plus FBS, 2 mM L-glutamine and penicillin/streptomycin solution (1x). RAW 264.7 cells were

cultured in phenol red-free Roswell Park Memorial Institute (RPMI) supplemented with FBS, 2 mM L-glutamine and penicillin/streptomycin solution (1x). Cells were amplified, stocked, and once thawed were kept in culture for a maximum 3 months.

2.1.6 Cell culture medium

Custom made medium used for cell treatments were purchased from Cell Culture technologies LLC. Custom medium contains glucose (3 g/L) as McCoy's 5A Modified Medium. Glutamine (2 mM), tyrosine (104 mg/L) were added at the moment of treatment.

2.2 Methods

2.2.1 General culture conditions

Cell lines were grown under 5% CO_2 at 37°C in their respective media. When passaging cells, growth medium was removed, washed with PBS and the cells incubated with a covering volume of trypsin. After the cells were detached, media was added to the cells to neutralize the trypsin and the cells seeded into a new plate.

2.2.2 Frozen storage cells

Cells were detached using trypsin, re-suspended in the culture medium and pelleted by centrifugation at 1200 rpm for 5 minutes. The cells were re-suspended in 1 ml of cell freezing medium (90% complete growth medium and 10% DMSO) and then moved in specific freezing vials. Vials wee then placed in polystyrene insulated boxes at -80°C.

2.2.3 Protein manipulation

Protein extraction: cells were washed twice in PBS solution and then lysed with RIPA lysis buffer supplemented with proteases and phosphatases inhibitors. Protein lysates were collected, kept in ice and centrifuged at 12000 rpm for 10 minutes. After centrifugation, the supernatant was collected and total proteins were quantified with Bradford assay.

Protein quantification: protein quantification is evaluated with Coomassie Brilliant Blue (Bradford protein assay), which binds to basics and aromatics amino acidic residues (especially arginine) of the proteins, leading to maximum absorption at 595 nm wavelength. Thus, Coomassie Brilliant Blue intensity is positively correlated to protein concentration. To obtain the standard curve of reference, we used Bovine Serum Albumine (BSA), diluting BSA 2 mg/ml concentrated in deionized water and then obtaining rising BSA concentrations from 2 µg/mL to 15 µg/mL. Then Bradford reagent is prepared diluting 1/5 of starting solution with Coomassie Brilliant Blue in 4/5 of deionized water. To run the assay, 5 µL of each sample, opportunely diluted in 45 µL of water, were added to 950 µl of the working solution. After 5 minutes incubation, the absorbance of each sample is evaluated at a wavelength of 595 nm, subtracting the blank value. From the values obtained from the standard curve it is possible to create a curve of absorbance in function of its concentration, thus, interpolating absorbance values to the standard curve, it is possible to calculate the final protein concentration. Correlation between absorbance and concentration is expressed by Lambert-Beer law: $A=\varepsilon dc$, where ε represents the molar extinction coefficient, d the path length and c represent sample concentration. For each Western Blotting experiment from 20 to 50 µg of total proteins are loaded in each lane on a 4–20% pre-cast Mini-PROTEAN TGX Gel.

Polyacrylamide gel electrophoresis: it is a technique utilized for proteins separation based on their ability to move within an electric current, based on the length of their polypeptide chains or of their molecular weight.

SDS polyacrylamide gel electrophoresis (SDS- PAGE) samples are boiled for 5 minutes in a sample buffer containing SDS and β-mercaptoethanol, which leads to disulphuric bonds reduction and destabilization of eventual protein tertiary structure. In addition, sample buffer is supplemented with bromophenol blue, ionizing coloured-tracking solution for the electrophoretic run, and glycerol, which increases sample density and promotes its stratification at the bottom of the loading well.

Once the samples are loaded in the stacking gel, an electric field is applied across the gel, causing the negatively-charged proteins to migrate across the gel

towards the positive electrode (anode). Stacking gel, characterized by very low acrylamide concentration (4%), is required to better stratify the samples before entering the separating gel. Proteins relative molecular mass is evaluated by comparison with protein ladder standard molecular weights, separated in the same gel. Running is carried on at 100V for almost 1 h.

Western blotting: Once the protein samples are run, in order to make the proteins accessible to antibody detection, they are moved from within the gel onto a membrane made of polyvinylidene difluoride (PVDF). The method for transferring the proteins is called blotting and uses the Trans-Blot Turbo Transfer Pack to pull protein from the gel into the PVDF membrane. The proteins embedded into the gel are transferred onto the membrane while maintaining the organization they had within the gel. Proteins transfer is carried out at 25V, 2.5A for 7 minutes (for proteins with low molecular weight) or 10 minutes (for proteins with high molecular weight). After blotting the PVDF membrane is incubated overnight in slow agitation at 4°C with specific primary antibodies in a blocking solution containing non-fat dry milk 3% and Tween 0.05%. After incubation, the membrane is washed three times with a washing solution containing PBS 1X and Tween 0.1% and, in order to reveal the specific protein, the membrane is incubated with horseradish peroxidase (HRP) conjugated secondary antibody for 1h at room temperature and then washed again for three times. In the chemiluminescence reaction horseradish peroxidase catalyzes the oxidation of luminol into a reagent which emits light when it decays. Since the oxidation of luminol is catalyzed by HRP, and the HRP is complexed with the protein of interest on the membrane, the amount and location of emission light is directly correlated with the location and amount of protein on the membrane. Chemiluminescent protein revelation is carried out with ECL Western Blotting reagents and developing of blots is carried out at the ChemiDoc (Biorad). Exposure is repeated, varying the time as needed for optimal detection.

2.2.4 Quantitative real-time RT-PCR (qRT-PCR)

Total RNA was extracted from tissue culture cells, grown as a monolayer, using RNasy Plus Mini Kit (Qiagen). RNA concentration and quality of the samples

were determined by measuring the UV absorbance at 260 nm and 280 nm on Nanodrop 1000 (Thermo Scientific) and 1µg of total RNA were reverse transcribed to strands of cDNA using iScript gDNA Clear DNA Synthesis Kit according to the manufacturer's instructions (Biorad). mRNA expression by qRT-PCR analysis was performed using Sso Advanced Universal SYBR Green Supermix (Biorad) for GLUT1 (qHsa CID0022232), HPD (qHsa CID0017734). Data were normalized on GAPDH (qHsa CED0038674).

2.2.5 Lactate assay

G-401 cells were plated in 24-well culture dishes and treated as reported in the Figures and described in the Results section. Lactate concentration was evaluated by using Lactate Colorimetric/Fluorometric Assay Kit (K607-100, Biovision). Cells culture medium were filtered with 0.2 µm filters and 20 µl/well of test samples were added to a 96-well plate and volume were adjusted to 50 µl/well with Lactate Assay Buffer. A total of 50 µl Reaction Mix, containing 46 µl of Lactate Assay Buffer, 2 µl of Lactate Enzyme Mix and 2 µl of Probe, were added to each well containing the Lactate Standards and test samples. The reaction was incubated for 30 minutes at room temperature protected from light and quantified measuring absorbance at 570 nm wavelength using a microplate reader. The lactate concentration was calculated by subtracting the 0 standard reading from all readings and applying the corrected absorbance to the Lactate Standard Curve to obtain the nmol of Lactate in the sample wells. Lactate concentration was normalized on cell counts.

2.2.6 ATP production

G-401 and 17.94 cells were plated in flat bottom white 96-well microplate and treated as reported in the Figures and described in the Results section. ATP concentration was evaluated by using ATPlite 1step (10 mL kit, PerkinElmer) based on the production of light caused by the reaction of ATP with added luciferase and D-luciferin, according to the reaction ATP+ D-luciferin + O_2 $\longrightarrow$ Oxyluciferin + AMP + PP_i + CO_2 + light. 30 minutes before starting the assay, the microplate was removed from the incubator to adapt to room temperature. The

lyophilized substrate solution was reconstituted with 10 mL of substrate buffer solution, mixed by inversion and left to stand for 5 min. 100 µl of the reconstituted solution were added to each well containing cells and the microplate were shaken for 2 minutes at 700 rpm using an orbital microplate shaker with an orbit diameter of 2 mm. For stabilize the luminescent signal the microplate was adapted to dark for 10 minutes and subsequently quantified measuring luminescence using a microplate reader. The emitted light is proportional to the ATP concentration and data were normalized on cell counts.

2.2.7 Mitochondria isolation

G-401 cells were plated in p100 dishes and treated as reported in the Figures and described in the Results section. Mitochondria isolation was performed by using Mammalian Mitochondria Isolation Kit for Tissue and Cultured Cells (K288-50, Biovision). 2 $x10^7$ cells were collected, centrifugated at 600 x g for 10 minutes and then the supernatant was removed carefully. 1 ml of Mitochondria Isolation Buffer were added to the cell pellet and vortexed for 5 seconds, followed by incubation on ice for 2 minutes. Then, 10 µl of Reagent A were added to cells, vortexed for 5 seconds, incubated on ice for 5 minutes while vortexing every minute for 5 seconds and centrifugated at 600 x g for 10 minutes at 4°C. The supernatant was collected in a separate tube and centrifugated at 7,000 x g for 10 minutes at 4°C. After centrifugation, the supernatant was discarded, the pellet washed with Mitochondria Isolation Buffer and centrifugated at 600 x g for 10 minutes at 4°C. After centrifugation, the pellet was resuspended in 100 µl of Storage Buffer and stored a -80°C for future use.

2.2.8 Succinate dehydrogenase activity

Mitochondria isolated from G-401 were used for the evaluation of succinate dehydrogenase activity assed by using the Succinate Dehydrogenase Activity Colorimetric Assay Kit (K660-100, Biovision). 20 µl/well of isolated mitochondria were added to a 96-well microplate and the volume adjusted to 50 µl with SDH Assay Buffer. For the SDH positive control, 20 µl of SDH Positive Control were added into a single well and the volume were adjusted to 50 µl with SDH Assay

Buffer. A total of 50 µl Reaction Mix, containing 46 µl of SDH Assay Buffer, 2 µl of SDH Substrate Mix and 2 µl of Probe, were added in each well containing the cells and the positive control. The absorbance was measured immediately at 600 nm wavelength in kinetic mode for 10-30 minutes using a microplate reader. In this assay, succinate dehydrogenase converts succinate to fumarate and transfers the electron to a probe, which changes the color from blue to a colorless product depending on the sample enzymatic activity, according to the reaction Succinate + SDH-FAD $\longrightarrow$ Fumarate + SDH-$FADH_2$ $\longrightarrow$ Product (colorless). Two different absorbance measurement at two different time points were chosen to calculate the amount of succinate dehydrogenase that generates 1.0 µmol of 2,6-Dichlorophenolindophenol (redox dye) per min and normalized to cell counts.

2.2.9 Fumarase activity

Mitochondria isolated from G-401 cells were used for the evaluation of fumarase activity assessed by using the Fumarase Activity Colorimetric assay Kit (K596-100, Biovision). 20 µl/well of isolated mitochondria were added to a 96-well microplate and the volume adjusted to 50 µl with Fumarase assay Buffer. A total of 50 µl Reaction Mix, containing 36 µl of Fumarase Assay Buffer, 2 µl of Fumarase Enzyme Mix, 10 µl of Fumarase Developer and 2 µl of Fumarate Substrates were added in each well containing the cells standard and the positive control. The absorbance was measured immediately at 450 nm wavelength in kinetic mode for 10-60 minutes using a microplate reader. In this assay, fumarase converts fumarate into malate, which then reacts with Enzyme Mix to form an intermediate that subsequently reduced the developer to a colored product, according to the reaction Fumarate + H_2O $\rightarrow$ Malate Intermediate $\rightarrow$ Color detection. Two different absorbance measurement a two different time points were chosen to calculate the amount of fumarase that generates 1.0 µmol of NADH per min and normalized to cell counts.

2.2.10 Fumarate detection

G-401 cells were plated in 24-well culture dishes and treated as reported in the Figures and described in the Results section. Fumarate detection was

performed by using Fumarate Detection Kit (ab102516, Abcam). Cells were collected and centrifugate at 13,000 x g for 10 minutes to remove insoluble materials. After centrifugation, 20 µl/well of supernatants were added to a 96-well microplate and diluted in the Fumarate Assay Buffer to a final volume of 50 µl. A 50 µl of reaction Mix, consisting of 90 µl of Fumarate assay Buffer, 8 µl of Fumarate Developer and 2 µl of Fumarate Enzyme Mix, were added to each well containing the Fumarate Standard and test samples. The reaction was incubated for 60 minutes at 37°C protected from the light and then quantified measuring absorbance at 450 nm wavelength using a microplate reader. The Fumarate Enzyme Mix recognizes fumarate as a specific substrate leading to proportional color development. The fumarate concentration was calculated by subtracting the 0 fumarate control from all sample readings and applying the corrected absorbance to the Fumarate Standard curve to obtain the µM of fumarate in the sample wells. Fumarate concentration were normalized on protein content.

2.2.11 Flow cytometry analysis

Tibial nerves were dissected from euthanized mice and mechanically dissociated to obtain a single cell suspension. Nerve were dissociated in a solution containing HEPES (25 mM), Hanks' Balanced Salt solution (HBSS, 1x), FBS 10% and dnase (10µM) by using the gentleMACS Octo Dissociator (Miltenyi Biotec). Cells were stained with anti-CD45-VioBlue conjugated antibody (130-110-664, Miltenyi Biotec), anti-F4/80-PE conjugated antibody (130-116-449, Miltenyi Biotec), and anti-CD64-APC conjugated antibody (130-126-950, Miltenyi Biotec). G-401 and 17.94 cells were plated in 12-well culture dishes and treated as reported in the Figures and described in the Results section. Cells were collected and centrifugated at 1,200 rpm for 5 minutes. After centrifugation the supernatants were resuspended in autoMACS Running Buffer (130-091-221), fixed, permeabilized and stained with anti-Ki-67-FITC conjugated antibody (130-117-691, Miltenyi Biotec), and anti-Glucose Transporter GLUT1-PE conjugated antibody (ab209449, Abcam). For glucose uptake assay, G-401 and 17.94 cells were washed with PBS and 2-NBDG-FITC (600470, Cayman Chemical) were added to a final concentration of 100 µg/ml in PBS. After 20

minutes of incubation, cells were detached and collected and centrifugated at 1,200 rpm for 5 minutes. After centrifugation, the pellet was resuspended in 200 µl of Cell-Based assay Buffer and centrifugated again. After staining, cells were subjected to flow cytometry by using a Miltenyi Biotec MACSQuant Analyzer 10. Results were analyzed by using FlowlogicTM Software.

2.2.12 H_2O_2 Assay

H_2O_2 level was assessed by using the Amplex Red® assay (Thermo Fisher Scientific). Tibial nerve tissue was rapidly removed and placed into modified Krebs/HEPES buffer [composition in mmol/l: 99.01 NaCl, 4.69 KCl, 2.50 CaCl2, 1.20 MgSO4, 1.03 KH2PO4, 25.0 NaHCO3, 20.0 Na-HEPES, and 5.6 glucose (pH 7.4)]. Samples were minced and incubated with Amplex red (100 µM) and HRP (1 U/ml) (1 h, 37°C) in modified Krebs/HEPES buffer protected from light. Fluorescence excitation and emission were at 540 and 590 nm, respectively. H_2O_2 production was calculated using H_2O_2 standard and expressed as µmol/l of mg of dry tissue. RAW 264.7 cells were seeded in 96-well plates (30.000 cells/well) and grown in phenol red-free Roswell Park Memorial Institute (RPMI). The cultured medium was replaced with Krebs-Ringer phosphate (KRP, composition in mM: 2 CaCl2; 5.4 KCl; 0.4 MgSO4; 135 NaCl; 10 D-glucose; 10 HEPES [pH 7.4]) added with SR59230A, propranolol, atenolol (all, 100 nM) or vehicle (0.01% DMSO in KRP) for 20 min at room temperature. Cells were activated by the addition of phorbol-myristate-acetate (PMA, 16 µM), along with Amplex Red (50 µM) and HRP (1 U/ml) at a total volume of 100 µl. Signal was detected 60 min after exposure to the stimuli, at 560 nm H_2O_2 release was calculated using H_2O_2 standards and expressed as nmol/l.

2.2.13 Immunofluorescence

The tumor and tibial nerve were dissected from anesthetized and transcardially perfused with PBS, followed by 4% paraformaldehyde, mice. The tibial nerve and the hindlimb were postfixed for 24 h, and cryoprotected in sucrose 30%. Immunofluorescence staining was performed according to standard procedures. Briefly, after the antibody retrieval with citrate buffer pH 6, tissue sections (10

μm) were incubated with the following primary antibodies: F4/80 [1: 50, MA516624, rat monoclonal (Cl:A3-1), RRID:AB_2538120 Thermo Fisher Scientific], PGP9.5 (1:250, ab108986, rabbit monoclonal, RRID:AB_ 10891773 Abcam), β1 receptor (1:400, ab3442, rabbit polyclonal, RRID:AB_ 10890808 Abcam), β2 receptor (1:100, ab182136, rabbit monoclonal, RRID:AB_2747383 Abcam), β3 receptor (1:100, ab94506, rabbit monoclonal, RRID:AB_ 10863818 Abcam) diluted in block solution (5% normal goat serum and normal donkey serum, in PBS and triton-x100, PBST) 1 h at room temperature. Sections were then incubated for 2 h in the dark with the fluorescent secondary antibody polyclonal, Alexa Fluor® 488 (1:600, Thermo Fisher Scientific) or Alexa Fluor® 594 (1:600, Thermo Fisher Scientific). Sections were coverslipped using a water-based mounting medium with 4′6′-diamidino-2-phenylindole (DAPI, Abcam). The analysis of negative controls (non-immune serum) was simultaneously performed to exclude the presence of non-specific immunofluorescent staining, cross-immunostaining, or fluorescence bleed-through. For histological evaluation, sections were stained with hematoxylin/eosin and based on the morphology, the boundaries of the nerve trunk corresponding to the epineurium were identified and reported in adjacent immunofluorescence images with dashed lines. The number of F4/80+ cells was counted in 104 μm2 boxes in the tibial nerve trunk.

2.2.14 Mechanical Allodynia

The measurement of mechanical paw withdrawal threshold (PWT) was carried out using von Frey filaments of increasing stiffness (0.02–2 g) applied to the plantar surface of the mouse hindpaw, according to the up-and-down paradigm. The 50% mechanical paw-withdrawal threshold (g) response was then calculated from the resulting scores.

2.2.15 *In vivo* experiments

BALB/c mice (male, 4 weeks old, Envigo RMS) were used. Mice were housed in a temperature- and humidity-controlled vivarium (12 h dark/light cycle, free access to food and water). Behavioral experiments were done in a quiet,

temperature-controlled (20–22°C) room between 9 am and 5 pm and were performed by an operator blinded to the drug treatment. Animals were anesthetized with a mixture of ketamine and xylazine (90 mg/kg and 3 mg/kg, respectively, i.p.) and euthanized with inhaled CO2 plus 10–50% O2. For cells inoculation, 50 µl of K7M2 (7 × 105) cells were suspended in PBS and injected para-tibial. Control groups (sham) were injected with 50 µl of PBS. K7M2 cell lines are isogenic with the BALB/c mouse strain. Tumor growth rate was evaluated by measuring tumor mass with a caliber, and tumor mass volume calculated as volume = [(length x width)2/2]. Mice were sacrificed at day 20 after K7M2 cells inoculation or sham. SR59230A, propranolol and atenolol (10 mg/kg i.p.) or vehicle (NaCl 0.9%) were administered twice a day (every 8 h) starting from day 10 after K7M2 cells inoculation, when a palpable tumor was present, or sham. Phenyl-alpha-tert-butyl nitrone (PBN, 100 mg/kg, i.p.) or vehicle (4% dimethyl sulfoxide, DMSO, 4% tween 80 in 0.9% NaCl) was given at day 14 after K7M2 cells inoculation.

2.2.16 Statistical analysis

The group of n = 6 animals for behavioral experiments was determined by sample size estimation using G*Power (v3.1) to detect size effect in a post-hoc test with type 1 and 2 error rates of 5 and 20% respectively. Mice were allocated to vehicle or treatment groups using a randomization procedure (http//:www.randomizer.org/). Investigators were blinded to the treatments, which were revealed only after data collection. No animals were excluded from experiments.

Densitometric analysis of the WB bands was performed by ImageJ software. Graphical representations were obtained by Graphpad Prims 8.0 (GraphPad Software, San Diego, CA) and statistical analyses were performed using Unpaired student's *t*-test, one-way and two-way ANOVA analysis of variance followed by Dunnett and Bonferroni's post hoc test as described in the figure legend and Results section. Differences were considered statistically significant when $p < 0.05$.

Chapter 3. Role of β-ARs in cancer-associated pain

3.1 Introduction

Although numerous clinical investigations have allowed us to identify some potential genetic markers involved in the onset and growth of pediatric cancers, they still remain the second leading cause of death in children. Different pharmacological compounds have been developed to target these altered signaling pathways. However, given the adaptability of tumor cells, targeting a single growth factor or a downstream signaling hub likely leads to a compensatory mechanism and many patients fail to benefit from these therapeutic approaches. As extensively described in the Introduction section, the β3-ARs have been proposed to contribute to the initiation and proliferation of several cancer types, including childhood cancers, by regulating inflammation, angiogenesis, cell motility and cellular immune response [147, 166, 170]. Different studies have elucidated the potential role of β3-ARs blockade to contrast tumor growth and progression.

The final goal of this project was to identify and characterize the involvement of β3-ARs in pediatric tumors, with a particular focus on cancer-evoked pain and neuroinflammation. Understanding the involvement of β3-ARs in cancer evoked pain in osteosarcoma can allow us to identify a novel therapeutic targets for this condition.

3.2 Results

3.2.1 K7M2 osteosarcoma cell inoculation induces tumor growth and allodynia in BALB/c mice.

As described in the Material and Methods section, K7M2 cell line is a murine cellular model of osteosarcoma. Therefore, para-tibial inoculation of K7M2 cells into the hindlimb of BALB/c mice, induced a rapid tumor growth in the soft tissue from the eighth day after K7M2 inoculation (Figure 14A). The increase in tumor growth is associated with a time-dependent (0-20 days) hindlimb thickness and

with a parallel increase in mechanical allodynia in the hind paw ipsilateral to the injected site compared to sham mice, as showed by mechanical paw-withdrawal threshold (PWT) that is considered the force at which withdrawal occurred after stimulation with a monofilament that delivers a constant pre-determinate force (Figure 14B). Reduction in the PWT correlates with increased mechanical allodynia. These results indicated a time-dependent association between the osteosarcoma tumor mass growth and the development of mechanical allodynia.

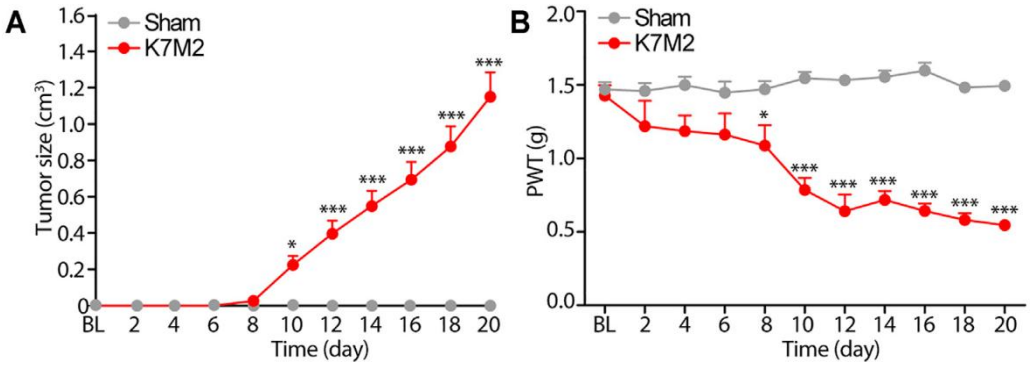

Figure 14. Tumor growth and mechanical allodynia induce by K7M2 osteosarcoma cells in BALB/c mice. A, 50 µl of K7M2 (7 x 10^5) cells were suspended in PBS and then injected para-tibial in BALB/c mice. Sham (control) were injected with 50 µl of PBS. Mice were sacrificed at day 20 after K7M2 cells inoculation or sham, and the tumor mass were measured. B, mechanical allodynia was measured from day 0 to day 20. BL, baseline. PWT, paw withdrawal threshold. N = 6. *p < 0.05, ***p < 0.001 K7M2 vs Sham. Two-way ANOVA and Bonferroni post hoc test.

3.2.2 Para-tibial K7M2 cells inoculation induces the recruitment of macrophages in tibial nerve.

To investigate the involvement of peripheral nerve macrophages in the development of pain in mouse model of neuropathic cancer pain, monocytes/macrophages inside the inoculated hindlimb were evaluated by flow cytometry and immunofluorescence analysis. Tibial nerve trunk ipsilateral to the inoculated hindlimb showed an increased number of F4/80+/CD64+ monocytes/macrophages associated with tumor growth. Sham did not increase the number of monocytes/macrophages inside the tibial nerve (Figure 15A, B),

suggesting an association between tumor growth in K7M2 osteosarcoma-bearing mice and an increased neuroinflammation in the tibial nerve, as indicated by the increased number of macrophages.

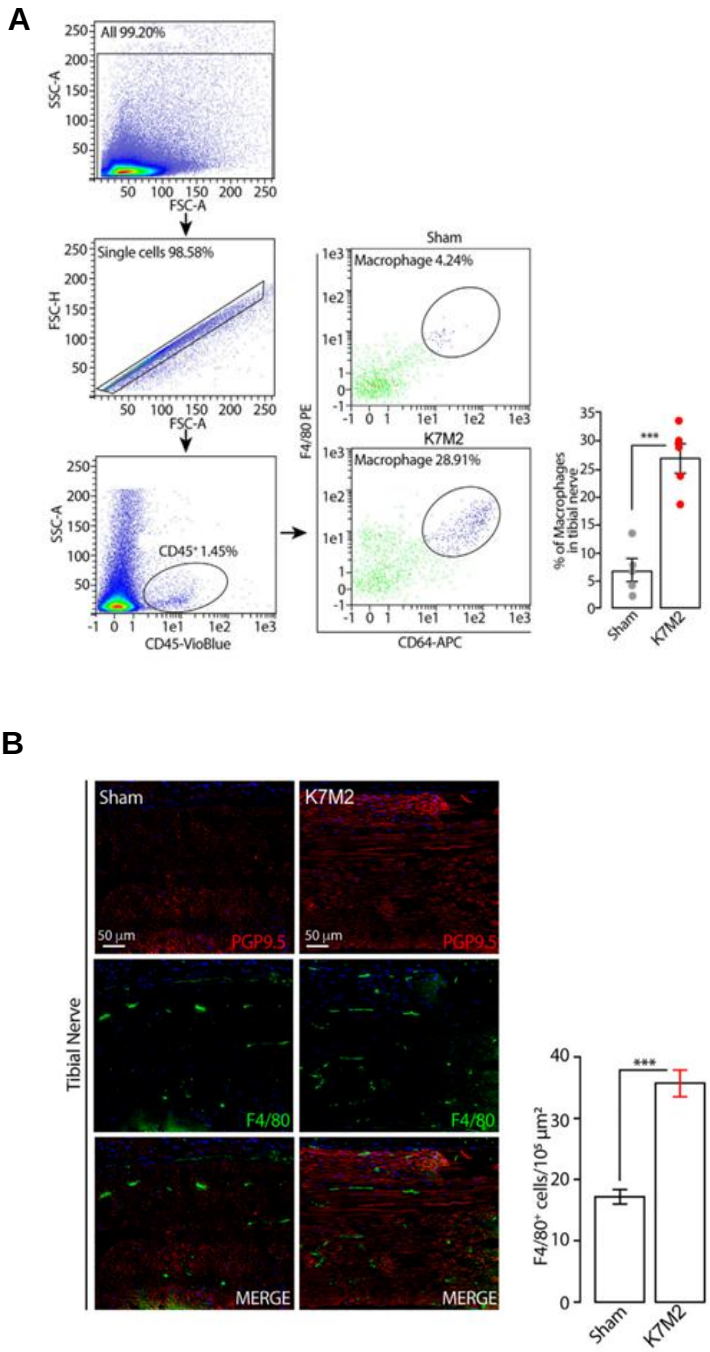

Figure 15. Tibial nerve displays an increased number of F4/80$^+$/CD64$^+$ monocytes/macrophages compared to sham. A, Gating strategy of flow cytometry analysis and relative quantification of F4/80$^+$/CD64$^+$ monocytes/macrophages in tibial nerve, compared to sham mice, after tibial nerve dissociation, and staining with anti-CD45-VioBlue conjugated antibody, anti-F4/80-PE conjugated antibody, and anti-CD64-APC conjugated

antibody. B, typical images and pooled data of F4/80$^+$ cells in the ipsilateral tibial nerve. Tumor and tibial nerve were dissected, fixed and then incubated with F4/80 and PGP9.5 (neuronal marker). N=6. *p < 0.05, ***p < 0.001 K7M2 vs Sham. Data are presented as mean ± SEM, data points overlaid. Unpaired student t-test.

3.2.3 *β*-ARs antagonism reduces osteosarcoma tumor growth and mechanical allodynia.

To investigate the possible involvement of the *β*-ARs in the modulation of tumor growth and mechanical allodynia induced by para-tibial inoculation of K7M2 osteosarcoma, mice were treated with the *β*1-antagonist atenolol, the *β*1/*β*2-antagonist propranolol and the *β*3-antagonist SR59230A. The treatments have been carried out 10 days after K7M2 osteosarcoma cells inoculation, when allodynia was already present. The treatment with the antagonist's propranolol and SR59230A induced a reduction in tumor size, while the treatment with atenolol reduced slightly, but not significantly, the tumor size, suggesting the crucial role of *β*2- and *β*3-ARs and a minor role of *β*1-ARs in regulating osteosarcoma tumor growth (Figure 16A). Interestingly, treatment with the *β*2- and *β*3-AR antagonists, but not with *β*1-antagonist, markedly reduced mechanical allodynia in K7M2 osteosarcoma-bearing mice (Figure 16B). To investigate the role of the *β*-ARs signaling in tumor and macrophages accumulating in the neuronal space, we first evaluated the expression of the three *β*-ARs in both tumor cells and macrophages inside the tibial nerve. Immunofluorescence analysis showed that tumor cells express all of the three *β*-ARs subtypes (Figure 16C), whereas macrophages located in the tibial nerve expressed only the *β*2- and *β*3-AR subtypes but not the *β*1-AR (Figure 16D). These results suggest that *β*1-AR blockade have a minor influence on osteosarcoma tumor growth and mechanical allodynia. In contrast, *β*2- and *β*3-AR blockade is able to impact osteosarcoma tumor growth and to attenuate mechanical allodynia resulting from osteosarcoma tumor growth.

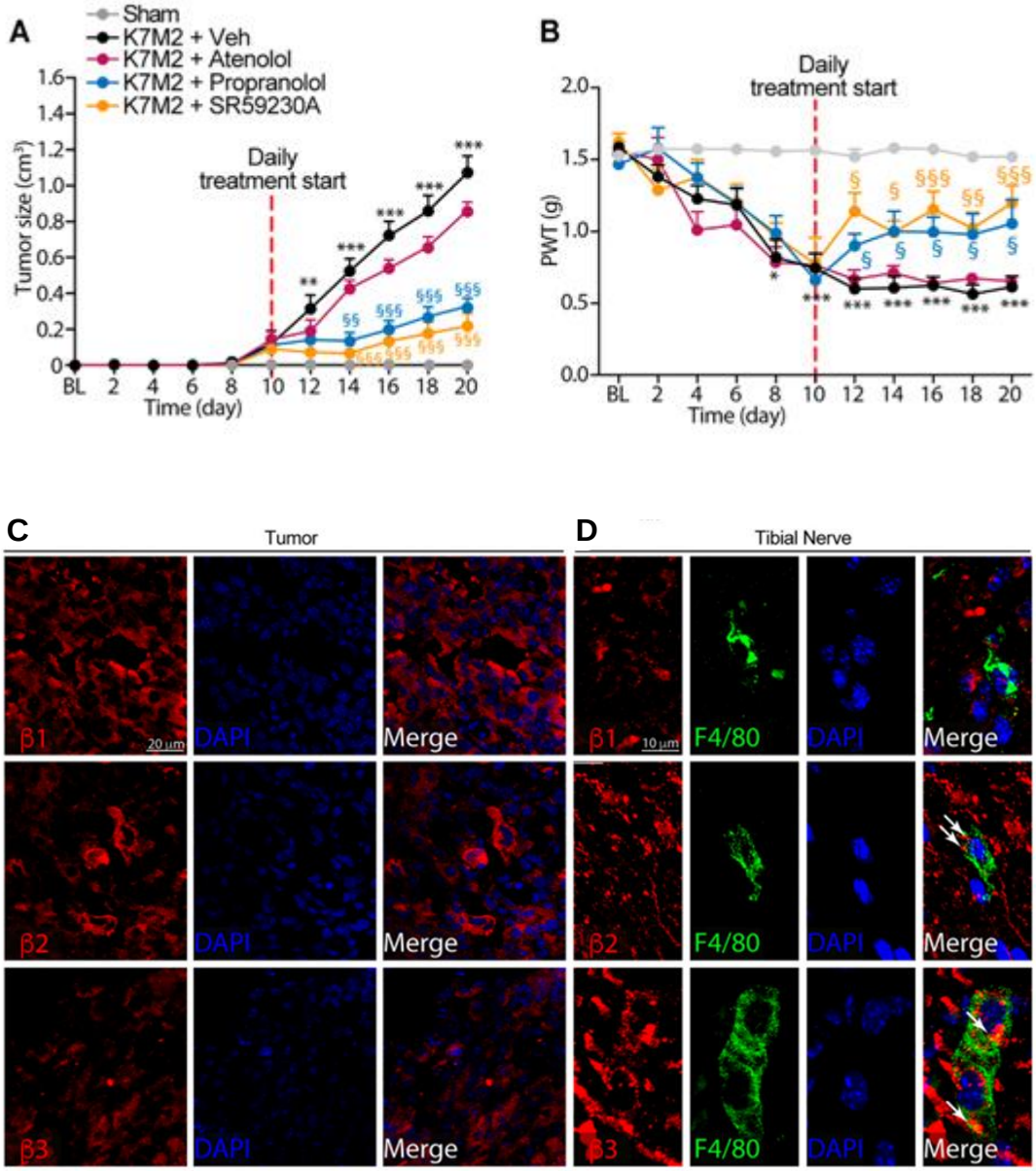

Figure 16. *β*2- and *β*3-AR, but not *β*1-AR antagonist treatment reduces K7M2 osteosarcoma growth and mechanical allodynia in BALB/c mice. A and B, time dependent increase in K7M2 osteosarcoma tumor growth and reduction of mechanical allodynia in BALB/c mice or sham administrated daily with atenolol (10 mg/kg i.p.), propanolol (10 mg/kg i.p.), SR59230A (10 mg/kg i.p.) or vehicle (Veh) after 10 days following cells inoculation. C and D, immunofluorescence images of *β*1-, *β*2- and *β*3-ARs expression in both tumor and macrophages, and F4/80^{+} expression in macrophages in tibial nerve after 20 days to para-tibial K7M2 osteosarcoma cells inoculation. BL, baseline. PWT, paw withdrawal threshold. N _ 6 mice. **p < 0.01, ***p < 0.001 vs Sham; §p < 0.05, §§p < 0.01, §§§p < 0.001 vs K7M2 + Veh. Data are presented as mean ± SEM. Two-way ANOVA and Bonferroni post hoc test.

3.2.4 *β*2- and *β*3-ARs antagonism impairs macrophages in BALB/c mice.

Given the efficacy of *β*2- and *β*3-ARs antagonists in reducing mechanical allodynia, we investigated if *β*2- and *β*3-ARs antagonism could modulate the number of macrophages recruited in the tibial nerve of K7M2 osteosarcoma-bearing mice. The treatment with propranolol and SR59230A showed a significant reduction in the number of macrophages located in the tibial nerve compared to vehicle-treated mice, whereas atenolol treatment had no effect in macrophages recruitment as showed by flow cytometry (Figure 17A) and immunofluorescence analysis (Figure 17B).

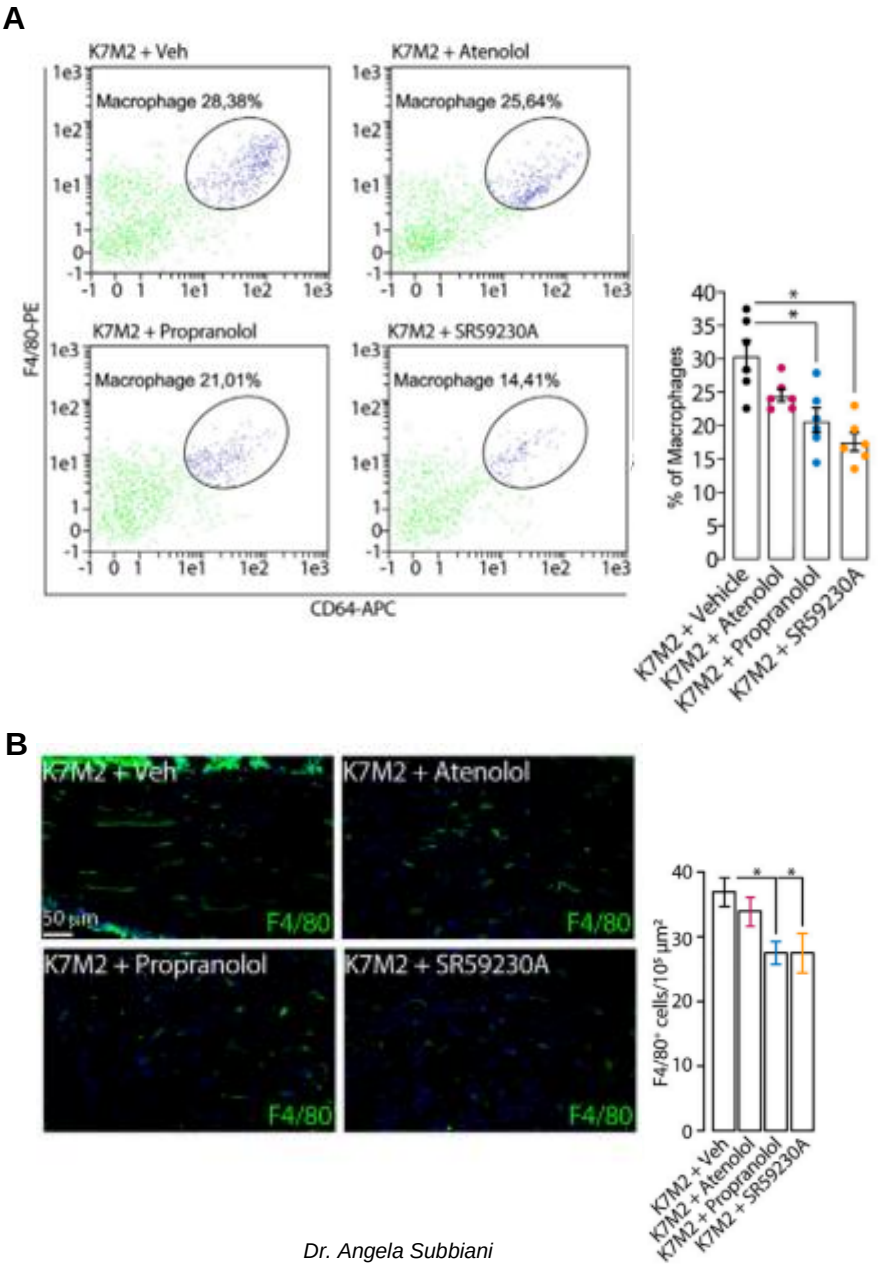

Figure 17. β2- and β3-AR antagonists reduce the number of macrophages in tibial nerve of K7M2 osteosarcoma-bearing mice. A and B, representative flow cytometry analysis and relative quantification of F4/80$^+$/CD64$^+$ macrophages, and immunofluorescence images and poled data of F4/80$^+$ macrophages after 20 days from para-tibial K7M2 osteosarcoma cell inoculation in BALB/c mice treated daily with atenolol (10 mg/kg i.p.), propanolol (10 mg/kg i.p.), SR59230A (10 mg/kg i.p.) or vehicle (Veh). N=6. *p < 0.05. Data are presented as mean ± SEM. One-way ANOVA and Bonferroni post hoc test.

3.2.5 β2- and β3-ARs antagonism regulates neuroinflammation responsible of mechanical allodynia.

Since it is established that the increase of the number of macrophages induces an increase in oxidative stress at the tissue levels and consequently pain [343, 456, 457], we evaluated the levels of ROS in K7M2 osteosarcoma-bearing mice and sham. Results showed an increase of H_2O_2 levels after para-tibial K7M2 osteosarcoma cell inoculation compared to sham mice. Interestingly, the treatment with β2- and β3-ARs antagonists, but not with β1-AR antagonist, significantly reduced H_2O_2 levels in tibial nerve (Figure 18A). Since macrophages showed no expression of the β1-AR subtype, we speculated that reduction of mechanical allodynia in K7M2 osteosarcoma-bearing mice after daily treatment with β2- and β3-ARs antagonists, was principally due to H_2O_2 release which lead to neuroinflammation, dependent on β2- and β3-ARs blockade on tibial macrophages. To validate this hypothesis, macrophages RAW 264.7 murine cells were stimulated with the pro-oxidant agent phorbol 12-myristate 13-acetate (PMA) (16μM) alone or in combination with the different β-AR antagonists. The treatment with PMA induced a release of H_2O_2 from RAW 264.7 cells, whereas the treatment with propranolol and SR59230A, but not with atenolol, reduced the H_2O_2 release (Figure 18B). To assess if the increase of H_2O_2 levels was associated with mechanical allodynia, K7M2 osteosarcoma-bearing mice were treated with the antioxidant PBN. Results showed that a single treatment with PBN at day 14 after cells inoculation, when mechanical allodynia was already present, was able to revert mechanical allodynia (Figure 18C). These data suggest that the accumulation of macrophages located in the tibial nerve of K7M2 osteosarcoma-bearing mice induces the development of

mechanical allodynia through the release of H_2O_2, and these processes are regulated by *β*2- and *β*3-ARs but not *β*1-ARs.

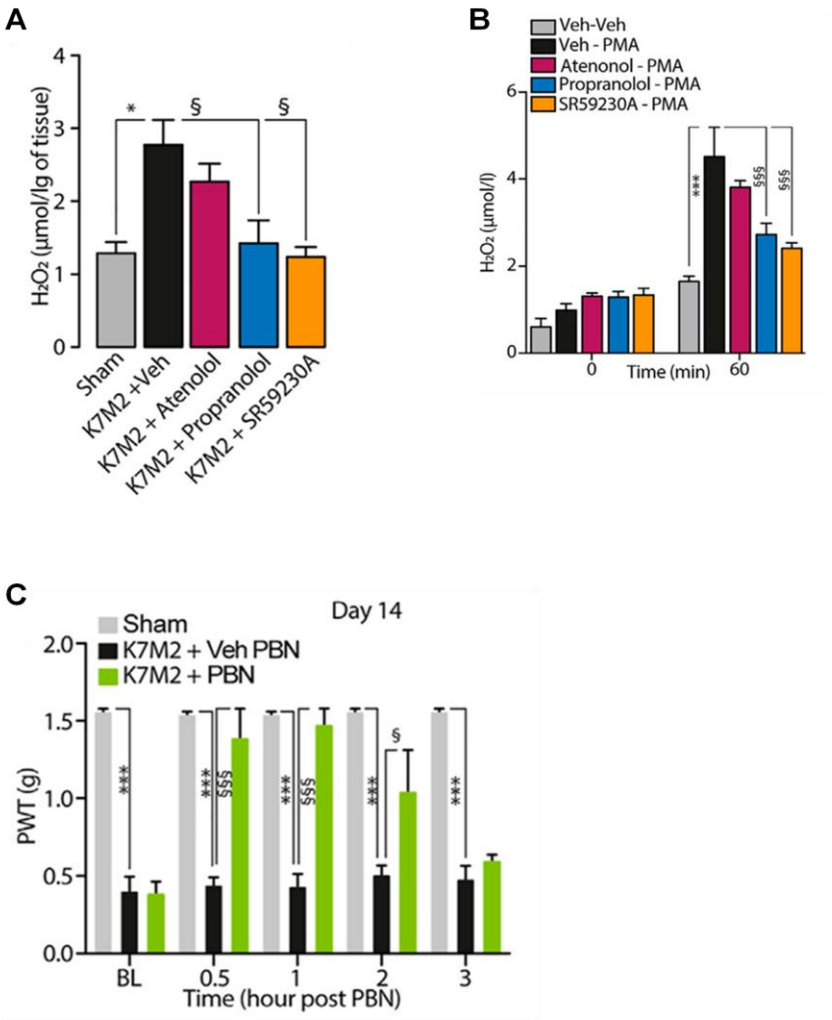

Figure 18. *β*2- and *β*3-ARs antagonism reduces neuroinflammation in tibial nerve of K7M2 osteosarcoma-bearing mice. A, H_2O_2 levels in tibial nerve after inoculation of K7M2 osteosarcoma cells or sham in BALB/c mice, and treated daily, starting from day 10, with atenolol (10 mg/kg, i.p.) propranolol (10 mg/kg, i.p.), SR59230A (10 mg/kg, i.p.) or vehicle (Veh). B, H_2O_2 content in macrophages RAW 264.7 cell line treated with PMA (16 µM) in combination with atenolol (100 nM), propanolol (100 nM) and SR59230A (100 nM) or Veh (n=3 independent experiments). C, mechanical allodynia at 14 days after para-tibial K7M2 osteosarcoma cell inoculation or sham in BALB/c mice treated with PBN (100 mg/kg, i.p.) or Veh. BL, baseline. PWT, paw withdrawal threshold. N=6 mice. *p < 0.05, ***p < 0.001 vs Sham, Veh-Veh; §p < 0.05, §§§p < 0.001 vs K7M2 + Veh, Veh-PMA, K7M2 + Veh PBN. Data are presented as mean ± SEM. One-way (A) or two-way (B-C) ANOVA and Bonferroni post hoc test.

3.3 Conclusion

These results showed that the development of mechanical allodynia in K7M2 osteosarcoma-bearing mice is associated with the recruitment of neuronal macrophages in the tibial nerve ipsilateral to tumor mass. Interestingly, the β2- and β3-ARs antagonism contributes not only in the reduction of tumor growth, but also in cancer pain. For this, targeting β2- and β3-ARs signaling, could be a promising strategy against tumor progression and the development of cancer-evoke pain in osteosarcoma.

3.4 Discussion

β-ARs are an essential component of the sympathetic nervous system, involved in the regulation of multiple physiological responses following activation by catecholamines [1]. Three types of β-ARs with different localization and function have been identified so far; the β1-, β2- and β3-ARs subtypes. The β3-ARs subtype exhibits a restricted expression pattern in humans, such as adipose tissue, myocardium, urinary bladder, brain and retina, where modulates multiple cellular processes including vasodilatation and cardiac function, thermogenesis and metabolism [3]. Increasing evidence suggested an emerging role of β3-ARs in the initiation, growth and progression of cancer [143, 144, 146]. Thus, modulation of β3-ARs signaling effectively reduces cancer metastasis, recurrence and mortality [103, 147, 168]. Moreover, recent studies have highlighted the involvement of β-ARs also in the modulation of various neuropathic pain [329-331]. Among β-ARs, the β2- and β3-ARs are the principal subtypes involved in pain generation by increasing the excitability of nociceptors and activation of immunoregulatory cells [328]. However, the mechanism by which these receptors promote the development and maintenance of pain is not yet fully understood.

Cancer-evoked pain is an important debilitating symptom related to tumor growth at both primary site and metastasis. It is considered a multi-step process that may results from direct infiltration by primary tumor or metastasis into a component of the central or peripheral nervous system, inflammatory responses or to compression of the nerve. Despite the increased interest, understanding

the molecular mechanism that underling the development and maintenance of cancer-evoked pain can allow us to identify novel therapeutic targets for this condition. Various studies have reported that β2- and β3-ARs may induce the activation of macrophages, T-cells and mast cells, as well as cytokine and chemokines, in various models of neuropathic pain following stress or pharmacological inhibition [458-461]. The role of the β-ARs, and in particular of the β3-ARs subtype, in cancer-evoked pain remains poorly investigated. To date, there are no clinical studies available that show whether the use of β-ARs antagonists might be effective in contrast cancer-evoked pain. However, a phase 2 study (https://clinicaltrials.gov/ct2/show/NCT01222091) investigated whether the concomitant treatment with propranolol and remifentanil (opioid) could improve thermal and mechanical hypersensitivity [462]. This study showed that the treatment in combination of these two drugs prevented the remifentanil-induced post infusion hyperalgesia, indicating β-ARs as possible pharmacological targets for preventing different types of pain.

To study the involvement of β3-ARs in modulating cancer-evoked pain in osteosarcoma, we have used an array of different *in vitro* and *in vivo* models. As such, we investigated primarily whether the treatment with β3-ARs antagonist might reduce osteosarcoma tumor growth in a syngeneic osteosarcoma murine model and whether β3-ARs targeting could be able to modulate mechanical allodynia developed with tumor growth and neuroinflammation since the expression of these receptors has been reported on tumor and inflammatory cells. First, we have found that the osteosarcoma-bearing mice developed sustained mechanical allodynia after 10 days from K7M2 osteosarcoma cells inoculation, but not in sham mice. Then, based on previous data that showed the crucial role of peripheral nerve macrophages in the induction and maintenance of mechanical allodynia, we wondered whether also in this cancer model, macrophages in the tibial nerve played a role in the development of cancer pain [343, 456, 463]. Results showed that the number of neural macrophages in the peripheral tibial nerve that runs ipsilateral to the tumor of osteosarcoma-bearing mice, were enhanced compared to sham mice. To evaluate the involvement of the β-ARs in the modulation of cancer-evoked pain in our cancer model, mice were treated daily with atenolol, propranolol and SR59230A, the β1-, β2- and β3-

ARs antagonists, respectively. Data showed that the treatment with atenolol had no effect in reducing mechanical allodynia, whereas the treatment with propranolol and SR59230A significantly reduced mechanical allodynia and tumor growth. These data confirm the involvement of the *β*2- and *β*3-ARs in the induction of cancer-evoked pain and in sustaining tumor growth and development as reported in previous data obtained in other cancer models [103, 147, 162, 164]. Next, we evaluated whether the *β*-ARs activity was correlated to the increase of neuronal macrophages and neuroinflammation in our model. Notably, the treatment with propranolol and SR59230A was able to reduce the number of macrophages in the peripheral tibial nerve compared to vehicle treated mice. These results suggested that the reduction in mechanical allodynia following the treatment with *β*2- and *β*3-ARs antagonisms were partially due to the reduction in macrophages localized in the tibial nerve, associated with a reduction of tumor size. As we observed the expression of all the three subtypes of *β*-ARs in osteosarcoma tumor cells but only *β*2- and *β*3-ARs expression on neuronal macrophages, we hypothesized that the *β*2- and *β*3-ARs signaling on neuronal macrophages could sustain the mechanical allodynia developed in osteosarcoma-bearing mice. Since oxidative stress results correlated to macrophages in tibial nerve and nociceptors activation in several pain models [342, 343, 464], we analyzed the amount of H_2O_2. Notably, the levels of H_2O_2 were increased in tibial nerve of osteosarcoma-bearing mice compared to sham mice, whereas the treatment with *β*2- and *β*3-ARs antagonists abrogated this effect. Accordingly, the treatment with an antioxidant transiently abrogated the established mechanical allodynia in osteosarcoma-bearing mice. Overall, these data suggest a role of *β*2- and *β*3-ARs in sustaining both tumor growth and cancer-evoked pain, and demonstrated that macrophages recruited into the peripheral tibial nerve and oxidative stress generation represent the cellular and molecular mediators for the development of painful conditions in a syngeneic osteosarcoma murine model. Moreover, these results demonstrated the ability of *β*-ARs antagonists in the modulation of both tumor growth and cancer-evoked pain, identifying the *β*-ARs, mainly the *β*2- and *β*3-ARs, as a promising therapeutic target for cancer therapy and associated pain.

Chapter 4. *β*3-ARs blockade impairs compensatory mechanism to overcome nutrient deprivation in malignant rhabdoid tumor of the kidney.

4.1 Introduction

The different and specific amino acid requirements of tumor cells provide the chance to target tumors via enzymatic reduction of amino acids or dietary restriction. Lowering serum tyrosine and phenylalanine was reported to limit growth and metastasis, and improve chemotherapy in various in vivo models of melanoma, hepatocarcinoma and lung cancer [426, 427]. Serum analysis conducted in malignant rhabdoid tumor patient's caring at Meyer Children's Hospital have shown a reduction in selected amino acid levels, including tyrosine and glutamine (Table 1.)

Amino acids	Mean SD (µmol/L)
Tyr	41 ± 27
Gln	349 ± 126

Normal value range (µmol/L): Tyr (44-114), Gln (399-823)

Table 1. Serum levels of tyrosine and glutamine in MRTK patients.

Given the reduction of these two amino acids in serum of patients with MRTK, we tried to mimic *in vitro* the effect of glutamine and tyrosine deprivation. In addition, G-401 cells were also deprived of phenylalanine, the precursor of tyrosine, to enforce the effect of tyrosine deprivation. In addition, since *β*3-ARs could be one of the players involved in regulating the compensatory mechanism following nutrient deprivation, understanding the involvement of *β*3-ARs signaling pathways during amino acids withdrawal will help to identify potential metabolic-related predictive biomarkers and/or potential therapeutic targets that can be further exploited for treatment approaches.

4.2 Results

4.2.1 Amino acid deprivation reduces cell survival and proliferation in G-401 cells.

To investigate whether deprivation of glutamine and tyrosine/phenylalanine could lead to survival advantages in MRTK tumor cells, G-401 cells were exposed to limited conditions for 24h, 48h and 72h as described in Materials and Methods. Deprivation of tyrosine/phenylalanine, glutamine or both, reduced cell survival and proliferation, assessed by measuring the number of cells and flow cytometry analysis of Ki-67, a nuclear marker for proliferating cells, respectively, in all conditions compared to control. Interestingly, G-401 cells exposed to glutamine deprivation do not show a reduction in cell survival and proliferation with respect to the tyrosine/phenylalanine and/or glutamine counterpart (Figure 19A, B).

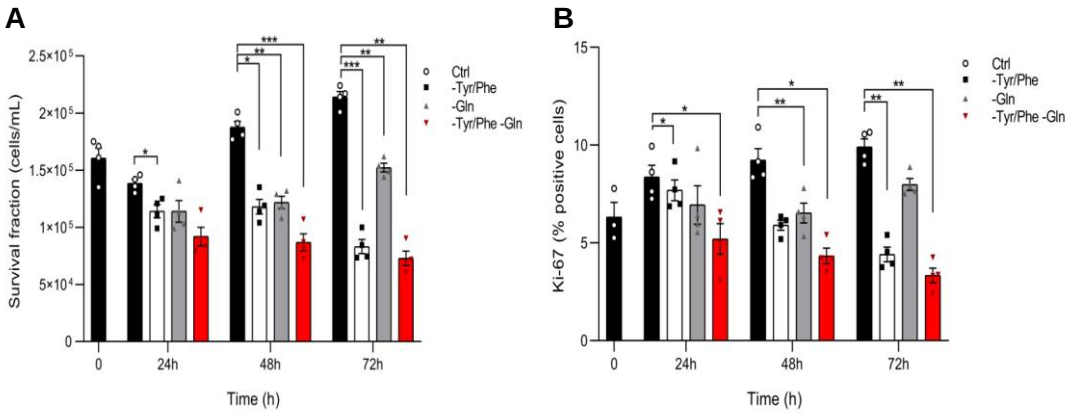

Figure 19. Tyrosine/phenylalanine and both tyrosine/phenylalanine and glutamine deprivation reduces cells survival and proliferation in G-401 cells. A, G-401 cells were subjected to tyrosine/phenylalanine (-Tyr/Phe), glutamine (-Gln) or both (-Tyr/Phe –Gln) deprivation for 24h, 48h and 72h and then the number of cells were count. B, flow cytometry analysis quantification of G-401 cells treated as in A and then stained with anti-Ki-67 conjugated antibody. N=4. *p < 0.05, **p < 0.01, vs Ctrl. Data are presented as mean ± SEM. Two- way ANOVA and Dunnett corrected (A, B).

4.2.2 Amino acids deprivation induces glucose uptake in G-401 cells.

After the unexpected results obtained following glutamine deprivation, we investigated the mechanism underlying G-401 survival during the absence of this nutrient. Upregulation of the glucose importer GLUT1 and subsequently glucose uptake has been demonstrated in many types of cancer to prevent cell death cells caused by growth factors deprivation [465, 466]. Therefore, we hypothesized that GLUT1 might be regulated and responsible for the cell survival of G-401 cells exposed to limited conditions.

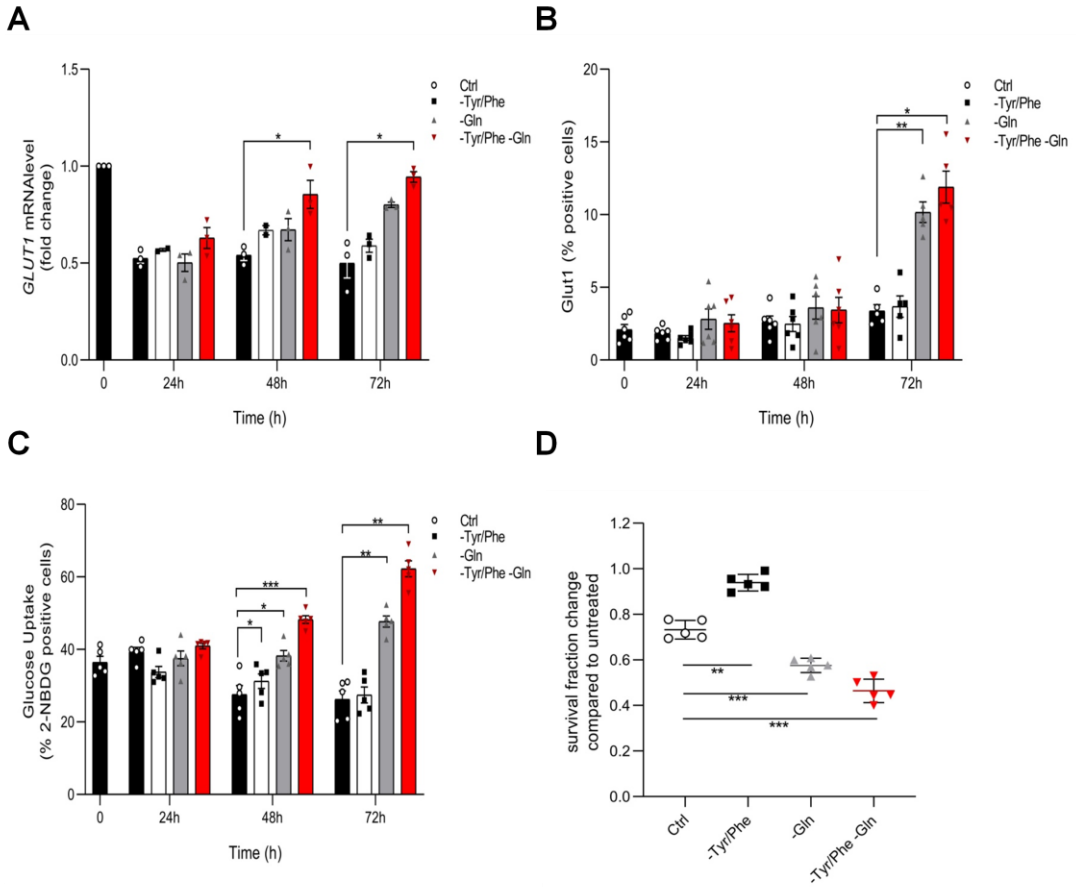

Figure 20. Glutamine and/or tyrosine/phenylalanine deprivation induces GLUT1 expression and glucose uptake in G-401 cells. A, G-401 cells were deprived of tyrosine/phenylalanine (-Tyr/Phe), glutamine (-Gln) or both (-Tyr/Phe –Gln) for 24h, 48h and 72h and then subjected to qRT-PCR to evaluated GLUT1 expression. B and C, flow cytometry analysis quantification of G-401 cells exposed to nutrient deprivation as in A and then stained with anti-GLUT1-FITC conjugated antibody and 2-NBDG. D, G-401 cells were

treated as in A for 2 days and then subjected to 2-DG treatment for further 3 days. Data are presented as the ratio of cell survival inhibition measured compared to untreated cells. N=3 (A), N=5 (B-D). *p < 0.05, **p < 0.01, ***p < 0.001 vs Ctrl. Data are presented as mean ± SEM. Two- way (A-C) and one-way (D) ANOVA and Dunnett corrected (A-D).

qRT-PCR analysis showed that glutamine and both glutamine and tyrosine/phenylalanine deprivation for 48h and 72h induced an increase in GLUT1 expression compared to control (Figure 20A). This increased expression of GLUT1 was further confirmed by flow cytometry analysis in the same conditions (Figure 20B). Given the increase of the expression of this transporter, we next evaluated the uptake of glucose in G-401 cells exposed to limited amino acids. The increased GLUT1 expression was paralleled by a significant increase in glucose uptake in the same conditions (Figure 20C). Thus, the hypothesis was that the unchanged cell survival and proliferation during glutamine deprivation was related to GLUT1 expression and glucose uptake in G-401 cells as a compensatory mechanism implemented by cells to survive during this condition. However, the increase of GLUT1 expression and glucose uptake in G-401 cells exposed to both amino acids deprivation, is not able to restore cell survival. Crucially, a single treatment with the metabolic poison 2-DG, which inhibits the glycolytic pathway, significantly impaired G-401 cells survival in absence of glutamine and both glutamine and tyrosine/phenylalanine (Figure 20D) compared to control.

4.2.3 Aerobic glycolysis is enhanced in G-401 cells following nutrient deprivation.

Since the increase in GLUT1 and glucose uptake, the expression of the key molecular components of the glycolytic pathway was analyzed in G-401 cells exposed to limited conditions. After 3 days of glutamine and/or tyrosine/phenylalanine deprivation, G-401 cells showed higher protein expression level by Western Blot analysis of the glycolytic enzyme HK2 compared to control and tyrosine/phenylalanine deprivation (Figure 21A).

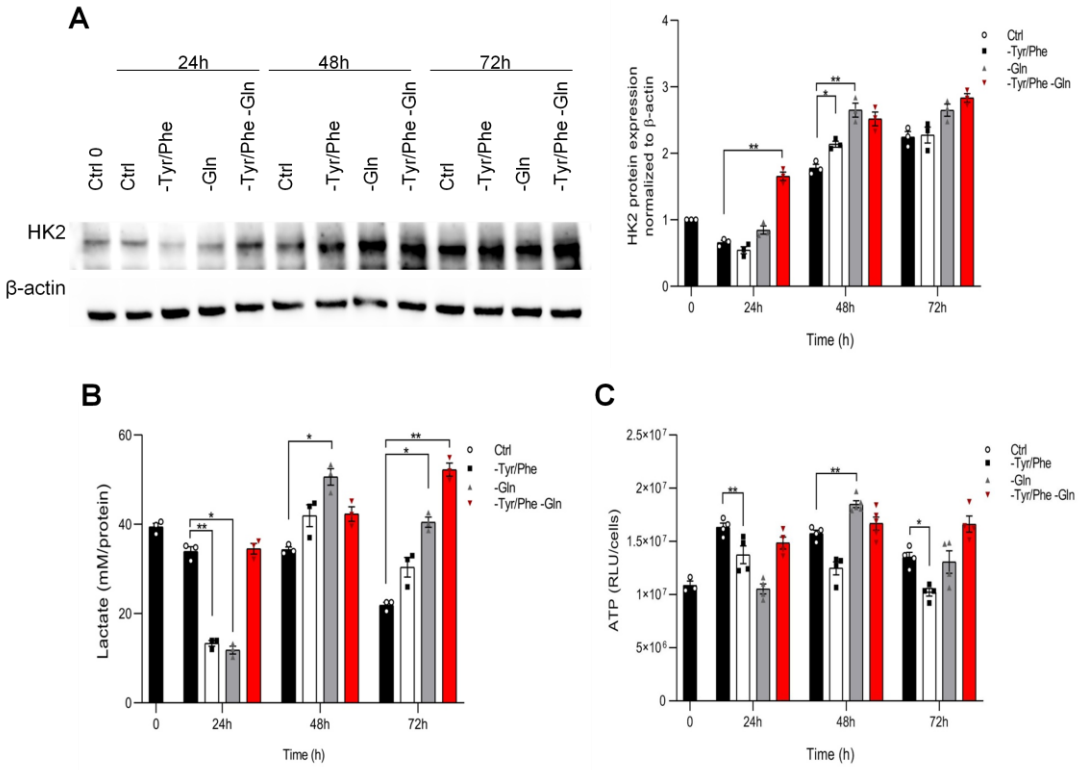

Figure 21. G-401 cells display higher aerobic glycolytic activity during glutamine and/or tyrosine/phenylalanine deprivation. A, Western Blot and relative densitometric analysis showing expression of HK2 in G-401 exposed to 24h, 48h and 72h of tyrosine/phenylalanine (-Tyr/Phe), glutamine (-Gln) or both (-Tyr/Phe –Gln) deprivation. Total protein lysates were subjected to Western Blot analysis as indicated. B, G-401 cells were treated as in A and then subjected to lactate assay. C, G-401 cells were treated as in A and then subjected to ATP assay. N=3 (A, B), N=5 (C). *p < 0.05, **p < 0.01, vs Ctrl. Data are presented as mean ± SEM. Two-way ANOVA and Dunnett corrected (A-C).

The increase in glycolysis-associated components was accompanied by reduced glucose respiration, assessed by extracellular lactate release in the same conditions (Figure 21B). This increased lactate production was paralleled by a significant increase in ATP production (Figure 21C). These data show that the enhanced glucose uptake in G-401 cells deprived of glutamine or both glutamine/phenylalanine have a glycolytic phenotype compared to control or to tyrosine/phenylalanine deprivation alone.

4.2.4 TCA cycle enzymes are upregulated in G-401 cells following amino acids withdrawal.

Tyrosine/phenylalanine and glutamine can be metabolized to fumarate and α-ketoglutarate, respectively, which can fuel the TCA cycle contributing to energy production and biosynthesis to support cell survival [467]. To investigate whether blocking the availability of these amino acids could impair the TCA cycle and mitochondrial function, we evaluated the production of fumarate and the activity of the enzymes of the TCA cycle. qRT-PCR analysis showed that glutamine deprivation induced a significant increase in HPD expression compared to control, tyrosine/phenylalanine and both tyrosine/phenylalanine and glutamine deprived G-401 cells in time dependent manner (Figure 22A). The increased expression of HPD during glutamine deprivation was paralleled to an increased fumarate production in the same conditions, whereas tyrosine/phenylalanine deprivation showed reduced production of this metabolite (Figure 22B), indicating that tyrosine/phenylalanine was an important source of fumarate in these conditions. Notably, although HPD expression appears to be lower after 48h and 72h of tyrosine/phenylalanine and glutamine withdrawal compared to control, no difference in fumarate production was observed. Thus, the hypothesis was that enhanced fumarate production during the simultaneous deprivation of both amino acids in G-401 cells was due to alternative mechanisms to maintain an active TCA cycle during limited conditions. This was further supported by the observation that succinate dehydrogenase and fumarate hydratase activity, two TCA cycle enzymes, were significantly increased in this condition compared to control (Figure 22C, D). These data suggest that even in the absence of tyrosine/phenylalanine and glutamine, G-401 cells might use other recycling pathways that provide intermediates that refilled the TCA cycle during limited conditions, including a small portion of glucose which was not metabolized by the glycolytic pathway. Indeed, no effect in G-401 cell survival (Figure 22E) and fumarate production (Figure 22F) was observed after treatment with NTBC, which inhibits HPD, in all conditions compared to control, confirming a compensatory mechanism in G-401 cells following tyrosine/phenylalanine and/or glutamine deprivation.

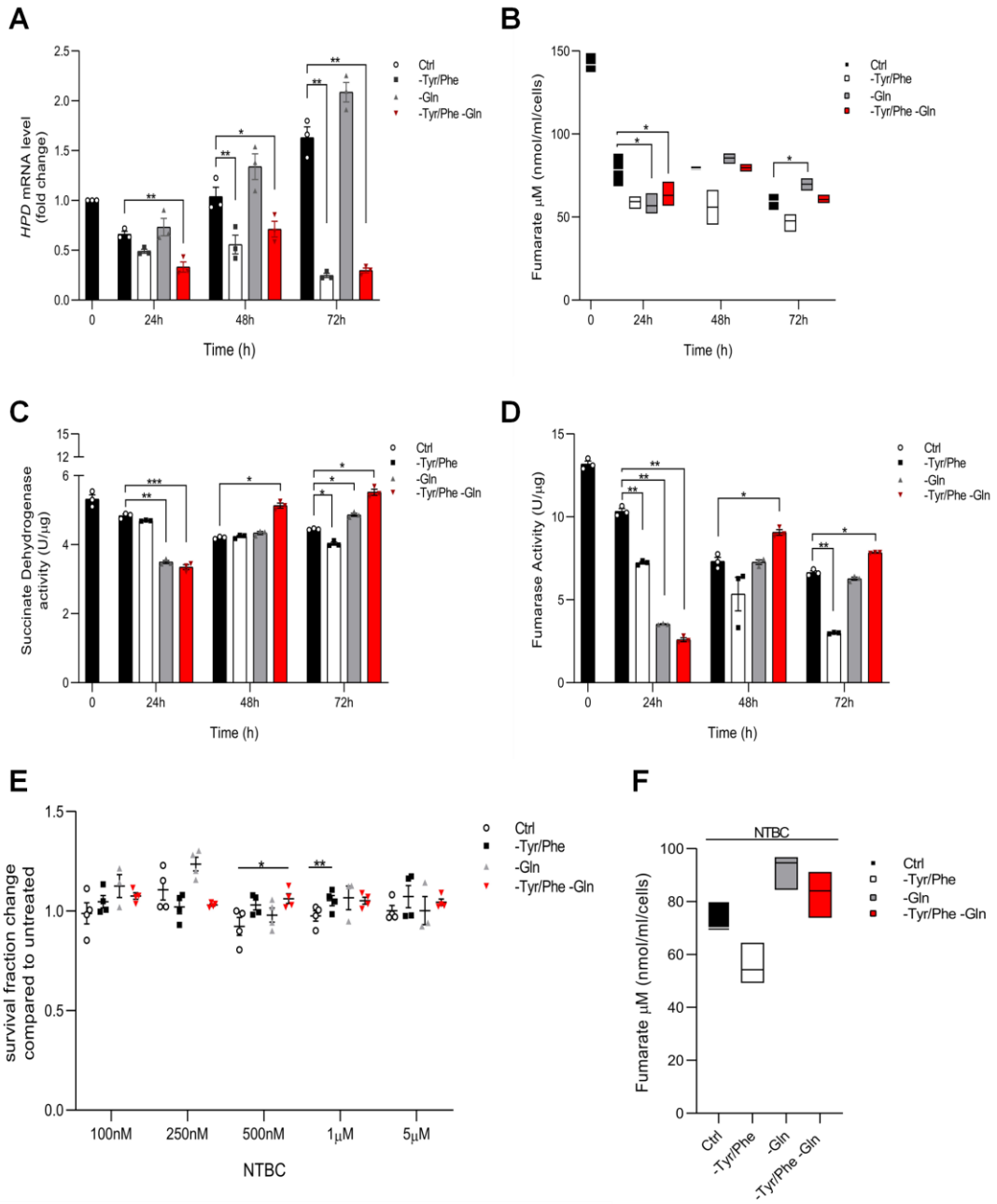

Figure 22. Succinate dehydrogenase and fumarate hydratase are upregulated during both long-term amino acid deprivation in G-401 cells lead to fumarate production. A, G-401 cells were deprived of tyrosine/phenylalanine (-Tyr/Phe), glutamine (-Gln) or both (-Tyr/Phe -Gln) for 24h, 48h and 72h and then subjected to qRT-PCR to evaluated HPD expression. B, G-401 cells were treated as in A and then evaluated the fumarate production assessed by using the fumarate assay. C, succinate dehydrogenase activity of mitochondria extracted from G-401 cells treated as in A. D, fumarate hydratase activity of mitochondria extracted from G-401 cells treated as in A. E, G-401 cells were treated as in A for 2 days and then subjected to NTBC treatment for further 2 days. Data are presented as the ratio of cell survival inhibition measured compared to untreated cells. F, G-401 cells were treated as in A for 2 days and then subjected to NTBC treatment for further 2 days and fumarate assay. N=3

(A-D, F), N=4 (E). *p < 0.05, **p < 0.01, vs Ctrl. Data are presented as mean ± SEM. Two-way (A-D, F) and one-way (E) ANOVA and Dunnett corrected (A-F).

4.2.5 β3-ARs blockade reverts the compensatory mechanism induced by nutrient deprivation.

Since it is established that the β3-ARs could modulate the expression of the glucose importer GLUTs and glucose uptake in adipocytes and skeletal muscles [468, 469], we analyzed the expression of GLUT1 and glucose uptake in G-401 cells following β3-ARs modulation. First, G-401 cells were exposed to tyrosine/phenylalanine and/or glutamine deprivation and then subjected to flow cytometry analysis. Deprivation of glutamine or both tyrosine/phenylalanine and glutamine increased β3-ARs expression already from 24h, with a maximum expression at 72h. Interestingly, also tyrosine/phenylalanine deprivation induced an increase of β3-ARs expression at 72h (Figure 23A), suggesting an activation of this receptor during stress conditions. Given the increased expression of β3-ARs in G-401 cells, we evaluated the possible correlation between β3-ARs and GLUT1 expression. G-401 cells were subjected to tyrosine/phenylalanine, glutamine and both deprivations and then treated with SR59230A (1 μM). After 2 days of treatment with the β3-AR antagonist, flow cytometry analysis showed a significantly reduced GLUT1 expression of G-401 cells compared to untreated during glutamine and both tyrosine/phenylalanine and glutamine deprivation (Figure 23B). This reduction in GLUT1 expression correlated whit a reduction of glucose uptake (Figure 23C) assessed by 2-NBDG staining and subsequent flow cytometry analysis in the same condition, indicating that β3-AR expression could modulates glucose metabolism in G-401 cells exposed to amino acid deprivation. Finally, we evaluated the effect of β3-ARs antagonism in G-401 cell survival during nutrient deprivation. The treatment with SR59230A showed a dose-dependent decrease in cell survival in response to the β3-AR antagonist during glutamine and both tyrosine/phenylalanine and glutamine deprivation (Figure 23D), suggesting that β3-ARs contributes to G-401cells adaptation and survival.

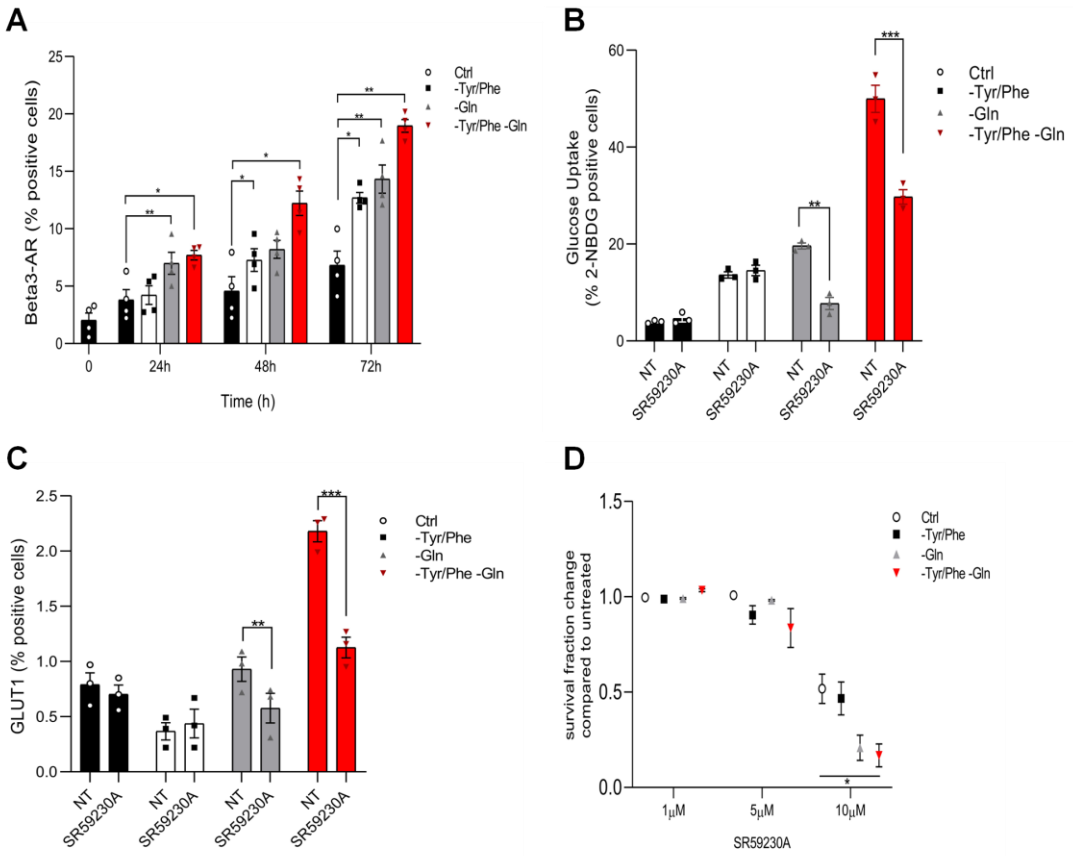

Figure 23. *β*3-ARs antagonism reduces glucose metabolism and survival in G-401 cells. A, flow cytometry analysis quantification of G-401 cells exposed to tyrosine/phenylalanine (-Tyr/Phe) and/or glutamine (-Gln) deprivation for 24h, 48h and 72h and then stained with anti-*β*3-AR-PE conjugated antibody. B and C, flow cytometry analysis quantification of G-401 cells exposed to nutrient deprivation as in A for 2 days and treated with SR59230A (1 μM) for further 2 days, and then stained with anti-GLUT1-FITC conjugated antibody and 2-NBDG. D, G-401 cells were treated as in A and then subjected to SR59230A treatment for further 2 days. Data are presented as the ratio of cell survival inhibition measured compared to untreated cells. N=4 (A), N=3 (B-C), N=6 (D). *p < 0.05, **p < 0.01, ***p < 0.001 vs Ctrl. Data are presented as mean ± SEM. Two-way ANOVA and Dunnett corrected (A, D) and Bonferroni (B-C) post hoc test.

4.3 Conclusion

*β*3-ARs expression is increased and plays a role in the regulation of MRTK cells during nutrient deprivation. The acquisition of a glycolytic phenotype via GLUT1 upregulation and subsequent glucose uptake could be involved in MRTK

aggressiveness. Further investigations are necessary to understand the involvement of *β*3-ARs in compensatory metabolic mechanisms in order to identify both potential metabolic related-biomarkers and therapeutic targets in MRTK.

4.4 Discussion

Nutrient deprivation is an environmental stress factor that can influence the behavior of cancer cells. Increased demand and overutilization of amino acids by tumor tissue may account for the reduced concentration of serum amino acids [426, 470]. The kidneys are one of the predominant organs where glutamine catabolism takes place, with a higher expression of glutamine catabolic enzymes and transporter than other organs, which correlates with poor prognosis [471, 472]. Moreover, low levels of tyrosine and phenylalanine have been demonstrated in the serum of several types of cancer, including renal cancers [426, 473]. In addition, deregulation of phenylalanine and tyrosine metabolism has been implicated in several types of disease such as Huntington's disease [474], tyrosinemia [475] and alkaptonuria [476]. Preliminary data that have been obtained in the last year of my PhD program suggest that *β*3-ARs signaling and modulation are also involved in the regulation of metabolic adaptation following nutrient deprivation in malignant rhabdoid tumor of the kidney. Based on the serum amino acids analysis carried out on patients with malignant rhabdoid tumor of the kidney, showing a reduction of these two aromatic amino acids levels, we have used G-401 cells to mimic *in vitro* the effect of serum amino acid deprivation. It has been reported, that cancers cells can undergo metabolic adaptation following nutrient deprivation to sustain growth and survival in many types of tumor [154, 477]. Metabolic adaptation is essential for the cancer cells to satisfy the different energetic requirements that support cancer cell from the initial proliferation, growth, survival and dissemination. First, we evaluated the impact of amino acid deprivation in G-401 cells in terms of survival and proliferation. Notably, tyrosine/phenylalanine or both tyrosine/phenylalanine and glutamine deprivation reduced cells survival and proliferation, in contrast, to control and glutamine withdrawal. Glutamine metabolism is an alternative energy source for cancer cells and is thought to be

a central metabolic pathway cooperating with glycolysis by providing intermediates for amino acids [478, 479] and lipid synthesis necessary to sustain the higher proliferation rate [480]. Many cancer types are also dependent on tyrosine and phenylalanine. Indeed, restriction of these two aromatic amino acids affects mitochondrial function, leading to apoptosis and inhibition of invasion [422, 481]. To identify the metabolic pathways associated with amino acids deprivation, we analyzed the expression of key glycolytic components and performed metabolic assays in G-401 cells exposed to limited conditions. The results showed that glutamine and both glutamine and tyrosine/phenylalanine deprivation in G-401 cells have a glycolytic phenotype. Indeed, G-401 cells showed and increased HK2, GLUT1 expression associated with increased glucose uptake and lactate secretion, during glutamine and both tyrosine/phenylalanine deprivation. As expected, targeting glycolytic metabolism in these conditions affected cell survival. This suggests that the acquisition of a glycolytic phenotype correlates with aggressive clinical features of G-401 cells. Indeed, malignant rhabdoid tumor of the kidney has a poorer prognosis and it has been reported that this cancer types show a high FDG-PET signal (i.e. higher glucose uptake) [482]. Consequently, 2-DG used in combination with standard therapy may be of clinical benefit to the malignant rhabdoid tumor of the kidney. To assess whether amino acids deprivation could be responsible for the TCA cycle and mitochondrial impairment, we analyzed the expression of the enzyme involved in the fumarate production and performed enzyme activity assay in G-401 cells during tyrosine/phenylalanine and/or glutamine deprivation. Dysfunction of succinate dehydrogenase and fumarate hydratase has been demonstrated involved in several types of cancer [483], and mutation of FH has been described in the pathogenesis of various pediatric cancers [484]. Surprisingly, TCA cycle enzyme activity was increased in G-401 cells exposed to simultaneous amino acids deprivation for 48h and 72h. This suggests that this enzymatic activity was due to alternative mechanisms to maintain an active TCA cycle during limited conditions. Indeed, targeting tyrosine metabolism in G-401 cells did not affect cell survival and fumarate production. A very recent study has shown a metabolic link between tyrosine and glutamine metabolism. In fact, deregulation of HPD expression increased the dependency and flux of glutamine

as a source of the TCA cycle in lung cancer. Therefore, combinational targeting could be exploited as a potentially promising anticancer therapy [425].
Next, we evaluated the molecular components that could be involved in the regulation of the compensatory metabolic mechanism that G-401 undergoes under nutrient deprivation. β3-ARs expression has been demonstrated involved in several types of cancer and the β3-ARs blockade has been previously described to reduce tumor growth and progression [103, 147]. To investigate the involvement of β3-ARs in G-401 cells, we analyzed the expression of this receptor during tyrosine/phenylalanine and/or glutamine deprivation. The results showed that nutrient deprivation induced β3-ARs expression in G-401 cells in a time dependent manner. Furthermore, it has been demonstrated that β3-ARs regulate the expression of GLUTs and increase the glucose uptake of adipocytes and skeletal muscles. As GLUT1 expression and glucose uptake were found to be upregulated in G-401 cells following amino acids deprivation, we hypothesized that β3-ARs could be responsible for the regulation of the altered metabolism observed in these cells. Notably, impairing β3-ARs signaling by treating G-401 with SR59230A, showed a reduction in GLUT1 expression and glucose uptake. Consequently, targeting β3-ARs with SR59230A impaired cell survival, indicating that β3-ARs targeting could have a potential therapeutic implication in G-401 cells during nutrient deprivation.

Alterations in other metabolic-related genes are also frequent in malignant rhabdoid tumor of the kidney. Pyruvate dehydrogenase kinase (PDK) has been recognized as an oncogene for its role in carcinogenesis and it has been reported to be upregulated in several cancers [485]. Preliminary data of microarray analysis showed an increased expression of PDK, in particular the isoform 4, in G-401 cells following both tyrosine/phenylalanine and glutamine deprivation. Conversely, no changes in PDK-4 expression in G-401 cells limited for tyrosine/phenylalanine or glutamine compared to control. In addition, aquaporin 5 (AQP5), a transmembrane protein that has been demonstrated to be involved in cell migration and proliferation [486], showed the same expression pattern of PDK-4. In G-401 cells exposed to amino acid deprivation, these genes could be activated in stress nutrient conditions and could confer an

advantage in terms of a compensatory mechanism. Future aims of the current study are the identification of one or more molecular players involved in the described compensatory mechanism. On one hand, *β*3-ARs could be used as a potential biomarker, since there are still difficulties in understanding the molecular mechanism that underlies the malignant rhabdoid tumor of the kidney; on the other hand, an interesting area of research could be the investigation of potential targeting approaches of the pathways that are controlled by the deregulated *β*3-ARs to be used as monotherapies or in association with current therapy. Amino acid deprivation strategies show great promise in the treatment of cancer. However, before amino acid depletion could be applied more broadly in the clinic, the metabolic dependencies of malignant rhabdoid tumor of the kidney and metabolic reprogramming need to be investigated in detail. Therefore, future application of amino acid depletion therapies in combination with targeted agents might represent a possible strategy against malignant rhabdoid tumor of the kidney.

A part of this study was published on *Frontiers in Pharmacology*: Bruno G, De Logu F, Souza Monteiro de Araujo D, Subbiani A, et al. *β2-and β3-Adrenergic Receptors Contribute to Cancer-Evoked Pain in a Mouse Model of Osteosarcoma via Modulation of Neural Macrophages*. DOI:10.3389/fphar.2021.697912. Published 27 Sep 2021.

Bibliography

1. Nergårdh, A., L.O. Boréus, and A.S. Naglo, *Characterization of the adrenergic beta-receptor in the urinary bladder of man and cat.* Acta Pharmacol Toxicol (Copenh), 1977. **40**(1): p. 14-21.

2. Ferguson, S.S., *Evolving concepts in G protein-coupled receptor endocytosis: the role in receptor desensitization and signaling.* Pharmacol Rev, 2001. **53**(1): p. 1-24.
3. Collins, S., *β-Adrenoceptor Signaling Networks in Adipocytes for Recruiting Stored Fat and Energy Expenditure.* Front Endocrinol (Lausanne), 2011. **2**: p. 102.
4. Pérez-Sayáns, M., et al., *Beta-adrenergic receptors in cancer: therapeutic implications.* Oncol Res, 2010. **19**(1): p. 45-54.
5. Neves, S.R., P.T. Ram, and R. Iyengar, *G protein pathways.* Science, 2002. **296**(5573): p. 1636-9.
6. Rockman, H.A., W.J. Koch, and R.J. Lefkowitz, *Seven-transmembrane-spanning receptors and heart function.* Nature, 2002. **415**(6868): p. 206-12.
7. Cazorla, O., et al., *The cAMP binding protein Epac regulates cardiac myofilament function.* Proc Natl Acad Sci U S A, 2009. **106**(33): p. 14144-9.
8. Burgoyne, J.R. and P. Eaton, *Oxidant sensing by protein kinases a and g enables integration of cell redox state with phosphoregulation.* Sensors (Basel), 2010. **10**(4): p. 2731-51.
9. Dorn, G.W., *GRK mythology: G-protein receptor kinases in cardiovascular disease.* J Mol Med (Berl), 2009. **87**(5): p. 455-63.
10. Lefkowitz, R.J., *G protein-coupled receptors. III. New roles for receptor kinases and beta-arrestins in receptor signaling and desensitization.* J Biol Chem, 1998. **273**(30): p. 18677-80.
11. Lefkowitz, R.J., et al., *Mechanisms of beta-adrenergic receptor desensitization and resensitization.* Adv Pharmacol, 1998. **42**: p. 416-20.
12. Pitcher, J.A., N.J. Freedman, and R.J. Lefkowitz, *G protein-coupled receptor kinases.* Annu Rev Biochem, 1998. **67**: p. 653-92.
13. Shukla, A.K., et al., *Distinct conformational changes in beta-arrestin report biased agonism at seven-transmembrane receptors.* Proc Natl Acad Sci U S A, 2008. **105**(29): p. 9988-93.
14. Goodman, O.B., et al., *Beta-arrestin acts as a clathrin adaptor in endocytosis of the beta2-adrenergic receptor.* Nature, 1996. **383**(6599): p. 447-50.
15. Krupnick, J.G., et al., *Arrestin/clathrin interaction. Localization of the clathrin binding domain of nonvisual arrestins to the carboxy terminus.* J Biol Chem, 1997. **272**(23): p. 15011-6.
16. Laporte, S.A., et al., *The beta2-adrenergic receptor/betaarrestin complex recruits the clathrin adaptor AP-2 during endocytosis.* Proc Natl Acad Sci U S A, 1999. **96**(7): p. 3712-7.
17. Gulick, T., et al., *Interleukin 1 and tumor necrosis factor inhibit cardiac myocyte beta-adrenergic responsiveness.* Proc Natl Acad Sci U S A, 1989. **86**(17): p. 6753-7.
18. Prabhu, S.D., *Cytokine-induced modulation of cardiac function.* Circ Res, 2004. **95**(12): p. 1140-53.
19. Wachsman, D.E., et al., *Kinetic studies of desensitization and resensitization of the relaxation response to beta-2 adrenoceptor agonists in isolated guinea pig trachea.* J Pharmacol Exp Ther, 1997. **280**(1): p. 332-45.
20. Ferguson, S.S. and M.G. Caron, *G protein-coupled receptor adaptation mechanisms.* Semin Cell Dev Biol, 1998. **9**(2): p. 119-27.
21. Wang, G., et al., *Nitric oxide regulates endocytosis by S-nitrosylation of dynamin.* Proc Natl Acad Sci U S A, 2006. **103**(5): p. 1295-300.
22. Martins, S.A., et al., *Towards the miniaturization of GPCR-based live-cell screening assays.* Trends Biotechnol, 2012. **30**(11): p. 566-74.

23. Merrifield, C.J., et al., *Endocytic vesicles move at the tips of actin tails in cultured mast cells.* Nat Cell Biol, 1999. **1**(1): p. 72-4.
24. Naga Prasad, S.V., et al., *Protein kinase activity of phosphoinositide 3-kinase regulates beta-adrenergic receptor endocytosis.* Nat Cell Biol, 2005. **7**(8): p. 785-96.
25. Seachrist, J.L., P.H. Anborgh, and S.S. Ferguson, *beta 2-adrenergic receptor internalization, endosomal sorting, and plasma membrane recycling are regulated by rab GTPases.* J Biol Chem, 2000. **275**(35): p. 27221-8.
26. Seachrist, J.L. and S.S. Ferguson, *Regulation of G protein-coupled receptor endocytosis and trafficking by Rab GTPases.* Life Sci, 2003. **74**(2-3): p. 225-35.
27. He, J., et al., *Proteomic analysis of beta1-adrenergic receptor interactions with PDZ scaffold proteins.* J Biol Chem, 2006. **281**(5): p. 2820-7.
28. Krueger, K.M., et al., *The role of sequestration in G protein-coupled receptor resensitization. Regulation of beta2-adrenergic receptor dephosphorylation by vesicular acidification.* J Biol Chem, 1997. **272**(1): p. 5-8.
29. Barak, L.S., et al., *A highly conserved tyrosine residue in G protein-coupled receptors is required for agonist-mediated beta 2-adrenergic receptor sequestration.* J Biol Chem, 1994. **269**(4): p. 2790-5.
30. Sibley, D.R., et al., *Phosphorylation/dephosphorylation of the beta-adrenergic receptor regulates its functional coupling to adenylate cyclase and subcellular distribution.* Proc Natl Acad Sci U S A, 1986. **83**(24): p. 9408-12.
31. Yu, S.S., R.J. Lefkowitz, and W.P. Hausdorff, *Beta-adrenergic receptor sequestration. A potential mechanism of receptor resensitization.* J Biol Chem, 1993. **268**(1): p. 337-41.
32. Zhang, J., et al., *A central role for beta-arrestins and clathrin-coated vesicle-mediated endocytosis in beta2-adrenergic receptor resensitization. Differential regulation of receptor resensitization in two distinct cell types.* J Biol Chem, 1997. **272**(43): p. 27005-14.
33. Zhang, J., et al., *Cellular trafficking of G protein-coupled receptor/beta-arrestin endocytic complexes.* J Biol Chem, 1999. **274**(16): p. 10999-1006.
34. Pippig, S., S. Andexinger, and M.J. Lohse, *Sequestration and recycling of beta 2-adrenergic receptors permit receptor resensitization.* Mol Pharmacol, 1995. **47**(4): p. 666-76.
35. Kelly, E., *G-protein-coupled receptor dephosphorylation at the cell surface.* Br J Pharmacol, 2006. **147**(3): p. 235-6.
36. Iyer, V.S. and J.M. Canty, *Regional desensitization of beta-adrenergic receptor signaling in swine with chronic hibernating myocardium.* Circ Res, 2005. **97**(8): p. 789-95.
37. Gupta, M.K., M.L. Mohan, and S.V. Naga Prasad, *G Protein-Coupled Receptor Resensitization Paradigms.* Int Rev Cell Mol Biol, 2018. **339**: p. 63-91.
38. Lin, F., H. Wang, and C.C. Malbon, *Gravin-mediated formation of signaling complexes in beta 2-adrenergic receptor desensitization and resensitization.* J Biol Chem, 2000. **275**(25): p. 19025-34.
39. Tao, J., H.Y. Wang, and C.C. Malbon, *Protein kinase A regulates AKAP250 (gravin) scaffold binding to the beta2-adrenergic receptor.* EMBO J, 2003. **22**(24): p. 6419-29.

40. Cong, M., et al., *Regulation of membrane targeting of the G protein-coupled receptor kinase 2 by protein kinase A and its anchoring protein AKAP79.* J Biol Chem, 2001. **276**(18): p. 15192-9.
41. Fraser, I.D., et al., *Assembly of an A kinase-anchoring protein-beta(2)-adrenergic receptor complex facilitates receptor phosphorylation and signaling.* Curr Biol, 2000. **10**(7): p. 409-12.
42. Tao, J. and C.C. Malbon, *G-protein-coupled receptor-associated A-kinase anchoring proteins AKAP5 and AKAP12: differential signaling to MAPK and GPCR recycling.* J Mol Signal, 2008. **3**: p. 19.
43. Nienaber, J.J., et al., *Inhibition of receptor-localized PI3K preserves cardiac beta-adrenergic receptor function and ameliorates pressure overload heart failure.* J Clin Invest, 2003. **112**(7): p. 1067-79.
44. Oudit, G.Y., et al., *Phosphoinositide 3-kinase gamma-deficient mice are protected from isoproterenol-induced heart failure.* Circulation, 2003. **108**(17): p. 2147-52.
45. Naga Prasad, S.V., et al., *Agonist-dependent recruitment of phosphoinositide 3-kinase to the membrane by beta-adrenergic receptor kinase 1. A role in receptor sequestration.* J Biol Chem, 2001. **276**(22): p. 18953-9.
46. Vasudevan, N.T., et al., *Inhibition of protein phosphatase 2A activity by PI3Kγ regulates β-adrenergic receptor function.* Mol Cell, 2011. **41**(6): p. 636-48.
47. Nahmias, C., et al., *Molecular characterization of the mouse beta 3-adrenergic receptor: relationship with the atypical receptor of adipocytes.* EMBO J, 1991. **10**(12): p. 3721-7.
48. Granneman, J.G., K.N. Lahners, and A. Chaudhry, *Molecular cloning and expression of the rat beta 3-adrenergic receptor.* Mol Pharmacol, 1991. **40**(6): p. 895-9.
49. Forrest, R.H. and J.G. Hickford, *Rapid communication: nucleotide sequences of the bovine, caprine, and ovine beta3-adrenergic receptor genes.* J Anim Sci, 2000. **78**(5): p. 1397-8.
50. Sasaki, N., et al., *Anti-obesity effects of selective agonists to the beta 3-adrenergic receptor in dogs. I. The presence of canine beta 3-adrenergic receptor and in vivo lipomobilization by its agonists.* J Vet Med Sci, 1998. **60**(4): p. 459-63.
51. Granneman, J.G., K.N. Lahners, and A. Chaudhry, *Characterization of the human beta 3-adrenergic receptor gene.* Mol Pharmacol, 1993. **44**(2): p. 264-70.
52. van Spronsen, A., et al., *The promoter and intron/exon structure of the human and mouse beta 3-adrenergic-receptor genes.* Eur J Biochem, 1993. **213**(3): p. 1117-24.
53. Hutchinson, D.S., et al., *Mouse beta 3a- and beta 3b-adrenoceptors expressed in Chinese hamster ovary cells display identical pharmacology but utilize distinct signalling pathways.* Br J Pharmacol, 2002. **135**(8): p. 1903-14.
54. Adachi, N., et al., *Differential.* J Biol Chem, 2019. **294**(7): p. 2569-2578.
55. Nantel, F., et al., *The human beta 3-adrenergic receptor is resistant to short term agonist-promoted desensitization.* Mol Pharmacol, 1993. **43**(4): p. 548-55.

56. Liggett, S.B., et al., *Structural basis for receptor subtype-specific regulation revealed by a chimeric beta 3/beta 2-adrenergic receptor.* Proc Natl Acad Sci U S A, 1993. **90**(8): p. 3665-9.
57. Hatakeyama, Y., et al., *Acute and chronic effects of FR-149175, a beta 3-adrenergic receptor agonist, on energy expenditure in Zucker fatty rats.* Am J Physiol Regul Integr Comp Physiol, 2004. **287**(2): p. R336-41.
58. Hutchinson, D.S., B.A. Evans, and R.J. Summers, *beta(3)-adrenoceptor regulation and relaxation responses in mouse ileum.* Br J Pharmacol, 2000. **129**(6): p. 1251-9.
59. Kurabayashi, T., D.G. Carey, and N.A. Morrison, *The beta 3-adrenergic receptor gene Trp64Arg mutation is overrepresented in obese women. Effects on weight, BMI, abdominal fat, blood pressure, and reproductive history in an elderly Australian population.* Diabetes, 1996. **45**(10): p. 1358-63.
60. Thomas, G.N., et al., *The Trp64Arg polymorphism of the beta3-adrenergic receptor gene and obesity in Chinese subjects with components of the metabolic syndrome.* Int J Obes Relat Metab Disord, 2000. **24**(5): p. 545-51.
61. Mo, W., et al., *The genetic polymorphisms of beta3-adrenergic receptor (AR) Trp64Arg and beta2-AR Gln27Glu are associated with obesity in Chinese male hypertensive patients.* Clin Chem Lab Med, 2007. **45**(4): p. 493-8.
62. Kadowaki, H., et al., *A mutation in the beta 3-adrenergic receptor gene is associated with obesity and hyperinsulinemia in Japanese subjects.* Biochem Biophys Res Commun, 1995. **215**(2): p. 555-60.
63. Takeuchi, S., et al., *ADRB3 polymorphism associated with BMI gain in Japanese men.* Exp Diabetes Res, 2012. **2012**: p. 973561.
64. Yamakita, M., et al., *The Trp64Arg polymorphism of the beta3-adrenergic receptor gene is associated with weight changes in obese Japanese men: a 4-year follow-up study.* J Physiol Anthropol, 2010. **29**(4): p. 133-9.
65. García-Rubi, E., et al., *Trp64Arg variant of the beta3-adrenoceptor and insulin resistance in obese postmenopausal women.* J Clin Endocrinol Metab, 1998. **83**(11): p. 4002-5.
66. Jesus, Í., et al., *Trp64Arg polymorphism of the ADRB3 gene associated with maximal fat oxidation and LDL-C levels in non-obese adolescents.* J Pediatr (Rio J), 2018. **94**(4): p. 425-431.
67. Szendrei, B., et al., *Influence of ADRB2 Gln27Glu and ADRB3 Trp64Arg polymorphisms on body weight and body composition changes after a controlled weight-loss intervention.* Appl Physiol Nutr Metab, 2016. **41**(3): p. 307-14.
68. Yang, H., et al., *The mutation of Trp64Arg in β3-adrenoreceptor-encoding gene is significantly associated with increased hypertension risk and elevated blood pressure: a meta-analysis.* Oncotarget, 2017. **8**(28): p. 46480-46490.
69. Li, Y.Y., et al., *Gene Trp64Arg Polymorphism and Essential Hypertension: A Meta-Analysis Including 9,555 Subjects.* Front Genet, 2018. **9**: p. 106.
70. Ferreira, C.E., et al., *The relationship between the Trp 64 Arg polymorphism of the beta 3-adrenoceptor gene and idiopathic overactive bladder.* Am J Obstet Gynecol, 2011. **205**(1): p. 82.e10-4.
71. Teitsma, C.A., J.J. de la Rosette, and M.C. Michel, *Are polymorphisms of the β(3)-adrenoceptor gene associated with an altered bladder function?* Neurourol Urodyn, 2013. **32**(3): p. 276-80.

72. Chen, Y., et al., *Stratified meta-analysis by ethnicity revealed that ADRB3 Trp64Arg polymorphism was associated with coronary artery disease in Asians, but not in Caucasians.* Medicine (Baltimore), 2020. **99**(4): p. e18914.
73. Carlsson, M., et al., *Common variants in the beta2-(Gln27Glu) and beta3-(Trp64Arg)--adrenoceptor genes are associated with elevated serum NEFA concentrations and type II diabetes.* Diabetologia, 2001. **44**(5): p. 629-36.
74. Masuo, K., et al., *Beta2- and beta3-adrenergic receptor polymorphisms are related to the onset of weight gain and blood pressure elevation over 5 years.* Circulation, 2005. **111**(25): p. 3429-34.
75. Hoffstedt, J., et al., *Polymorphism of the human beta3-adrenoceptor gene forms a well-conserved haplotype that is associated with moderate obesity and altered receptor function.* Diabetes, 1999. **48**(1): p. 203-5.
76. Mentuccia, D., et al., *Association between a novel variant of the human type 2 deiodinase gene Thr92Ala and insulin resistance: evidence of interaction with the Trp64Arg variant of the beta-3-adrenergic receptor.* Diabetes, 2002. **51**(3): p. 880-3.
77. Corella, D., et al., *Gender specific associations of the Trp64Arg mutation in the beta3-adrenergic receptor gene with obesity-related phenotypes in a Mediterranean population: interaction with a common lipoprotein lipase gene variation.* J Intern Med, 2001. **250**(4): p. 348-60.
78. Aoyama, M., et al., *Phenotypic linkage between single-nucleotide polymorphisms of beta3-adrenergic receptor gene and NADH dehydrogenase subunit-2 gene, with special reference to eating behavior.* Biochem Biophys Res Commun, 2003. **309**(1): p. 261-5.
79. Piétri-Rouxel, F., et al., *The biochemical effect of the naturally occurring Trp64-->Arg mutation on human beta3-adrenoceptor activity.* Eur J Biochem, 1997. **247**(3): p. 1174-9.
80. Kimura, K., et al., *Mutated human beta3-adrenergic receptor (Trp64Arg) lowers the response to beta3-adrenergic agonists in transfected 3T3-L1 preadipocytes.* Horm Metab Res, 2000. **32**(3): p. 91-6.
81. Perfetti, R., et al., *Pancreatic beta-cells expressing the Arg64 variant of the beta(3)-adrenergic receptor exhibit abnormal insulin secretory activity.* J Mol Endocrinol, 2001. **27**(2): p. 133-44.
82. Vrydag, W., A.E. Alewijnse, and M.C. Michel, *Do gene polymorphisms alone or in combination affect the function of human beta3-adrenoceptors?* Br J Pharmacol, 2009. **156**(1): p. 127-34.
83. Huang, Q., et al., *Trp64Arg (rs4994) polymorphism of β3-adrenergic receptor gene is associated with hyperuricemia in a Chinese male population.* Clin Chem Lab Med, 2013. **51**(9): p. 1755-60.
84. Voruganti, V.S., et al., *Genetic variation in APOJ, LPL, and TNFRSF10B affects plasma fatty acid distribution in Alaskan Eskimos.* Am J Clin Nutr, 2010. **91**(6): p. 1574-83.
85. Hamilton, G., et al., *Candidate gene association study of insulin signaling genes and Alzheimer's disease: evidence for SOS2, PCK1, and PPARgamma as susceptibility loci.* Am J Med Genet B Neuropsychiatr Genet, 2007. **144B**(4): p. 508-16.
86. Grazia Perrone, M. and A. Scilimati, *β(3)-Adrenoceptor agonists and (antagonists as) inverse agonists history, perspective, constitutive activity, and stereospecific binding.* Methods Enzymol, 2010. **484**: p. 197-230.
87. Baker, J.G., *The selectivity of beta-adrenoceptor agonists at human beta1-, beta2- and beta3-adrenoceptors.* Br J Pharmacol, 2010. **160**(5): p. 1048-61.

88. Hoffmann, C., et al., *Comparative pharmacology of human beta-adrenergic receptor subtypes--characterization of stably transfected receptors in CHO cells.* Naunyn Schmiedebergs Arch Pharmacol, 2004. **369**(2): p. 151-9.
89. Niu, X., et al., *β3-Adrenoreceptor stimulation protects against myocardial infarction injury via eNOS and nNOS activation.* PLoS One, 2014. **9**(6): p. e98713.
90. Mitidieri, E., et al., *β.* Pharmacol Res, 2017. **124**: p. 100-104.
91. Wang, Z., et al., *The protective effects of the β3 adrenergic receptor agonist BRL37344 against liver steatosis and inflammation in a rat model of high-fat diet-induced nonalcoholic fatty liver disease (NAFLD).* Mol Med, 2020. **26**(1): p. 54.
92. Michel, M.C., *Do β-adrenoceptor agonists induce homologous or heterologous desensitization in rat urinary bladder?* Naunyn Schmiedebergs Arch Pharmacol, 2014. **387**(3): p. 215-24.
93. Puzzo, D., et al., *CL316,243, a β3-adrenergic receptor agonist, induces muscle hypertrophy and increased strength.* Sci Rep, 2016. **5**: p. 37504.
94. Karimi Galougahi, K., et al., *β3 Adrenergic Stimulation Restores Nitric Oxide/Redox Balance and Enhances Endothelial Function in Hyperglycemia.* J Am Heart Assoc, 2016. **5**(2).
95. Keam, S.J., *Mirabegron: Pediatric First Approval.* Paediatr Drugs, 2021. **23**(4): p. 411-415.
96. Chapple, C.R., et al., *Mirabegron in overactive bladder: a review of efficacy, safety, and tolerability.* Neurourol Urodyn, 2014. **33**(1): p. 17-30.
97. Biers, S.M., J.M. Reynard, and A.F. Brading, *The effects of a new selective beta3-adrenoceptor agonist (GW427353) on spontaneous activity and detrusor relaxation in human bladder.* BJU Int, 2006. **98**(6): p. 1310-4.
98. Bianchetti, A. and L. Manara, *In vitro inhibition of intestinal motility by phenylethanolaminotetralines: evidence of atypical beta-adrenoceptors in rat colon.* Br J Pharmacol, 1990. **100**(4): p. 831-9.
99. Tanyeri, P., et al., *Involvement of serotonin receptor subtypes in the antidepressant-like effect of beta receptor agonist Amibegron (SR 58611A): an experimental study.* Pharmacol Biochem Behav, 2013. **105**: p. 12-6.
100. Vasina, V., et al., *The beta3-adrenoceptor agonist SR58611A ameliorates experimental colitis in rats.* Neurogastroenterol Motil, 2008. **20**(9): p. 1030-41.
101. Sun, J., et al., *β3 adrenergic receptor antagonist SR59230A exerts beneficial effects on right ventricular performance in monocrotaline-induced pulmonary arterial hypertension.* Exp Ther Med, 2020. **19**(1): p. 489-498.
102. Russell, S.T., K. Hirai, and M.J. Tisdale, *Role of beta3-adrenergic receptors in the action of a tumour lipid mobilizing factor.* Br J Cancer, 2002. **86**(3): p. 424-8.
103. Calvani, M., et al., *β3-Adrenoreceptor Blockade Induces Stem Cells Differentiation in Melanoma Microenvironment.* Int J Mol Sci, 2020. **21**(4).
104. Parmee, E.R., et al., *Discovery of L-755,507: a subnanomolar human beta 3 adrenergic receptor agonist.* Bioorg Med Chem Lett, 1998. **8**(9): p. 1107-12.
105. Hu, B., et al., *(4-Piperidin-1-yl)phenyl amides: potent and selective human beta(3) agonists.* J Med Chem, 2001. **44**(9): p. 1456-66.
106. Arch, J.R., et al., *Atypical beta-adrenoceptor on brown adipocytes as target for anti-obesity drugs.* Nature, 1984. **309**(5964): p. 163-5.
107. Schena, G. and M.J. Caplan, *Everything You Always Wanted to Know about β.* Cells, 2019. **8**(4).

108. Hodis, J., R. Vaclavíková, and H. Farghali, *Beta-3 agonist-induced lipolysis and nitric oxide production: relationship to PPARgamma agonist/antagonist and AMP kinase modulation.* Gen Physiol Biophys, 2011. **30**(1): p. 90-9.
109. Banfi, S., et al., *Increased thermogenesis by a noncanonical pathway in ANGPTL3/8-deficient mice.* Proc Natl Acad Sci U S A, 2018. **115**(6): p. E1249-E1258.
110. Mattsson, C.L., et al., *β_1-Adrenergic receptors increase UCP1 in human MADS brown adipocytes and rescue cold-acclimated β_3-adrenergic receptor-knockout mice via nonshivering thermogenesis.* Am J Physiol Endocrinol Metab, 2011. **301**(6): p. E1108-18.
111. Larsen, T.M., et al., *Effect of a 28-d treatment with L-796568, a novel beta(3)-adrenergic receptor agonist, on energy expenditure and body composition in obese men.* Am J Clin Nutr, 2002. **76**(4): p. 780-8.
112. van Baak, M.A., et al., *Acute effect of L-796568, a novel beta 3-adrenergic receptor agonist, on energy expenditure in obese men.* Clin Pharmacol Ther, 2002. **71**(4): p. 272-9.
113. Cypess, A.M., et al., *Identification and importance of brown adipose tissue in adult humans.* N Engl J Med, 2009. **360**(15): p. 1509-17.
114. Baskin, A.S., et al., *Regulation of Human Adipose Tissue Activation, Gallbladder Size, and Bile Acid Metabolism by a β3-Adrenergic Receptor Agonist.* Diabetes, 2018. **67**(10): p. 2113-2125.
115. Gauthier, C., et al., *Functional beta3-adrenoceptor in the human heart.* J Clin Invest, 1996. **98**(2): p. 556-62.
116. Moniotte, S., et al., *Upregulation of beta(3)-adrenoceptors and altered contractile response to inotropic amines in human failing myocardium.* Circulation, 2001. **103**(12): p. 1649-55.
117. Trappanese, D.M., et al., *Chronic β1-adrenergic blockade enhances myocardial β3-adrenergic coupling with nitric oxide-cGMP signaling in a canine model of chronic volume overload: new insight into mechanisms of cardiac benefit with selective β1-blocker therapy.* Basic Res Cardiol, 2015. **110**(1): p. 456.
118. Gauthier, C., D. Langin, and J.L. Balligand, *Beta3-adrenoceptors in the cardiovascular system.* Trends Pharmacol Sci, 2000. **21**(11): p. 426-31.
119. Balligand, J.L., *Cardiac salvage by tweaking with beta-3-adrenergic receptors.* Cardiovasc Res, 2016. **111**(2): p. 128-33.
120. Cannavo, A., D. Liccardo, and W.J. Koch, *Targeting cardiac β-adrenergic signaling via GRK2 inhibition for heart failure therapy.* Front Physiol, 2013. **4**: p. 264.
121. Moniotte, S. and J.L. Balligand, *Potential use of beta(3)-adrenoceptor antagonists in heart failure therapy.* Cardiovasc Drug Rev, 2002. **20**(1): p. 19-26.
122. Mongillo, M., et al., *Compartmentalized phosphodiesterase-2 activity blunts beta-adrenergic cardiac inotropy via an NO/cGMP-dependent pathway.* Circ Res, 2006. **98**(2): p. 226-34.
123. García-Prieto, J., et al., *β3 adrenergic receptor selective stimulation during ischemia/reperfusion improves cardiac function in translational models through inhibition of mPTP opening in cardiomyocytes.* Basic Res Cardiol, 2014. **109**(4): p. 422.
124. Sharma, V., et al., *Metoprolol increases the expression of beta(3)-adrenoceptors in the diabetic heart: effects on nitric oxide signaling and forkhead transcription factor-3.* Eur J Pharmacol, 2008. **595**(1-3): p. 44-51.

125. Zhang, Z., et al., *Nebivolol protects against myocardial infarction injury via stimulation of beta 3-adrenergic receptors and nitric oxide signaling.* PLoS One, 2014. **9**(5): p. e98179.
126. Aragón, J.P., et al., *Beta3-adrenoreceptor stimulation ameliorates myocardial ischemia-reperfusion injury via endothelial nitric oxide synthase and neuronal nitric oxide synthase activation.* J Am Coll Cardiol, 2011. **58**(25): p. 2683-91.
127. Igawa, Y., et al., *Functional and molecular biological evidence for a possible beta3-adrenoceptor in the human detrusor muscle.* Br J Pharmacol, 1999. **126**(3): p. 819-25.
128. Otsuka, A., et al., *Expression and functional role of beta-adrenoceptors in the human urinary bladder urothelium.* Naunyn Schmiedebergs Arch Pharmacol, 2008. **377**(4-6): p. 473-81.
129. Rouget, C., et al., *Modulation of nerve-evoked contractions by β3-adrenoceptor agonism in human and rat isolated urinary bladder.* Pharmacol Res, 2014. **80**: p. 14-20.
130. Gillespie, J.I., et al., *Beta adrenergic modulation of spontaneous microcontractions and electrical field-stimulated contractions in isolated strips of rat urinary bladder from normal animals and animals with partial bladder outflow obstruction.* Naunyn Schmiedebergs Arch Pharmacol, 2015. **388**(7): p. 719-26.
131. Michel, M.C. and C. Korstanje, *β3-Adrenoceptor agonists for overactive bladder syndrome: Role of translational pharmacology in a repositioning clinical drug development project.* Pharmacol Ther, 2016. **159**: p. 66-82.
132. Procino, G., et al., *β3 adrenergic receptor in the kidney may be a new player in sympathetic regulation of renal function.* Kidney Int, 2016. **90**(3): p. 555-67.
133. Shen, H., et al., *Expression of β-adrenergic receptor subtypes in human normal and dilated ureter.* Int Urol Nephrol, 2017. **49**(10): p. 1771-1778.
134. Chen, S.F., C.L. Lee, and H.C. Kuo, *Changes in sensory proteins in the bladder urothelium of patients with chronic kidney disease and end-stage renal disease.* Low Urin Tract Symptoms, 2019. **11**(2): p. O202-O208.
135. Rodriguez, M., et al., *Evidence for the presence of beta 3-adrenergic receptor mRNA in the human brain.* Brain Res Mol Brain Res, 1995. **29**(2): p. 369-75.
136. Stemmelin, J., et al., *Stimulation of the beta3-Adrenoceptor as a novel treatment strategy for anxiety and depressive disorders.* Neuropsychopharmacology, 2008. **33**(3): p. 574-87.
137. Claustre, Y., et al., *Effects of the beta3-adrenoceptor (Adrb3) agonist SR58611A (amibegron) on serotonergic and noradrenergic transmission in the rodent: relevance to its antidepressant/anxiolytic-like profile.* Neuroscience, 2008. **156**(2): p. 353-64.
138. Gibbs, M.E., D.S. Hutchinson, and R.J. Summers, *Role of beta-adrenoceptors in memory consolidation: beta3-adrenoceptors act on glucose uptake and beta2-adrenoceptors on glycogenolysis.* Neuropsychopharmacology, 2008. **33**(10): p. 2384-97.
139. Dal Monte, M., L. Filippi, and P. Bagnoli, *Beta3-adrenergic receptors modulate vascular endothelial growth factor release in response to hypoxia through the nitric oxide pathway in mouse retinal explants.* Naunyn Schmiedebergs Arch Pharmacol, 2013. **386**(4): p. 269-78.

140. Casini, G., et al., *The β-adrenergic system as a possible new target for pharmacologic treatment of neovascular retinal diseases.* Prog Retin Eye Res, 2014. **42**: p. 103-29.
141. Escarcega González, C.E., et al., *β-Adrenoceptor Blockade for Infantile Hemangioma Therapy: Do β3-Adrenoceptors Play a Role?* J Vasc Res, 2018. **55**(3): p. 159-168.
142. Prey, S., et al., *Mast cells as possible targets of propranolol therapy: an immunohistological study of beta-adrenergic receptors in infantile haemangiomas.* Histopathology, 2014. **65**(3): p. 436-9.
143. Moretti, S., et al., *β-adrenoceptors are upregulated in human melanoma and their activation releases pro-tumorigenic cytokines and metalloproteases in melanoma cell lines.* Lab Invest, 2013. **93**(3): p. 279-90.
144. Montoya, A., et al., *Use of non-selective β-blockers is associated with decreased tumor proliferative indices in early stage breast cancer.* Oncotarget, 2017. **8**(4): p. 6446-6460.
145. Watkins, J.L., et al., *Clinical impact of selective and nonselective beta-blockers on survival in patients with ovarian cancer.* Cancer, 2015. **121**(19): p. 3444-51.
146. Zheng, M., et al., *ADRB3 expression in tumor cells is a poor prognostic factor and promotes proliferation in non-small cell lung carcinoma.* Cancer Immunol Immunother, 2020. **69**(11): p. 2345-2355.
147. Bruno, G., et al., *β3-adrenoreceptor blockade reduces tumor growth and increases neuronal differentiation in neuroblastoma via SK2/S1P.* Oncogene, 2020. **39**(2): p. 368-384.
148. Pasha, A., et al., *β3-Adrenoreceptor Activity Limits Apigenin Efficacy in Ewing Sarcoma Cells: A Dual Approach to Prevent Cell Survival.* Int J Mol Sci, 2019. **20**(9).
149. Antoni, M.H., et al., *The influence of bio-behavioural factors on tumour biology: pathways and mechanisms.* Nat Rev Cancer, 2006. **6**(3): p. 240-8.
150. Cole, S.W. and A.K. Sood, *Molecular pathways: beta-adrenergic signaling in cancer.* Clin Cancer Res, 2012. **18**(5): p. 1201-6.
151. Lutgendorf, S.K., et al., *Social isolation is associated with elevated tumor norepinephrine in ovarian carcinoma patients.* Brain Behav Immun, 2011. **25**(2): p. 250-5.
152. Entschladen, F., et al., *Tumour-cell migration, invasion, and metastasis: navigation by neurotransmitters.* Lancet Oncol, 2004. **5**(4): p. 254-8.
153. Sloan, E.K., et al., *The sympathetic nervous system induces a metastatic switch in primary breast cancer.* Cancer Res, 2010. **70**(18): p. 7042-52.
154. Palm, D., et al., *The norepinephrine-driven metastasis development of PC-3 human prostate cancer cells in BALB/c nude mice is inhibited by beta-blockers.* Int J Cancer, 2006. **118**(11): p. 2744-9.
155. Thaker, P.H., et al., *Chronic stress promotes tumor growth and angiogenesis in a mouse model of ovarian carcinoma.* Nat Med, 2006. **12**(8): p. 939-44.
156. Inbar, S., et al., *Do stress responses promote leukemia progression? An animal study suggesting a role for epinephrine and prostaglandin-E2 through reduced NK activity.* PLoS One, 2011. **6**(4): p. e19246.
157. Goldfarb, Y., et al., *Improving postoperative immune status and resistance to cancer metastasis: a combined perioperative approach of immunostimulation and prevention of excessive surgical stress responses.* Ann Surg, 2011. **253**(4): p. 798-810.

158. Cole, S.W., et al., *Sympathetic nervous system regulation of the tumour microenvironment.* Nat Rev Cancer, 2015. **15**(9): p. 563-72.
159. Huang, X.E., et al., *Possible association of beta2- and beta3-adrenergic receptor gene polymorphisms with susceptibility to breast cancer.* Breast Cancer Res, 2001. **3**(4): p. 264-9.
160. Babol, K., et al., *An association between the Trp64Arg polymorphism in the beta3-adrenergic receptor gene and endometrial cancer and obesity.* J Exp Clin Cancer Res, 2004. **23**(4): p. 669-74.
161. Perrone, M.G., et al., *Upregulation of beta3-adrenergic receptor mRNA in human colon cancer: a preliminary study.* Oncology, 2008. **75**(3-4): p. 224-9.
162. Magnon, C., et al., *Autonomic nerve development contributes to prostate cancer progression.* Science, 2013. **341**(6142): p. 1236361.
163. Chisholm, K.M., et al., *β-Adrenergic receptor expression in vascular tumors.* Mod Pathol, 2012. **25**(11): p. 1446-51.
164. Lamkin, D.M., et al., *Chronic stress enhances progression of acute lymphoblastic leukemia via β-adrenergic signaling.* Brain Behav Immun, 2012. **26**(4): p. 635-41.
165. Rains, S.L., C.N. Amaya, and B.A. Bryan, *Beta-adrenergic receptors are expressed across diverse cancers.* Oncoscience, 2017. **4**(7-8): p. 95-105.
166. Dal Monte, M., et al., *Functional involvement of β3-adrenergic receptors in melanoma growth and vascularization.* J Mol Med (Berl), 2013. **91**(12): p. 1407-19.
167. Sereni, F., et al., *Role of host β1- and β2-adrenergic receptors in a murine model of B16 melanoma: functional involvement of β3-adrenergic receptors.* Naunyn Schmiedebergs Arch Pharmacol, 2015. **388**(12): p. 1317-31.
168. Dal Monte, M., et al., *β3-adrenergic receptor activity modulates melanoma cell proliferation and survival through nitric oxide signaling.* Naunyn Schmiedebergs Arch Pharmacol, 2014. **387**(6): p. 533-43.
169. Cai, H.Y., et al., *The essential role for aromatic cluster in the β3 adrenergic receptor.* Acta Pharmacol Sin, 2012. **33**(8): p. 1062-8.
170. Calvani, M., et al., *Norepinephrine promotes tumor microenvironment reactivity through β3-adrenoreceptors during melanoma progression.* Oncotarget, 2015. **6**(7): p. 4615-32.
171. Calvani, M., et al., *β.* Br J Pharmacol, 2019. **176**(14): p. 2509-2524.
172. Harris, A.L., *Hypoxia--a key regulatory factor in tumour growth.* Nat Rev Cancer, 2002. **2**(1): p. 38-47.
173. Calvani, M., et al., *Preliminary Study on β3-Adrenoreceptor as Predictor Marker of Relapse in Ewing Sarcoma Patients.* Biomedicines, 2020. **8**(10).
174. Gupta, M.K., et al., *An assessment of the role of reactive oxygen species and redox signaling in norepinephrine-induced apoptosis and hypertrophy of H9c2 cardiac myoblasts.* Antioxid Redox Signal, 2006. **8**(5-6): p. 1081-93.
175. Xu, Q., et al., *Myocardial oxidative stress contributes to transgenic β_2-adrenoceptor activation-induced cardiomyopathy and heart failure.* Br J Pharmacol, 2011. **162**(5): p. 1012-28.
176. Brixius, K., et al., *Mechanisms of beta 3-adrenoceptor-induced eNOS activation in right atrial and left ventricular human myocardium.* Br J Pharmacol, 2004. **143**(8): p. 1014-22.
177. Hadi, T., et al., *Beta3 adrenergic receptor stimulation in human macrophages inhibits NADPHoxidase activity and induces catalase expression via PPARγ activation.* Biochim Biophys Acta Mol Cell Res, 2017. **1864**(10): p. 1769-1784.

178. Burke, A.J., et al., *The yin and yang of nitric oxide in cancer progression.* Carcinogenesis, 2013. **34**(3): p. 503-12.
179. Sikora, A.G., et al., *Targeted inhibition of inducible nitric oxide synthase inhibits growth of human melanoma in vivo and synergizes with chemotherapy.* Clin Cancer Res, 2010. **16**(6): p. 1834-44.
180. Yoshioka, Y., et al., *Noradrenaline increases intracellular glutathione in human astrocytoma U-251 MG cells by inducing glutamate-cysteine ligase protein via β3-adrenoceptor stimulation.* Eur J Pharmacol, 2016. **772**: p. 51-61.
181. Ferrucci, V., et al., *Natural compounds for pediatric cancer treatment.* Naunyn Schmiedebergs Arch Pharmacol, 2016. **389**(2): p. 131-49.
182. Schoenfeld, J.D., et al., *Redox active metals and H.* Redox Biol, 2018. **14**: p. 417-422.
183. Calvani, M., A. Pasha, and C. Favre, *Nutraceutical Boom in Cancer: Inside the Labyrinth of Reactive Oxygen Species.* Int J Mol Sci, 2020. **21**(6).
184. Collaborators, G.C.C., *The global burden of childhood and adolescent cancer in 2017: an analysis of the Global Burden of Disease Study 2017.* Lancet Oncol, 2019. **20**(9): p. 1211-1225.
185. Siegel, R.L., et al., *Cancer Statistics, 2021.* CA Cancer J Clin, 2021. **71**(1): p. 7-33.
186. Messerschmitt, P.J., et al., *Osteosarcoma.* J Am Acad Orthop Surg, 2009. **17**(8): p. 515-27.
187. Mirabello, L., R.J. Troisi, and S.A. Savage, *International osteosarcoma incidence patterns in children and adolescents, middle ages and elderly persons.* Int J Cancer, 2009. **125**(1): p. 229-34.
188. Abate, M.E., et al., *Non-metastatic osteosarcoma of the extremities in children aged 5 years or younger.* Pediatr Blood Cancer, 2010. **55**(4): p. 652-4.
189. Pakos, E.E., et al., *Prognostic factors and outcomes for osteosarcoma: an international collaboration.* Eur J Cancer, 2009. **45**(13): p. 2367-75.
190. Ottaviani, G. and N. Jaffe, *The epidemiology of osteosarcoma.* Cancer Treat Res, 2009. **152**: p. 3-13.
191. Linabery, A.M. and J.A. Ross, *Trends in childhood cancer incidence in the U.S. (1992-2004).* Cancer, 2008. **112**(2): p. 416-32.
192. Gatta, G., et al., *Childhood cancer survival in Europe and the United States.* Cancer, 2002. **95**(8): p. 1767-72.
193. Sampo, M.M., et al., *Osteosarcoma in Finland from 1971 through 1990: a nationwide study of epidemiology and outcome.* Acta Orthop, 2008. **79**(6): p. 861-6.
194. Picci, P., et al., *Survival in high-grade osteosarcoma: improvement over 21 years at a single institution.* Ann Oncol, 2010. **21**(6): p. 1366-1373.
195. Longhi, A., et al., *Osteosarcoma in patients older than 65 years.* J Clin Oncol, 2008. **26**(33): p. 5368-73.
196. Robling, A.G., A.B. Castillo, and C.H. Turner, *Biomechanical and molecular regulation of bone remodeling.* Annu Rev Biomed Eng, 2006. **8**: p. 455-98.
197. Datta, H.K., et al., *The cell biology of bone metabolism.* J Clin Pathol, 2008. **61**(5): p. 577-87.
198. Capulli, M., R. Paone, and N. Rucci, *Osteoblast and osteocyte: games without frontiers.* Arch Biochem Biophys, 2014. **561**: p. 3-12.
199. Franz-Odendaal, T.A., B.K. Hall, and P.E. Witten, *Buried alive: how osteoblasts become osteocytes.* Dev Dyn, 2006. **235**(1): p. 176-90.

200. Chan, G.K. and G. Duque, *Age-related bone loss: old bone, new facts.* Gerontology, 2002. **48**(2): p. 62-71.
201. Crockett, J.C., et al., *New knowledge on critical osteoclast formation and activation pathways from study of rare genetic diseases of osteoclasts: focus on the RANK/RANKL axis.* Osteoporos Int, 2011. **22**(1): p. 1-20.
202. Charles, J.F. and A.O. Aliprantis, *Osteoclasts: more than 'bone eaters'.* Trends Mol Med, 2014. **20**(8): p. 449-59.
203. Aarden, E.M., E.H. Burger, and P.J. Nijweide, *Function of osteocytes in bone.* J Cell Biochem, 1994. **55**(3): p. 287-99.
204. Mutsaers, A.J. and C.R. Walkley, *Cells of origin in osteosarcoma: mesenchymal stem cells or osteoblast committed cells?* Bone, 2014. **62**: p. 56-63.
205. Xiao, W., et al., *Mesenchymal stem cell transformation and sarcoma genesis.* Clin Sarcoma Res, 2013. **3**(1): p. 10.
206. Uccelli, A., L. Moretta, and V. Pistoia, *Mesenchymal stem cells in health and disease.* Nat Rev Immunol, 2008. **8**(9): p. 726-36.
207. Jo, V.Y. and C.D. Fletcher, *WHO classification of soft tissue tumours: an update based on the 2013 (4th) edition.* Pathology, 2014. **46**(2): p. 95-104.
208. Shimizu, T., et al., *c-MYC overexpression with loss of Ink4a/Arf transforms bone marrow stromal cells into osteosarcoma accompanied by loss of adipogenesis.* Oncogene, 2010. **29**(42): p. 5687-99.
209. Wang, J.Y., et al., *Generation of Osteosarcomas from a Combination of Rb Silencing and c-Myc Overexpression in Human Mesenchymal Stem Cells.* Stem Cells Transl Med, 2017. **6**(2): p. 512-526.
210. Yang, Y., et al., *Genetically transforming human osteoblasts to sarcoma: development of an osteosarcoma model.* Genes Cancer, 2017. **8**(1-2): p. 484-494.
211. Rubio, R., et al., *The differentiation stage of p53-Rb-deficient bone marrow mesenchymal stem cells imposes the phenotype of in vivo sarcoma development.* Oncogene, 2013. **32**(41): p. 4970-80.
212. Pietrovito, L., et al., *Bone marrow-derived mesenchymal stem cells promote invasiveness and transendothelial migration of osteosarcoma cells via a mesenchymal to amoeboid transition.* Mol Oncol, 2018. **12**(5): p. 659-676.
213. Sottnik, J.L., et al., *Osteocytes serve as a progenitor cell of osteosarcoma.* J Cell Biochem, 2014. **115**(8): p. 1420-9.
214. Wittrant, Y., et al., *RANKL/RANK/OPG: new therapeutic targets in bone tumours and associated osteolysis.* Biochim Biophys Acta, 2004. **1704**(2): p. 49-57.
215. Lamora, A., et al., *TGF-β Signaling in Bone Remodeling and Osteosarcoma Progression.* J Clin Med, 2016. **5**(11).
216. Verrecchia, F. and F. Rédini, *Transforming Growth Factor-β Signaling Plays a Pivotal Role in the Interplay Between Osteosarcoma Cells and Their Microenvironment.* Front Oncol, 2018. **8**: p. 133.
217. Paparella, M.L., et al., *Osteosarcoma of the jaw: an analysis of a series of 74 cases.* Histopathology, 2013. **63**(4): p. 551-7.
218. Bielack, S.S., et al., *Prognostic factors in high-grade osteosarcoma of the extremities or trunk: an analysis of 1,702 patients treated on neoadjuvant cooperative osteosarcoma study group protocols.* J Clin Oncol, 2002. **20**(3): p. 776-90.
219. *StatPearls*. 2021.

220. Weiss, A., et al., *Telangiectatic osteosarcoma: the St. Jude Children's Research Hospital's experience.* Cancer, 2007. **109**(8): p. 1627-37.
221. Bacci, G., et al., *Telangiectatic osteosarcoma of the extremity: neoadjuvant chemotherapy in 24 cases.* Acta Orthop Scand, 2001. **72**(2): p. 167-72.
222. Zhong, J., et al., *Clarifying prognostic factors of small cell osteosarcoma: A pooled analysis of 20 cases and the literature.* J Bone Oncol, 2020. **24**: p. 100305.
223. Righi, A., et al., *Small cell osteosarcoma: clinicopathologic, immunohistochemical, and molecular analysis of 36 cases.* Am J Surg Pathol, 2015. **39**(5): p. 691-9.
224. Malhas, A.M., et al., *Low-grade central osteosarcoma: a difficult condition to diagnose.* Sarcoma, 2012. **2012**: p. 764796.
225. Hang, J.F. and P.C. Chen, *Parosteal osteosarcoma.* Arch Pathol Lab Med, 2014. **138**(5): p. 694-9.
226. Lee, S.J., et al., *Surface osteosarcoma: Predictors of outcomes.* J Surg Oncol, 2021. **124**(4): p. 646-654.
227. Raymond, A.K., *Surface osteosarcoma.* Clin Orthop Relat Res, 1991(270): p. 140-8.
228. Nouri, H., et al., *Surface osteosarcoma: Clinical features and therapeutic implications.* J Bone Oncol, 2015. **4**(4): p. 115-23.
229. Rickel, K., F. Fang, and J. Tao, *Molecular genetics of osteosarcoma.* Bone, 2017. **102**: p. 69-79.
230. Wong, F.L., et al., *Cancer incidence after retinoblastoma. Radiation dose and sarcoma risk.* JAMA, 1997. **278**(15): p. 1262-7.
231. Smida, J., et al., *Genomic alterations and allelic imbalances are strong prognostic predictors in osteosarcoma.* Clin Cancer Res, 2010. **16**(16): p. 4256-67.
232. Mejia-Guerrero, S., et al., *Characterization of the 12q15 MDM2 and 12q13-14 CDK4 amplicons and clinical correlations in osteosarcoma.* Genes Chromosomes Cancer, 2010. **49**(6): p. 518-25.
233. Tsuchiya, T., et al., *Analysis of the p16INK4, p14ARF, p15, TP53, and MDM2 genes and their prognostic implications in osteosarcoma and Ewing sarcoma.* Cancer Genet Cytogenet, 2000. **120**(2): p. 91-8.
234. Patiño-García, A., et al., *Genetic and epigenetic alterations of the cell cycle regulators and tumor suppressor genes in pediatric osteosarcomas.* J Pediatr Hematol Oncol, 2003. **25**(5): p. 362-7.
235. Overholtzer, M., et al., *The presence of p53 mutations in human osteosarcomas correlates with high levels of genomic instability.* Proc Natl Acad Sci U S A, 2003. **100**(20): p. 11547-52.
236. Miller, C.W., et al., *Alterations of the p53, Rb and MDM2 genes in osteosarcoma.* J Cancer Res Clin Oncol, 1996. **122**(9): p. 559-65.
237. Paulson, Q.X., et al., *Transgenic expression of E2F3a causes DNA damage leading to ATM-dependent apoptosis.* Oncogene, 2008. **27**(36): p. 4954-61.
238. Hurst, C.D., et al., *Inactivation of the Rb pathway and overexpression of both isoforms of E2F3 are obligate events in bladder tumours with 6p22 amplification.* Oncogene, 2008. **27**(19): p. 2716-27.
239. Olsson, A.Y., et al., *Role of E2F3 expression in modulating cellular proliferation rate in human bladder and prostate cancer cells.* Oncogene, 2007. **26**(7): p. 1028-37.

240. Sadikovic, B., et al., *Expression analysis of genes associated with human osteosarcoma tumors shows correlation of RUNX2 overexpression with poor response to chemotherapy.* BMC Cancer, 2010. **10**: p. 202.
241. Steliarova-Foucher, E., et al., *International incidence of childhood cancer, 2001-10: a population-based registry study.* Lancet Oncol, 2017. **18**(6): p. 719-731.
242. Tomlinson, G.E., et al., *Rhabdoid tumor of the kidney in the National Wilms' Tumor Study: age at diagnosis as a prognostic factor.* J Clin Oncol, 2005. **23**(30): p. 7641-5.
243. Fanburg-Smith, J.C., et al., *Extrarenal rhabdoid tumors of soft tissue: a clinicopathologic and immunohistochemical study of 18 cases.* Ann Diagn Pathol, 1998. **2**(6): p. 351-62.
244. Heck, J.E., et al., *Epidemiology of rhabdoid tumors of early childhood.* Pediatr Blood Cancer, 2013. **60**(1): p. 77-81.
245. Ahmed, H.U., et al., *Part I: Primary malignant non-Wilms' renal tumours in children.* Lancet Oncol, 2007. **8**(8): p. 730-7.
246. Zhanghuang, C., et al., *Clinical and Molecular Differentiation Between Malignant Rhabdoid Tumor of the Kidney and Normal Tissue: A Two-Case Report.* Front Oncol, 2021. **11**: p. 659709.
247. van den Heuvel-Eibrink, M.M., et al., *Malignant rhabdoid tumours of the kidney (MRTKs), registered on recent SIOP protocols from 1993 to 2005: a report of the SIOP renal tumour study group.* Pediatr Blood Cancer, 2011. **56**(5): p. 733-7.
248. Vujanić, G.M., et al., *Rhabdoid tumour of the kidney: a clinicopathological study of 22 patients from the International Society of Paediatric Oncology (SIOP) nephroblastoma file.* Histopathology, 1996. **28**(4): p. 333-40.
249. Molenaar, W.M., et al., *Molecular markers of primitive neuroectodermal tumors and other pediatric central nervous system tumors. Monoclonal antibodies to neuronal and glial antigens distinguish subsets of primitive neuroectodermal tumors.* Lab Invest, 1989. **61**(6): p. 635-43.
250. Kodet, R., et al., *Rhabdomyosarcomas with intermediate-filament inclusions and features of rhabdoid tumors. Light microscopic and immunohistochemical study.* Am J Surg Pathol, 1991. **15**(3): p. 257-67.
251. Ogino, S., T.Y. Ro, and R.W. Redline, *Malignant rhabdoid tumor: A phenotype? An entity?--A controversy revisited.* Adv Anat Pathol, 2000. **7**(3): p. 181-90.
252. Douglass, E.C., et al., *Malignant rhabdoid tumor: a highly malignant childhood tumor with minimal karyotypic changes.* Genes Chromosomes Cancer, 1990. **2**(3): p. 210-6.
253. Rosty, C., et al., *Cytogenetic and molecular analysis of a t(1;22)(p36;q11.2) in a rhabdoid tumor with a putative homozygous deletion of chromosome 22.* Genes Chromosomes Cancer, 1998. **21**(2): p. 82-9.
254. Versteege, I., et al., *Truncating mutations of hSNF5/INI1 in aggressive paediatric cancer.* Nature, 1998. **394**(6689): p. 203-6.
255. Kwon, H., et al., *Nucleosome disruption and enhancement of activator binding by a human SW1/SNF complex.* Nature, 1994. **370**(6489): p. 477-81.
256. Owen-Hughes, T., et al., *Persistent site-specific remodeling of a nucleosome array by transient action of the SWI/SNF complex.* Science, 1996. **273**(5274): p. 513-6.
257. Lee, D., et al., *Interaction of E1 and hSNF5 proteins stimulates replication of human papillomavirus DNA.* Nature, 1999. **399**(6735): p. 487-91.

258. Biegel, J.A., et al., *Mutations of the INI1 rhabdoid tumor suppressor gene in medulloblastomas and primitive neuroectodermal tumors of the central nervous system.* Clin Cancer Res, 2000. **6**(7): p. 2759-63.
259. DeCristofaro, M.F., et al., *Alteration of hSNF5/INI1/BAF47 detected in rhabdoid cell lines and primary rhabdomyosarcomas but not Wilms' tumors.* Oncogene, 1999. **18**(52): p. 7559-65.
260. Sévenet, N., et al., *Constitutional mutations of the hSNF5/INI1 gene predispose to a variety of cancers.* Am J Hum Genet, 1999. **65**(5): p. 1342-8.
261. Hoot, A.C., et al., *Immunohistochemical analysis of hSNF5/INI1 distinguishes renal and extra-renal malignant rhabdoid tumors from other pediatric soft tissue tumors.* Am J Surg Pathol, 2004. **28**(11): p. 1485-91.
262. Sigauke, E., et al., *Absence of expression of SMARCB1/INI1 in malignant rhabdoid tumors of the central nervous system, kidneys and soft tissue: an immunohistochemical study with implications for diagnosis.* Mod Pathol, 2006. **19**(5): p. 717-25.
263. Wang, X., et al., *SMARCB1-mediated SWI/SNF complex function is essential for enhancer regulation.* Nat Genet, 2017. **49**(2): p. 289-295.
264. Charboneau, A., et al., *P-Akt expression distinguishes two types of malignant rhabdoid tumors.* J Cell Physiol, 2006. **209**(2): p. 422-7.
265. Yamaoka, B., et al., *Exosomal miR-214-3p as a potential novel biomarker for rhabdoid tumor of the kidney.* Pediatr Surg Int, 2021.
266. Langley, P., et al., *The societal impact of pain in the European Union: health-related quality of life and healthcare resource utilization.* J Med Econ, 2010. **13**(3): p. 571-81.
267. Dahlhamer, J., et al., *Prevalence of Chronic Pain and High-Impact Chronic Pain Among Adults - United States, 2016.* MMWR Morb Mortal Wkly Rep, 2018. **67**(36): p. 1001-1006.
268. van Hecke, O., et al., *Neuropathic pain in the general population: a systematic review of epidemiological studies.* Pain, 2014. **155**(4): p. 654-662.
269. Janevic, M.R., et al., *Racial and Socioeconomic Disparities in Disabling Chronic Pain: Findings From the Health and Retirement Study.* J Pain, 2017. **18**(12): p. 1459-1467.
270. Macfarlane, G.J., et al., *Can large surveys conducted on highly selected populations provide valid information on the epidemiology of common health conditions? An analysis of UK Biobank data on musculoskeletal pain.* Br J Pain, 2015. **9**(4): p. 203-12.
271. Jeffries, L.J., S.F. Milanese, and K.A. Grimmer-Somers, *Epidemiology of adolescent spinal pain: a systematic overview of the research literature.* Spine (Phila Pa 1976), 2007. **32**(23): p. 2630-7.
272. King, S., et al., *The epidemiology of chronic pain in children and adolescents revisited: a systematic review.* Pain, 2011. **152**(12): p. 2729-2738.
273. Dubin, A.E. and A. Patapoutian, *Nociceptors: the sensors of the pain pathway.* J Clin Invest, 2010. **120**(11): p. 3760-72.
274. Basbaum, A.I., et al., *Cellular and molecular mechanisms of pain.* Cell, 2009. **139**(2): p. 267-84.
275. Oh, S.B., et al., *Chemokines and glycoprotein120 produce pain hypersensitivity by directly exciting primary nociceptive neurons.* J Neurosci, 2001. **21**(14): p. 5027-35.
276. Dawes, J.M., et al., *CXCL5 mediates UVB irradiation-induced pain.* Sci Transl Med, 2011. **3**(90): p. 90ra60.

277. Hucho, T. and J.D. Levine, *Signaling pathways in sensitization: toward a nociceptor cell biology.* Neuron, 2007. **55**(3): p. 365-76.
278. Bandell, M., et al., *Noxious cold ion channel TRPA1 is activated by pungent compounds and bradykinin.* Neuron, 2004. **41**(6): p. 849-57.
279. Obata, K., et al., *TRPA1 induced in sensory neurons contributes to cold hyperalgesia after inflammation and nerve injury.* J Clin Invest, 2005. **115**(9): p. 2393-401.
280. Schmidt, M., et al., *Nociceptive signals induce trafficking of TRPA1 to the plasma membrane.* Neuron, 2009. **64**(4): p. 498-509.
281. Pinho-Ribeiro, F.A., W.A. Verri, and I.M. Chiu, *Nociceptor Sensory Neuron-Immune Interactions in Pain and Inflammation.* Trends Immunol, 2017. **38**(1): p. 5-19.
282. Julius, D., *TRP channels and pain.* Annu Rev Cell Dev Biol, 2013. **29**: p. 355-84.
283. Chuang , H.H., et al., *Bradykinin and nerve growth factor release the capsaicin receptor from PtdIns(4,5)P2-mediated inhibition.* Nature, 2001. **411**(6840): p. 957-62.
284. Prescott, E.D. and D. Julius, *A modular PIP2 binding site as a determinant of capsaicin receptor sensitivity.* Science, 2003. **300**(5623): p. 1284-8.
285. Jin, X. and R.W. Gereau, *Acute p38-mediated modulation of tetrodotoxin-resistant sodium channels in mouse sensory neurons by tumor necrosis factor-alpha.* J Neurosci, 2006. **26**(1): p. 246-55.
286. Liu, X.J., et al., *TLR signaling adaptor protein MyD88 in primary sensory neurons contributes to persistent inflammatory and neuropathic pain and neuroinflammation.* Sci Rep, 2016. **6**: p. 28188.
287. Alessandri-Haber, N., et al., *A transient receptor potential vanilloid 4-dependent mechanism of hyperalgesia is engaged by concerted action of inflammatory mediators.* J Neurosci, 2006. **26**(14): p. 3864-74.
288. Todaka, H., et al., *Warm temperature-sensitive transient receptor potential vanilloid 4 (TRPV4) plays an essential role in thermal hyperalgesia.* J Biol Chem, 2004. **279**(34): p. 35133-8.
289. Michalick, L. and W.M. Kuebler, *TRPV4-A Missing Link Between Mechanosensation and Immunity.* Front Immunol, 2020. **11**: p. 413.
290. Binshtok, A.M., et al., *Nociceptors are interleukin-1beta sensors.* J Neurosci, 2008. **28**(52): p. 14062-73.
291. Chiu, I.M., C.A. von Hehn, and C.J. Woolf, *Neurogenic inflammation and the peripheral nervous system in host defense and immunopathology.* Nat Neurosci, 2012. **15**(8): p. 1063-7.
292. Matsuda, M., Y. Huh, and R.R. Ji, *Roles of inflammation, neurogenic inflammation, and neuroinflammation in pain.* J Anesth, 2019. **33**(1): p. 131-139.
293. Cook, A.D., et al., *Immune Cytokines and Their Receptors in Inflammatory Pain.* Trends Immunol, 2018. **39**(3): p. 240-255.
294. Sun, J., et al., *Substance P enhances NF-kappaB transactivation and chemokine response in murine macrophages via ERK1/2 and p38 MAPK signaling pathways.* Am J Physiol Cell Physiol, 2008. **294**(6): p. C1586-96.
295. Yaraee, R., et al., *Effect of neuropeptides (SP and CGRP) on antigen presentation by macrophages.* Immunopharmacol Immunotoxicol, 2005. **27**(3): p. 395-404.
296. Gao, Y.J. and R.R. Ji, *Chemokines, neuronal-glial interactions, and central processing of neuropathic pain.* Pharmacol Ther, 2010. **126**(1): p. 56-68.

297. White, F.A., et al., *Excitatory monocyte chemoattractant protein-1 signaling is up-regulated in sensory neurons after chronic compression of the dorsal root ganglion.* Proc Natl Acad Sci U S A, 2005. **102**(39): p. 14092-7.
298. Willemen, H.L., et al., *Monocytes/Macrophages control resolution of transient inflammatory pain.* J Pain, 2014. **15**(5): p. 496-506.
299. Bang, S., et al., *GPR37 regulates macrophage phagocytosis and resolution of inflammatory pain.* J Clin Invest, 2018. **128**(8): p. 3568-3582.
300. Park, C.K., et al., *Resolving TRPV1- and TNF-α-mediated spinal cord synaptic plasticity and inflammatory pain with neuroprotectin D1.* J Neurosci, 2011. **31**(42): p. 15072-85.
301. Qu, L. and M.J. Caterina, *Accelerating the reversal of inflammatory pain with NPD1 and its receptor GPR37.* J Clin Invest, 2018. **128**(8): p. 3246-3249.
302. Kanashiro, A., et al., *The role of neutrophils in neuro-immune modulation.* Pharmacol Res, 2020. **151**: p. 104580.
303. McNamee, K.E., et al., *IL-17 induces hyperalgesia via TNF-dependent neutrophil infiltration.* Pain, 2011. **152**(8): p. 1838-1845.
304. Carreira, E.U., et al., *Neutrophils recruited by CXCR1/2 signalling mediate post-incisional pain.* Eur J Pain, 2013. **17**(5): p. 654-63.
305. Pinho-Ribeiro, F.A., et al., *Blocking Neuronal Signaling to Immune Cells Treats Streptococcal Invasive Infection.* Cell, 2018. **173**(5): p. 1083-1097.e22.
306. Chiu, I.M., et al., *Bacteria activate sensory neurons that modulate pain and inflammation.* Nature, 2013. **501**(7465): p. 52-7.
307. Rittner, H.L., et al., *Mycobacteria attenuate nociceptive responses by formyl peptide receptor triggered opioid peptide release from neutrophils.* PLoS Pathog, 2009. **5**(4): p. e1000362.
308. Forsythe, P. and J. Bienenstock, *The mast cell-nerve functional unit: a key component of physiologic and pathophysiologic responses.* Chem Immunol Allergy, 2012. **98**: p. 196-221.
309. Nigrovic, P.A. and D.M. Lee, *Mast cells in inflammatory arthritis.* Arthritis Res Ther, 2005. **7**(1): p. 1-11.
310. Chatterjea, D. and T. Martinov, *Mast cells: versatile gatekeepers of pain.* Mol Immunol, 2015. **63**(1): p. 38-44.
311. Rudick, C.N., et al., *Mast cell-derived histamine mediates cystitis pain.* PLoS One, 2008. **3**(5): p. e2096.
312. Milenkovic, N., et al., *Nociceptive tuning by stem cell factor/c-Kit signaling.* Neuron, 2007. **56**(5): p. 893-906.
313. Vincent, L., et al., *Mast cell activation contributes to sickle cell pathobiology and pain in mice.* Blood, 2013. **122**(11): p. 1853-62.
314. Jolly, P.S., et al., *Transactivation of sphingosine-1-phosphate receptors by FcepsilonRI triggering is required for normal mast cell degranulation and chemotaxis.* J Exp Med, 2004. **199**(7): p. 959-70.
315. Green, D.P., et al., *A Mast-Cell-Specific Receptor Mediates Neurogenic Inflammation and Pain.* Neuron, 2019. **101**(3): p. 412-420.e3.
316. Weaver, J.L., et al., *Hematopoietic pannexin 1 function is critical for neuropathic pain.* Sci Rep, 2017. **7**: p. 42550.
317. Bravo, D., et al., *Interactions of pannexin 1 with NMDA and P2X7 receptors in central nervous system pathologies: Possible role on chronic pain.* Pharmacol Res, 2015. **101**: p. 86-93.

318. Riol-Blanco, L., et al., *Nociceptive sensory neurons drive interleukin-23-mediated psoriasiform skin inflammation.* Nature, 2014. **510**(7503): p. 157-61.
319. Mikami, N., et al., *Calcitonin gene-related peptide regulates type IV hypersensitivity through dendritic cell functions.* PLoS One, 2014. **9**(1): p. e86367.
320. Abbott, C.A., et al., *Prevalence and characteristics of painful diabetic neuropathy in a large community-based diabetic population in the U.K.* Diabetes Care, 2011. **34**(10): p. 2220-4.
321. Costigan, M., J. Scholz, and C.J. Woolf, *Neuropathic pain: a maladaptive response of the nervous system to damage.* Annu Rev Neurosci, 2009. **32**: p. 1-32.
322. Szok, D., et al., *Therapeutic Approaches for Peripheral and Central Neuropathic Pain.* Behav Neurol, 2019. **2019**: p. 8685954.
323. Borsook, D., *Neurological diseases and pain.* Brain, 2012. **135**(Pt 2): p. 320-44.
324. Freeman, R., *Not all neuropathy in diabetes is of diabetic etiology: differential diagnosis of diabetic neuropathy.* Curr Diab Rep, 2009. **9**(6): p. 423-31.
325. Yang, Y., et al., *Mutations in SCN9A, encoding a sodium channel alpha subunit, in patients with primary erythermalgia.* J Med Genet, 2004. **41**(3): p. 171-4.
326. Patel, R. and A.H. Dickenson, *Neuronal hyperexcitability in the ventral posterior thalamus of neuropathic rats: modality selective effects of pregabalin.* J Neurophysiol, 2016. **116**(1): p. 159-70.
327. Navratilova, E., C.W. Atcherley, and F. Porreca, *Brain Circuits Encoding Reward from Pain Relief.* Trends Neurosci, 2015. **38**(11): p. 741-750.
328. Hartung, J.E., B.P. Ciszek, and A.G. Nackley, *β2- and β3-adrenergic receptors drive COMT-dependent pain by increasing production of nitric oxide and cytokines.* Pain, 2014. **155**(7): p. 1346-1355.
329. Zhang, X., et al., *Sustained stimulation of β.* Brain Behav Immun, 2018. **73**: p. 520-532.
330. Kanno, T., T. Yaguchi, and T. Nishizaki, *Noradrenaline stimulates ATP release from DRG neurons by targeting beta(3) adrenoceptors as a factor of neuropathic pain.* J Cell Physiol, 2010. **224**(2): p. 345-51.
331. Fávaro-Moreira, N.C., C.A. Parada, and C.H. Tambeli, *Blockade of β_1-, β_2- and β_3-adrenoceptors in the temporomandibular joint induces antinociception especially in female rats.* Eur J Pain, 2012. **16**(9): p. 1302-10.
332. Rayment, C., et al., *Neuropathic cancer pain: prevalence, severity, analgesics and impact from the European Palliative Care Research Collaborative-Computerised Symptom Assessment study.* Palliat Med, 2013. **27**(8): p. 714-21.
333. Cleeland, C.S., et al., *Are the symptoms of cancer and cancer treatment due to a shared biologic mechanism? A cytokine-immunologic model of cancer symptoms.* Cancer, 2003. **97**(11): p. 2919-25.
334. Koike, H. and G. Sobue, *Paraneoplastic neuropathy.* Handb Clin Neurol, 2013. **115**: p. 713-26.
335. Delanian, S., J.L. Lefaix, and P.F. Pradat, *Radiation-induced neuropathy in cancer survivors.* Radiother Oncol, 2012. **105**(3): p. 273-82.
336. Edwards, H.L., M.R. Mulvey, and M.I. Bennett, *Cancer-Related Neuropathic Pain.* Cancers (Basel), 2019. **11**(3).

337. Sahenk, Z., et al., *Taxol neuropathy. Electrodiagnostic and sural nerve biopsy findings.* Arch Neurol, 1994. **51**(7): p. 726-9.
338. Seretny, M., et al., *Incidence, prevalence, and predictors of chemotherapy-induced peripheral neuropathy: A systematic review and meta-analysis.* Pain, 2014. **155**(12): p. 2461-2470.
339. Kudel, I., et al., *Predictors and consequences of multiple persistent postmastectomy pains.* J Pain Symptom Manage, 2007. **34**(6): p. 619-27.
340. Lee, B.H., et al., *Behavioral characteristics of a mouse model of cancer pain.* Yonsei Med J, 2005. **46**(2): p. 252-9.
341. Asai, H., et al., *Heat and mechanical hyperalgesia in mice model of cancer pain.* Pain, 2005. **117**(1-2): p. 19-29.
342. Antoniazzi, C.T.D., et al., *Transient receptor potential ankyrin 1 (TRPA1) plays a critical role in a mouse model of cancer pain.* Int J Cancer, 2019. **144**(2): p. 355-365.
343. De Logu, F., et al., *Peripheral Nerve Resident Macrophages and Schwann Cells Mediate Cancer-Induced Pain.* Cancer Res, 2021. **81**(12): p. 3387-3401.
344. Ghilardi, J.R., et al., *Selective blockade of the capsaicin receptor TRPV1 attenuates bone cancer pain.* J Neurosci, 2005. **25**(12): p. 3126-31.
345. Tsuzuki, S., et al., *Skeletal complications in cancer patients with bone metastases.* Int J Urol, 2016. **23**(10): p. 825-832.
346. Lozano-Ondoua, A.N., A.M. Symons-Liguori, and T.W. Vanderah, *Cancer-induced bone pain: Mechanisms and models.* Neurosci Lett, 2013. **557 Pt A**: p. 52-9.
347. Shiozawa, Y., et al., *Bone marrow as a metastatic niche for disseminated tumor cells from solid tumors.* Bonekey Rep, 2015. **4**: p. 689.
348. Zheng, Y., et al., *The role of the bone microenvironment in skeletal metastasis.* J Bone Oncol, 2013. **2**(1): p. 47-57.
349. Buenrostro, D., S.I. Park, and J.A. Sterling, *Dissecting the role of bone marrow stromal cells on bone metastases.* Biomed Res Int, 2014. **2014**: p. 875305.
350. Clohisy, D.R. and P.W. Mantyh, *Bone cancer pain and the role of RANKL/OPG.* J Musculoskelet Neuronal Interact, 2004. **4**(3): p. 293-300.
351. Lingueglia, E., *[Acid-Sensing Ion Channels (ASICs) in pain].* Biol Aujourdhui, 2014. **208**(1): p. 13-20.
352. Holzer, P., *Acid-sensitive ion channels and receptors.* Handb Exp Pharmacol, 2009(194): p. 283-332.
353. Reyes, J.P., S.M. Sims, and S.J. Dixon, *P2 receptor expression, signaling and function in osteoclasts.* Front Biosci (Schol Ed), 2011. **3**: p. 1101-18.
354. Kaan, T.K., et al., *Systemic blockade of P2X3 and P2X2/3 receptors attenuates bone cancer pain behaviour in rats.* Brain, 2010. **133**(9): p. 2549-64.
355. Franceschini, A. and E. Adinolfi, *P2X receptors: New players in cancer pain.* World J Biol Chem, 2014. **5**(4): p. 429-36.
356. Kitano, Y., et al., *Gene expression of bone matrix proteins and endothelin receptors in endothelin-1-deficient mice revealed by in situ hybridization.* J Bone Miner Res, 1998. **13**(2): p. 237-44.
357. Kasperk, C.H., et al., *Endothelin-1 is a potent regulator of human bone cell metabolism in vitro.* Calcif Tissue Int, 1997. **60**(4): p. 368-74.
358. Peters, C.M., et al., *Endothelin and the tumorigenic component of bone cancer pain.* Neuroscience, 2004. **126**(4): p. 1043-52.

359. Park, S.H., et al., *Role of the Bone Microenvironment in the Development of Painful Complications of Skeletal Metastases.* Cancers (Basel), 2018. **10**(5).
360. Hiraoka, K., et al., *Inhibition of bone and muscle metastases of lung cancer cells by a decrease in the number of monocytes/macrophages.* Cancer Sci, 2008. **99**(8): p. 1595-602.
361. Zelenka, M., M. Schäfers, and C. Sommer, *Intraneural injection of interleukin-1beta and tumor necrosis factor-alpha into rat sciatic nerve at physiological doses induces signs of neuropathic pain.* Pain, 2005. **116**(3): p. 257-263.
362. Zhang, X.C., et al., *Tumor necrosis factor-α induces sensitization of meningeal nociceptors mediated via local COX and p38 MAP kinase actions.* Pain, 2011. **152**(1): p. 140-149.
363. Di Pompo, G., et al., *Intratumoral acidosis fosters cancer-induced bone pain through the activation of the mesenchymal tumor-associated stroma in bone metastasis from breast carcinoma.* Oncotarget, 2017. **8**(33): p. 54478-54496.
364. Hanahan, D. and R.A. Weinberg, *Hallmarks of cancer: the next generation.* Cell, 2011. **144**(5): p. 646-74.
365. Cairns, R.A., I.S. Harris, and T.W. Mak, *Regulation of cancer cell metabolism.* Nat Rev Cancer, 2011. **11**(2): p. 85-95.
366. WARBURG, O., *On the origin of cancer cells.* Science, 1956. **123**(3191): p. 309-14.
367. Fantin, V.R., J. St-Pierre, and P. Leder, *Attenuation of LDH-A expression uncovers a link between glycolysis, mitochondrial physiology, and tumor maintenance.* Cancer Cell, 2006. **9**(6): p. 425-34.
368. Moreno-Sánchez, R., et al., *Energy metabolism in tumor cells.* FEBS J, 2007. **274**(6): p. 1393-418.
369. Guppy, M., E. Greiner, and K. Brand, *The role of the Crabtree effect and an endogenous fuel in the energy metabolism of resting and proliferating thymocytes.* Eur J Biochem, 1993. **212**(1): p. 95-9.
370. Ancey, P.B., C. Contat, and E. Meylan, *Glucose transporters in cancer - from tumor cells to the tumor microenvironment.* FEBS J, 2018. **285**(16): p. 2926-2943.
371. Vander Heiden, M.G., L.C. Cantley, and C.B. Thompson, *Understanding the Warburg effect: the metabolic requirements of cell proliferation.* Science, 2009. **324**(5930): p. 1029-33.
372. Gatenby, R.A. and R.J. Gillies, *Why do cancers have high aerobic glycolysis?* Nat Rev Cancer, 2004. **4**(11): p. 891-9.
373. Christofk, H.R., et al., *The M2 splice isoform of pyruvate kinase is important for cancer metabolism and tumour growth.* Nature, 2008. **452**(7184): p. 230-3.
374. Vander Heiden, M.G., et al., *Evidence for an alternative glycolytic pathway in rapidly proliferating cells.* Science, 2010. **329**(5998): p. 1492-9.
375. Mazurek, S., *Pyruvate kinase type M2: a key regulator within the tumour metabolome and a tool for metabolic profiling of tumours.* Ernst Schering Found Symp Proc, 2007(4): p. 99-124.
376. Luo, W., et al., *Pyruvate kinase M2 is a PHD3-stimulated coactivator for hypoxia-inducible factor 1.* Cell, 2011. **145**(5): p. 732-44.
377. Mazurek, S., *Pyruvate kinase type M2: a key regulator of the metabolic budget system in tumor cells.* Int J Biochem Cell Biol, 2011. **43**(7): p. 969-80.

378. Keller, K.E., I.S. Tan, and Y.S. Lee, *SAICAR stimulates pyruvate kinase isoform M2 and promotes cancer cell survival in glucose-limited conditions.* Science, 2012. **338**(6110): p. 1069-72.
379. Keller, K.E., et al., *SAICAR induces protein kinase activity of PKM2 that is necessary for sustained proliferative signaling of cancer cells.* Mol Cell, 2014. **53**(5): p. 700-9.
380. Gui, D.Y., C.A. Lewis, and M.G. Vander Heiden, *Allosteric regulation of PKM2 allows cellular adaptation to different physiological states.* Sci Signal, 2013. **6**(263): p. pe7.
381. Anastasiou, D., et al., *Inhibition of pyruvate kinase M2 by reactive oxygen species contributes to cellular antioxidant responses.* Science, 2011. **334**(6060): p. 1278-83.
382. Kim, J.W., et al., *Evaluation of myc E-box phylogenetic footprints in glycolytic genes by chromatin immunoprecipitation assays.* Mol Cell Biol, 2004. **24**(13): p. 5923-36.
383. David, C.J., et al., *HnRNP proteins controlled by c-Myc deregulate pyruvate kinase mRNA splicing in cancer.* Nature, 2010. **463**(7279): p. 364-8.
384. Iqbal, M.A., et al., *Missense mutations in pyruvate kinase M2 promote cancer metabolism, oxidative endurance, anchorage independence, and tumor growth in a dominant negative manner.* J Biol Chem, 2014. **289**(12): p. 8098-105.
385. Song, M., et al., *AKT as a Therapeutic Target for Cancer.* Cancer Res, 2019. **79**(6): p. 1019-1031.
386. Barthel, A., et al., *Regulation of GLUT1 gene transcription by the serine/threonine kinase Akt1.* J Biol Chem, 1999. **274**(29): p. 20281-6.
387. Taha, C., et al., *Opposite translational control of GLUT1 and GLUT4 glucose transporter mRNAs in response to insulin. Role of mammalian target of rapamycin, protein kinase b, and phosphatidylinositol 3-kinase in GLUT1 mRNA translation.* J Biol Chem, 1999. **274**(46): p. 33085-91.
388. Albanell, J., et al., *mTOR signalling in human cancer.* Clin Transl Oncol, 2007. **9**(8): p. 484-93.
389. Chiang, C.T., et al., *Diosgenin, a naturally occurring steroid, suppresses fatty acid synthase expression in HER2-overexpressing breast cancer cells through modulating Akt, mTOR and JNK phosphorylation.* FEBS Lett, 2007. **581**(30): p. 5735-42.
390. Semenza, G.L., et al., *Transcriptional regulation of genes encoding glycolytic enzymes by hypoxia-inducible factor 1.* J Biol Chem, 1994. **269**(38): p. 23757-63.
391. Hu, C.J., et al., *Differential roles of hypoxia-inducible factor 1alpha (HIF-1alpha) and HIF-2alpha in hypoxic gene regulation.* Mol Cell Biol, 2003. **23**(24): p. 9361-74.
392. Semenza, G.L., *Targeting HIF-1 for cancer therapy.* Nat Rev Cancer, 2003. **3**(10): p. 721-32.
393. Dang, C.V., et al., *The c-Myc target gene network.* Semin Cancer Biol, 2006. **16**(4): p. 253-64.
394. Draoui, N. and O. Feron, *Lactate shuttles at a glance: from physiological paradigms to anti-cancer treatments.* Dis Model Mech, 2011. **4**(6): p. 727-32.
395. Moellering, R.E., et al., *Acid treatment of melanoma cells selects for invasive phenotypes.* Clin Exp Metastasis, 2008. **25**(4): p. 411-25.
396. Mathupala, S.P., A. Rempel, and P.L. Pedersen, *Aberrant glycolytic metabolism of cancer cells: a remarkable coordination of genetic,*

transcriptional, post-translational, and mutational events that lead to a critical role for type II hexokinase. J Bioenerg Biomembr, 1997. **29**(4): p. 339-43.
397. Dang, C.V., et al., *Oncogenes in tumor metabolism, tumorigenesis, and apoptosis.* J Bioenerg Biomembr, 1997. **29**(4): p. 345-54.
398. Dang, C.V., *c-Myc target genes involved in cell growth, apoptosis, and metabolism.* Mol Cell Biol, 1999. **19**(1): p. 1-11.
399. Tran, Q., et al., *Targeting Cancer Metabolism - Revisiting the Warburg Effects.* Toxicol Res, 2016. **32**(3): p. 177-93.
400. Kim, J.W., et al., *HIF-1-mediated expression of pyruvate dehydrogenase kinase: a metabolic switch required for cellular adaptation to hypoxia.* Cell Metab, 2006. **3**(3): p. 177-85.
401. Papandreou, I., et al., *HIF-1 mediates adaptation to hypoxia by actively downregulating mitochondrial oxygen consumption.* Cell Metab, 2006. **3**(3): p. 187-97.
402. Snell, K. and D.A. Duff, *Branched-chain amino acid metabolism and alanine formation in rat muscles in vitro. Mitochondrial-cytosolic interrelationships.* Biochem J, 1985. **225**(3): p. 737-43.
403. Amelio, I., et al., *Serine and glycine metabolism in cancer.* Trends Biochem Sci, 2014. **39**(4): p. 191-8.
404. DeBerardinis, R.J., *Serine metabolism: some tumors take the road less traveled.* Cell Metab, 2011. **14**(3): p. 285-6.
405. Nikiforov, M.A., et al., *A functional screen for Myc-responsive genes reveals serine hydroxymethyltransferase, a major source of the one-carbon unit for cell metabolism.* Mol Cell Biol, 2002. **22**(16): p. 5793-800.
406. Li, Z. and H. Zhang, *Reprogramming of glucose, fatty acid and amino acid metabolism for cancer progression.* Cell Mol Life Sci, 2016. **73**(2): p. 377-92.
407. Snell, K., Y. Natsumeda, and G. Weber, *The modulation of serine metabolism in hepatoma 3924A during different phases of cellular proliferation in culture.* Biochem J, 1987. **245**(2): p. 609-12.
408. Kikuchi, G., *The glycine cleavage system: composition, reaction mechanism, and physiological significance.* Mol Cell Biochem, 1973. **1**(2): p. 169-87.
409. Labuschagne, C.F., et al., *Serine, but not glycine, supports one-carbon metabolism and proliferation of cancer cells.* Cell Rep, 2014. **7**(4): p. 1248-58.
410. Feun, L.G., M.T. Kuo, and N. Savaraj, *Arginine deprivation in cancer therapy.* Curr Opin Clin Nutr Metab Care, 2015. **18**(1): p. 78-82.
411. Phang, J.M., et al., *Proline metabolism and cancer: emerging links to glutamine and collagen.* Curr Opin Clin Nutr Metab Care, 2015. **18**(1): p. 71-7.
412. Phang, J.M., et al., *The proline regulatory axis and cancer.* Front Oncol, 2012. **2**: p. 60.
413. D'Aniello, C., et al., *Proline Metabolism in Tumor Growth and Metastatic Progression.* Front Oncol, 2020. **10**: p. 776.
414. Neurauter, G., et al., *Serum phenylalanine concentrations in patients with ovarian carcinoma correlate with concentrations of immune activation markers and of isoprostane-8.* Cancer Lett, 2008. **272**(1): p. 141-7.
415. Ploder, M., et al., *Serum phenylalanine in patients post trauma and with sepsis correlate to neopterin concentrations.* Amino Acids, 2008. **35**(2): p. 303-7.

416. Porta, F., et al., *Tyrosine metabolism in health and disease: slow-release amino acids therapy improves tyrosine homeostasis in phenylketonuria.* J Pediatr Endocrinol Metab, 2020. **33**(12): p. 1519-1523.
417. Hitosugi, T., et al., *Tyrosine phosphorylation of mitochondrial pyruvate dehydrogenase kinase 1 is important for cancer metabolism.* Mol Cell, 2011. **44**(6): p. 864-77.
418. Shiman, R. and D.W. Gray, *Formation and fate of tyrosine. Intracellular partitioning of newly synthesized tyrosine in mammalian liver.* J Biol Chem, 1998. **273**(52): p. 34760-9.
419. Fernstrom, J.D. and M.H. Fernstrom, *Tyrosine, phenylalanine, and catecholamine synthesis and function in the brain.* J Nutr, 2007. **137**(6 Suppl 1): p. 1539S-1547S; discussion 1548S.
420. Dunkley, P.R., et al., *Tyrosine hydroxylase phosphorylation: regulation and consequences.* J Neurochem, 2004. **91**(5): p. 1025-43.
421. Le Bourdellès, B., et al., *Phosphorylation of human recombinant tyrosine hydroxylase isoforms 1 and 2: an additional phosphorylated residue in isoform 2, generated through alternative splicing.* J Biol Chem, 1991. **266**(26): p. 17124-30.
422. Fu, Y.M., et al., *Specific amino acid dependency regulates invasiveness and viability of androgen-independent prostate cancer cells.* Nutr Cancer, 2003. **45**(1): p. 60-73.
423. Joza, N., et al., *Essential role of the mitochondrial apoptosis-inducing factor in programmed cell death.* Nature, 2001. **410**(6828): p. 549-54.
424. Fu, Y.M. and G.G. Meadows, *Specific amino acid dependency regulates the cellular behavior of melanoma.* J Nutr, 2007. **137**(6 Suppl 1): p. 1591S-1596S; discussion 1597S-1598S.
425. Tong, M., et al., *Loss of tyrosine catabolic enzyme HPD promotes glutamine anaplerosis through mTOR signaling in liver cancer.* Cell Rep, 2021. **36**(8): p. 109617.
426. Wiggins, T., et al., *Tyrosine, phenylalanine, and tryptophan in gastroesophageal malignancy: a systematic review.* Cancer Epidemiol Biomarkers Prev, 2015. **24**(1): p. 32-8.
427. Nguyen, T.N., H.Q. Nguyen, and D.H. Le, *Unveiling prognostics biomarkers of tyrosine metabolism reprogramming in liver cancer by cross-platform gene expression analyses.* PLoS One, 2020. **15**(6): p. e0229276.
428. Uchino, H., et al., *Transport of amino acid-related compounds mediated by L-type amino acid transporter 1 (LAT1): insights into the mechanisms of substrate recognition.* Mol Pharmacol, 2002. **61**(4): p. 729-37.
429. Kaira, K., et al., *Fluorine-18-alpha-methyltyrosine positron emission tomography for diagnosis and staging of lung cancer: a clinicopathologic study.* Clin Cancer Res, 2007. **13**(21): p. 6369-78.
430. Suzuki, M., et al., *An experimental study on O-[18F]fluoromethyl-L-tyrosine for differentiation between tumor and inflammatory tissues.* Ann Nucl Med, 2005. **19**(7): p. 589-95.
431. Kaira, K., et al., *Assessment of therapy response in lung cancer with ^{18}F-α-methyl tyrosine PET.* AJR Am J Roentgenol, 2010. **195**(5): p. 1204-11.
432. Bhutia, Y.D., et al., *Amino Acid transporters in cancer and their relevance to "glutamine addiction": novel targets for the design of a new class of anticancer drugs.* Cancer Res, 2015. **75**(9): p. 1782-8.
433. Nicklin, P., et al., *Bidirectional transport of amino acids regulates mTOR and autophagy.* Cell, 2009. **136**(3): p. 521-34.

434. Timmerman, L.A., et al., *Glutamine sensitivity analysis identifies the xCT antiporter as a common triple-negative breast tumor therapeutic target.* Cancer Cell, 2013. **24**(4): p. 450-65.
435. Moreadith, R.W. and A.L. Lehninger, *The pathways of glutamate and glutamine oxidation by tumor cell mitochondria. Role of mitochondrial NAD(P)+-dependent malic enzyme.* J Biol Chem, 1984. **259**(10): p. 6215-21.
436. Gameiro, P.A., et al., *In vivo HIF-mediated reductive carboxylation is regulated by citrate levels and sensitizes VHL-deficient cells to glutamine deprivation.* Cell Metab, 2013. **17**(3): p. 372-85.
437. Mullen, A.R., et al., *Reductive carboxylation supports growth in tumour cells with defective mitochondria.* Nature, 2011. **481**(7381): p. 385-8.
438. Metallo, C.M., et al., *Reductive glutamine metabolism by IDH1 mediates lipogenesis under hypoxia.* Nature, 2011. **481**(7381): p. 380-4.
439. DeBerardinis, R.J., et al., *Beyond aerobic glycolysis: transformed cells can engage in glutamine metabolism that exceeds the requirement for protein and nucleotide synthesis.* Proc Natl Acad Sci U S A, 2007. **104**(49): p. 19345-50.
440. Le, A., et al., *Glucose-independent glutamine metabolism via TCA cycling for proliferation and survival in B cells.* Cell Metab, 2012. **15**(1): p. 110-21.
441. Yang, C., et al., *Glutamine oxidation maintains the TCA cycle and cell survival during impaired mitochondrial pyruvate transport.* Mol Cell, 2014. **56**(3): p. 414-424.
442. Lane, A.N. and T.W. Fan, *Regulation of mammalian nucleotide metabolism and biosynthesis.* Nucleic Acids Res, 2015. **43**(4): p. 2466-85.
443. Hosios, A.M., et al., *Amino Acids Rather than Glucose Account for the Majority of Cell Mass in Proliferating Mammalian Cells.* Dev Cell, 2016. **36**(5): p. 540-9.
444. Cunningham, J.T., et al., *Protein and nucleotide biosynthesis are coupled by a single rate-limiting enzyme, PRPS2, to drive cancer.* Cell, 2014. **157**(5): p. 1088-103.
445. Liu, Y.C., et al., *Global regulation of nucleotide biosynthetic genes by c-Myc.* PLoS One, 2008. **3**(7): p. e2722.
446. Goswami, M.T., et al., *Role and regulation of coordinately expressed de novo purine biosynthetic enzymes PPAT and PAICS in lung cancer.* Oncotarget, 2015. **6**(27): p. 23445-61.
447. Sullivan, L.B., et al., *Supporting Aspartate Biosynthesis Is an Essential Function of Respiration in Proliferating Cells.* Cell, 2015. **162**(3): p. 552-63.
448. Patel, D., et al., *Aspartate Rescues S-phase Arrest Caused by Suppression of Glutamine Utilization in KRas-driven Cancer Cells.* J Biol Chem, 2016. **291**(17): p. 9322-9.
449. Gao, P., et al., *c-Myc suppression of miR-23a/b enhances mitochondrial glutaminase expression and glutamine metabolism.* Nature, 2009. **458**(7239): p. 762-5.
450. Bott, A.J., et al., *Oncogenic Myc Induces Expression of Glutamine Synthetase through Promoter Demethylation.* Cell Metab, 2015. **22**(6): p. 1068-77.
451. Zhao, X., et al., *SLC1A5 glutamine transporter is a target of MYC and mediates reduced mTORC1 signaling and increased fatty acid oxidation in long-lived Myc hypomorphic mice.* Aging Cell, 2019. **18**(3): p. e12947.
452. Pérez-Escuredo, J., et al., *Lactate promotes glutamine uptake and metabolism in oxidative cancer cells.* Cell Cycle, 2016. **15**(1): p. 72-83.

453. Son, J., et al., *Glutamine supports pancreatic cancer growth through a KRAS-regulated metabolic pathway.* Nature, 2013. **496**(7443): p. 101-5.
454. Matés, J.M., et al., *Glutaminase isoenzymes as key regulators in metabolic and oxidative stress against cancer.* Curr Mol Med, 2013. **13**(4): p. 514-34.
455. Reynolds, M.R., et al., *Control of glutamine metabolism by the tumor suppressor Rb.* Oncogene, 2014. **33**(5): p. 556-66.
456. De Logu, F., et al., *Schwann cell TRPA1 mediates neuroinflammation that sustains macrophage-dependent neuropathic pain in mice.* Nat Commun, 2017. **8**(1): p. 1887.
457. De Logu, F., et al., *Macrophages and Schwann cell TRPA1 mediate chronic allodynia in a mouse model of complex regional pain syndrome type I.* Brain Behav Immun, 2020. **88**: p. 535-546.
458. Laukova, M., et al., *Acute stress differently modulates β1, β2 and β3 adrenoceptors in T cells, but not in B cells, from the rat spleen.* Neuroimmunomodulation, 2012. **19**(2): p. 69-78.
459. Slota, C., et al., *Norepinephrine preferentially modulates memory CD8 T cell function inducing inflammatory cytokine production and reducing proliferation in response to activation.* Brain Behav Immun, 2015. **46**: p. 168-79.
460. Chi, D.S., et al., *MAPK-dependent regulation of IL-1- and beta-adrenoreceptor-induced inflammatory cytokine production from mast cells: implications for the stress response.* BMC Immunol, 2004. **5**: p. 22.
461. Chiarella, S.E., et al., *β_2-Adrenergic agonists augment air pollution-induced IL-6 release and thrombosis.* J Clin Invest, 2014. **124**(7): p. 2935-46.
462. Chu, L.F., et al., *Modulation of remifentanil-induced postinfusion hyperalgesia by the β-blocker propranolol in humans.* Pain, 2012. **153**(5): p. 974-981.
463. De Logu, F., et al., *Oxidative stress mediates thalidomide-induced pain by targeting peripheral TRPA1 and central TRPV4.* BMC Biol, 2020. **18**(1): p. 197.
464. Brusco, I., et al., *Dacarbazine alone or associated with melanoma-bearing cancer pain model induces painful hypersensitivity by TRPA1 activation in mice.* Int J Cancer, 2020. **146**(10): p. 2797-2809.
465. Gonzalez-Menendez, P., et al., *GLUT1 protects prostate cancer cells from glucose deprivation-induced oxidative stress.* Redox Biol, 2018. **17**: p. 112-127.
466. Jóźwiak, P., et al., *Glucose-dependent glucose transporter 1 expression and its impact on viability of thyroid cancer cells.* Oncol Rep, 2015. **33**(2): p. 913-20.
467. Lieu, E.L., et al., *Amino acids in cancer.* Exp Mol Med, 2020. **52**(1): p. 15-30.
468. Dallner, O.S., et al., *Beta3-adrenergic receptors stimulate glucose uptake in brown adipocytes by two mechanisms independently of glucose transporter 4 translocation.* Endocrinology, 2006. **147**(12): p. 5730-9.
469. Milagro, F.I., et al., *A beta3-adrenergic agonist increases muscle GLUT1/GLUT4 ratio, and regulates liver glucose utilization in diabetic rats.* Diabetes Obes Metab, 1999. **1**(2): p. 97-104.
470. Sirniö, P., et al., *Alterations in serum amino-acid profile in the progression of colorectal cancer: associations with systemic inflammation, tumour stage and patient survival.* Br J Cancer, 2019. **120**(2): p. 238-246.
471. Hoerner, C.R., V.J. Chen, and A.C. Fan, *The 'Achilles Heel' of Metabolism in Renal Cell Carcinoma: Glutaminase Inhibition as a Rational Treatment Strategy.* Kidney Cancer, 2019. **3**(1): p. 15-29.

472. Abu Aboud, O., et al., *Glutamine Addiction in Kidney Cancer Suppresses Oxidative Stress and Can Be Exploited for Real-Time Imaging.* Cancer Res, 2017. **77**(23): p. 6746-6758.
473. Mustafa, A., et al., *Serum amino acid levels as a biomarker for renal cell carcinoma.* J Urol, 2011. **186**(4): p. 1206-12.
474. Herman, S., et al., *Alterations in the tyrosine and phenylalanine pathways revealed by biochemical profiling in cerebrospinal fluid of Huntington's disease subjects.* Sci Rep, 2019. **9**(1): p. 4129.
475. Chinsky, J.M., et al., *Diagnosis and treatment of tyrosinemia type I: a US and Canadian consensus group review and recommendations.* Genet Med, 2017. **19**(12).
476. Zatkova, A., L. Ranganath, and L. Kadasi, *Alkaptonuria: Current Perspectives.* Appl Clin Genet, 2020. **13**: p. 37-47.
477. Derle, A., et al., *The role of metabolic adaptation to nutrient stress in pancreatic cancer.* Cell Stress, 2018. **2**(12): p. 332-339.
478. Cao, M.D., et al., *Metabolic characterization of triple negative breast cancer.* BMC Cancer, 2014. **14**: p. 941.
479. DeBerardinis, R.J. and T. Cheng, *Q's next: the diverse functions of glutamine in metabolism, cell biology and cancer.* Oncogene, 2010. **29**(3): p. 313-24.
480. Mashima, T., H. Seimiya, and T. Tsuruo, *De novo fatty-acid synthesis and related pathways as molecular targets for cancer therapy.* Br J Cancer, 2009. **100**(9): p. 1369-72.
481. Ge, X., et al., *Activation of caspases and cleavage of Bid are required for tyrosine and phenylalanine deficiency-induced apoptosis of human A375 melanoma cells.* Arch Biochem Biophys, 2002. **403**(1): p. 50-8.
482. Pirro, V., A. Skanjeti, and E. Pelosi, *18F-fluorodeoxyglucose-positron emission tomography in the characterization of suspected rhabdoid renal tumor recurrence: a case report.* J Pediatr Hematol Oncol, 2007. **29**(1): p. 69-71.
483. King, A., M.A. Selak, and E. Gottlieb, *Succinate dehydrogenase and fumarate hydratase: linking mitochondrial dysfunction and cancer.* Oncogene, 2006. **25**(34): p. 4675-82.
484. Schmidt, C., M. Sciacovelli, and C. Frezza, *Fumarate hydratase in cancer: A multifaceted tumour suppressor.* Semin Cell Dev Biol, 2020. **98**: p. 15-25.
485. Atas, E., M. Oberhuber, and L. Kenner, *The Implications of PDK1-4 on Tumor Energy Metabolism, Aggressiveness and Therapy Resistance.* Front Oncol, 2020. **10**: p. 583217.
486. De Ieso, M.L. and A.J. Yool, *Mechanisms of Aquaporin-Facilitated Cancer Invasion and Metastasis.* Front Chem, 2018. **6**: p. 135.